Iranian Gas Institute

ISSN: 2588-5596

JGT

JOURNAL OF GAS TECHNOLOGY

Volume 10 • Issue 2 • Winter 2025 • www.jgt.irangi.org

Journal of Gas Technology, JGT

Volume 10, Issue 2, Winter 2025

Publisher
Iranian Gas Institute

Director-in-Charge
Mohammadreza Omidkhah

Editor-in-Chief
Ali Vatani

Deputy Editor
Hedayat Azizpour

Associate Editor
Mastaneh Hajipour

Executive Manager
Hamidreza Karimi

Editorial Board Members
Ali Vatani, University of Tehran
Mohammadreza Omidkhah, Tarbiat Modares University
Mohamadreza Jafari Nasr, Research Institute of Petroleum Industry
Vahid Taghikhani, Sharif University of Technology
Mahmood Moshfeghian, Oklahoma State University
Mojtaba Shariati Niasar, University of Tehran
Reza Mosayebi Behbahani, Petroleum University of Technology
Rahbar Rahimi, University of Sistan and Baluchestan
Seyed Hesam Najibi, Petroleum University of Technology
Seyed Alireza Tabatabaei-Nezhad, Sahand University of Technology
Riyaz Kharrat, Petroleum University of Technology
Toraj Mohammadi, Iran University of Science and Technology
Seyed Reza Shadizadeh, Petroleum University of Technology
Bahman Tohidi, Heriot-Watt University
Fariborz Rashidi, Amirkabir University of Technology
Masoud Soroush, Drexel University - United States
Mahmoud Jamiolahmady, Heriot-Watt University Institute, Scotland
Amir Hossein Mohammadi, University of KwaZulu-Natal, South Africa

Technical Editor
Masoud Aghajani & Mortaza Zivdar

Layout
Hamidreza karimi

Cover Design
Hamidreza karimi

Contact Information
https://jgt.irangi.org
Email: ijgt.igi@gmail.com

EISSN: 2588-5596

Open Access Journal
Journal of Gas Technology is a peer reviewed, open access journal.

JOURNAL OF GAS TECHNOLOGY

Volume 10, Issue 2, Winter 2025

Annual Names of Reviewers

Ali Vatani
University of Tehran

Mastaneh Hajipour
Islamic Azad University, Science and Research Branch

Saeid Jamshidi
Sharif University of Technology

Hedayat Azizpour
University of Tehran

Morteza Zivdar
University of Sistan and Baluchestan

Masoud Aghajani
Petroleum University of Technology

Seyyed Hossein Hosseini
Ilam University

Davod Mohebbi-Kalhori
University of Sistan and Baluchestan

Mohammad Reza Sardashti Birjandi
University of Sistan and Baluchestanh

Mohammadreza Bagheri
Hakim Sabzevari University

Masoud Bijani
Garmsar University

Ebrahim Biniaz Delijani
Islamic Azad University, Science and Research Branch

Mahdi Razavifar
University of Tabriz

Zeinab Hamidzadeh
Islamic Azad University, Science and Research Branch

Yasin Khalili
Amirkabir University of Technology

Amir Hossein Mohammadi
University of KwaZulu-Natal, South Africa

Sara Tarashi
University of Tehran

kazem kashefi
Research Institute of Petroleum Industry

kamran keynejad
University of Tehran

Table of Contents

JOURNAL OF GAS TECHNOLOGY

Volume 10 / Issue 2 / Winter 2025 / Pages 5-20

Journal Home page: https://jgt.irangi.org

Enhancement of Ternary LNG Mixture Separation Process by Using Dividing Wall Column

Mahmoud Hemmati[1], Morteza Zivdar[2*], Taleb Zarei[3], Rahbar Rahimi[2]

1. Ph.D. Student, Department of Chemical Engineering, Faculty of Engineering, University of Sistan and Baluchestan, Zahedan, Iran
2. Professor, Department of Chemical Engineering, Faculty of Engineering, University of Sistan and Baluchestan, Zahedan, Iran
3. Professor, Department of Mechanical Engineering, University of Hormozgan, Bandar Abbas, Iran

ARTICLE INFO

ORIGINAL RESEARCH ARTICLE

Article History:
Received: 02 October 2025
Revised: 16 November 2025
Accepted: 16 December 2025

Keywords:
Dividing wall column
Optimization
Aspen plus
Total Annual Cost
Energy Efficiency
Ternary Hydrocarbon Separation
Process Intensification

DOR: 20.1001.1/jgt.2026.2076264.1063

ABSTRACT

The dividing wall column (DWC) represents a form of process intensification that offers the potential to lower energy usage and initial investment costs in distillation practices. This research undertakes a systematic optimization and economic comparison between DWC and a traditional distillation column process for the separation of a three-component mixture of N-Pentane, N-Hexane, and N-Heptane. The analysis delves into the exergy flows and economic aspects of these two processes in detail. In this study the sequential quadratic programming (SQP) optimization method was used to minimize the total reboiler and condenser duties and the Peng Robinson model is applied to predict the vapor-liquid equilibrium (VLE) of the systems under study. In this study, DWC is evaluated against a conventional two-column distillation setup in terms of total annual cost (TAC) and energy consumption under the same feed ratio conditions. The results show that implementing DWC leads to a 37% decrease in TAC and a 38% reduction in energy requirements. This research proposes the use of dividing wall columns as an alternative to traditional distillation columns, providing a new method for separating hydrocarbons that emphasizes economic efficiency and encourages the adoption of innovative practices for energy conservation and environmental protection.

How to cite this article
M. Hemmati, M. Zivdar, R. Rahimi, T. Zarei, Enhancement of Ternary LNG Mixture Separation Process by using Dividing Wall Column. Journal of Gas Technology. 2025; 10(2): 5-20. (https://jgt.irangi.org/article_737827.html)

* Corresponding author.
E-mail address: mzivdar@eng.usb.ac.ir, (M. Zivdar).

Available online 30 December 2025
2588-5596/© 2016 The Authors. Published by Iranian Gas Institute.
This is an open access article under the CC BY license. (https://creativecommons.org/licenses/by/4.0)

1. Introduction

The increase in energy costs and economic difficulties has highlighted the necessity for natural gas and liquid recovery facilities to improve their sophistication and efficiency. Essentially, the latest NGL plants are structured to lower both fixed and operational expenses without compromising on their production levels. Two crucial factors that can significantly impact process performance are process configuration and plant operation (Mehrpooya, Vatani et al. 2010). Distillation is widely recognized as one of the most frequently utilized processes in chemical industries and petrochemical (Shahruddin, Uzuman et al. 2025).

Distillation is recognized as one of the most energy-demanding separation methods, responsible for consuming more than 40% of the energy consumed in the petrochemical and chemical industry. Additionally, it constitutes roughly 95% of the total energy used for separation in both the refining and chemical processing sectors. Despite its significant energy requirements, distillation continues to be a fundamental separation technique because of its straightforwardness and efficiency. As of now, there are approximately 40,000 operational distillation columns utilized in more than 200 distinct processes (Biasi, Zemp et al. 2024). In today's energy-conscious society, conventional distillation processes are both cost and energy intensive. It is crucial to enhance the sustainability and economic viability of distillation systems. Heat-integrated distillation columns, such as the dividing-wall column (DWC), have been proposed and investigated for NGL recovery processes. Dividing-wall column, as a practical intensification technology, demonstrates significant advantages in this regard. Because of its compact equipment design and minimized remixing effects, a DWC necessitates lower capital and operating costs for the separation of multicomponent mixtures compared to traditional distillation setups (Li, Guan et al. 2024). The Dividing Wall Column was first designed by R.O. Wright in 1949 as an improved column setup. It includes a vertical partition wall that divides the column into a main section and a pre-fractionation section. This wall helps reduce the remixing of intermediate components, leading to higher energy efficiency compared to traditional distillation sequences. The inaugural industrial deployment of a DWC occurred at BASF in 1985. Since then, only over 200 DWCs have been erected globally. One obstacle hindering widespread DWC adoption is the challenging task of tightly managing the vapor split ratio, which typically operates within a narrow range (Song, Cui et al. 2024). With reference to Fig 1. the distinction between the Dividing Wall Column (DWC) and the Simple Distillation Column (SDC) is clearly visible. The DWC features a vertical dividing wall that separates it into two sections: the prefractionator on the left side and the main column on the remaining side. The ternary feed is initially introduced into the prefractionator, where it is separated into two primary binary mixtures. These mixtures then flow into the main column, bypassing the dividing wall, for further refinement and separation into three pure products. (Yuan, Zhang et al. 2024). the three-component feed (A, B, C) enters from the pre-fractionator side. In this section, the heaviest and lightest are separated. The lightest composition (A) and part of the composition with the middle boiling point (B) travel to the top of the wall and the lightest component (A) leave the top of the tower as a distillate. The heaviest composition (C) along with a part of (B) deflected towards the bottom of the wall and the heaviest composition exits from the bottom of the tower. The middle boiling point (B), which moves up and down the wall along with the light and heavy currents, is separated on the back side of the wall and exits from the middle of the tower by a tensile flow (Ränger, Halvorsen et al. 2025). Therefore, the DWC is two different distillation columns in one unit separated by a wall. Since two separation steps are being merged into one unit, it can be referred to as process integration. So, compared with conventional distillation columns, DWCs reduce plant space, equipment investment, and energy consumption (Kolbe and Wenzel 2004, Liu, Zhao et al. 2022). This innovative column design effectively addresses the issue of re-mixing the intermediate component, setting it apart from conventional direct or indirect SDC sequences.

When evaluating design options for multi-component separation, the primary measure is often used total annual cost (TAC). Processes with lower TAC are generally more energy-efficient, as energy usage is a key factor influencing costs. However, a more comprehensive insight can be gained by examining metrics directly linked to energy analysis and TAC. Researchers have employed energy analysis and TAC to assess the effectiveness of various distillation alternatives a wide range of systems including hydrocarbons, alcohols, aldehydes, ketones, amines. Yanyang et al.(Wu, Zhang et al. 2020) optimized TAC and total energy loss simultaneously for separation of the three diols. In this study, DWC was evaluated against both a side rectifier configuration and a conventional distillation column in terms of energy consumption and total annual costs, while using an equal number of stages. The findings revealed a 47.60% reduction in energy requirements and a 35.40% decrease in TAC when using DWC compared to the traditional distillation column. Furthermore, compared to the side rectifier configuration, DWC exhibited a 48.00% reduction in energy consumption and a 34.11% decrease in total annual costs. Li et al. (Li, Zhang et al. 2020)optimized DWC to separate ternary mixtures of alcohol systems. In this work, used response surface methodology (RSM) to obtain optimal operation parameters and compared with to the conventional process. Result showed that DWC can decrease energy consumption and total annual cost by 25.43%, 33.39%, and 28.73% respectively and increase thermodynamic efficiency. In an tray to reduce the costs related with DWC, Wu et al. (Wu, Zhang et al. 2020) precented Sequential quadratic programming (SQP) to optimize the separation of the ternary components. As a result, illustrated that DWC can reduce total annual costs (TACs) and energy requirements significantly compared with traditional two-column distillation process. In another work, to separate azeotrope three components, Wang et al. (Wang, Song et al. 2023) proposed the use DWC. They obtained an energy saving of 37% and TAC 43.5% compared conventional azeotrope distillation. The advantages of this new technology are reducing energy consumption, reducing investment costs, high thermodynamic efficiency, and reducing the required space. Natalie et al. (Czarnecki, Giannetti et al. 2024) conducted research on how the positioning of walls affects the economics and energy consumption in a simulated chemical system. Their goal was to create an azeotropic composition of water and isopropanol. Different wall placement sequences such as direct conventional, indirect conventional, middle wall divided wall column (DWC), top wall DWC, and bottom wall DWC were analyzed through Aspen Plus simulations. The results showed that the middle wall DWC option required a fixed capital investment of at least 8% less, while achieving energy savings of 14% compared to conventional sequences. In order to improve the intensification process, Andrade et al.(Andrade, Andrade et al. 2024) compared two improved setups for the downstream separation phase of the Methanol-to-Olefins (MTO) process to enhance the intensification process. They found that the configuration with two DWCs was more efficient, saving 15.56% energy in the reboiler, cutting total annual costs by 7.68%, and lowering daily CO_2 emissions by 11.33 tons, representing a 14.19% reduction compared to the traditional method.

To design DWC, in 1992 Triantafyllou and Smith presented the first methods to design DWCS (FUGK) (Di Pretoro, Ciranna et al. 2021). The minimum vapor flow rate (V_min) was presented by Halvorsen (Halvorsen and Skogestad 2011). In another research, Lavasani et al. (Lavasani, Rahimi et al. 2018) used response surface methodology (RSM) to design and optimize the parameters of the DWC. In a similar work (2020), Chunli et al. studied (RSM) method to obtain optimal parameters (Li, Zhang et al. 2020). Finally, Ceron et al. (Buitimea-Cerón, Hahn et al. 2021) evaluated three methodologies to design and optimize DWCs. They showed that the Sotudeh and Shahraki (S&S) method was the most efficient technique.

In distillation sequences, intricate columns that are thermally connected and operate based on the concept of process enhancements are employed to reduce the remixing of non-essential elements. As a result, this leads to a more energy-efficient separation process and the potential for reducing operational and investment costs. Among these complex columns, dividing-wall columns (DWC) are commonly considered as a favored option in distillation sequence design scenarios (Li, Finn et al. 2023). By eschewing remixing, DWCs typically achieve a 20-40% reduction in energy consumption compared to the most efficient conventional two-column sequence. Each single DWC shell substitutes for two traditional columns, along with their related ancillary equipment (such as one condenser, one reboilers, and fewer pumps and vessels), resulting in potential capital cost savings of up to 30%. This decreased energy usage not only results in a diminished carbon footprint and lower greenhouse gas emissions but also aligns with the principles of green engineering.

The main importance of this study lies in introducing novel methods for separating a ternary mixture of N-Pentane, N-Hexane, and N-Heptane. New methods against traditional techniques, considering criteria such as energy consumption, initial investments, and greenhouse gas emissions were evaluated. The most effective operational conditions were determined by simulation. The final separation technique is developed by analyzing economic, environmental, overall energy consumption, and thermodynamic efficiency indicators.

1.1. Example of Application

The distillation process plays a key role in chemical, petrochemical, and refinery industries, despite high energy consumption. DWCs can be the best alternative to traditional distillation columns (Battisti, Machado et al. 2020). In 1985, BASF installed the first industrial DWC. In 2010 Asprion et al. (Asprion and Kaibel 2010) reported more than 60 DWCs were put in by BASF. In 2010 Yildirim et al reported. In 2010 Yildirim et al reported there are 125 DWCs in the world which 116 are to separate ternary components. The author expected this number to increase to 350 in 2015 (Yildirim, Kiss et al. 2011). Later, Li et al. (Li, Li et al. 2019) expressed there were more than 300 DWCs. It was promised that DWC could be a popular distillation device in 2070 (Schultz, Stewart et al. 2002, Wu, Zhang et al. 2020). Most of the DWCs are of the packing type and some of them are of the tray type. Reported that the diameter of these columns is 0.6 to 4 meters and the largest middle wall tower with a height of 107 meters and a diameter of 5 meters is active in Africa. DWCs can be used in the azeotropic process, extractive process, and reactive distillation process which will be investigated in the following sections (Yildirim, Kiss et al. 2011). However, one of the strategies to intensify the process is to set up and use the DWC towers, but their application is minuscule on the industrial and pilot scale (Shi, Zhao et al. 2020).

In this study, two setups, including a traditional distillation column and a DWC process, were utilized to separate N-Pentane, N-Hexane, and N-Heptane. The Aspentech Aspen Plus was used to acquire the operation conditions and accurate design variables. The effective sensitivity analysis device sensitivity analysis was adopted to minimize the total condenser and reboiler duties needed in the simulations. Several optimization variables were adopted: split vapor ratio and liquid ratio, reflux ratio, divided wall location, feed stage, side stream location and total number of stages. DWC and conventional distillation column were compared to indicate the advantage of DWC process for separation of hydrocarbon mixtures in terms of (total annual cost) TAC, exergy loss (El) and CO_2 emissions.

2. Simulation and Performance Evaluation Methods

2.1. Simulation Condition and Methods

In this work, the simulation software Aspen Plus was applied to execute a steady-state simulation and optimization of the separation of N-Pentane (A), N-Hexane (B), and N-Heptane (C) systems in a DWC and conventional distillation column. In addition, the feed fresh mol ratio of A, B and C was 0.3,0.3 and 0.4 and feed ratio was 3600 Kmol/h. The boiling point of A, B and C was 35.9 °C, 68.3 °C and 98 °C. degrees centigrade at one atmospheric pressure (Figure 1). All the product purities are set as 99.5 mol% in two processes. In this simulation, the two columns are assumed to be at atmospheric pressure for easy operation. Process simulations were carried in Aspen Plus V8.0. The Peng Robinson model is applied to predict the vapor-liquid equilibrium (VLE) of the systems under study, with the binary interaction parameters carefully selected from Aspen Plus default databank.

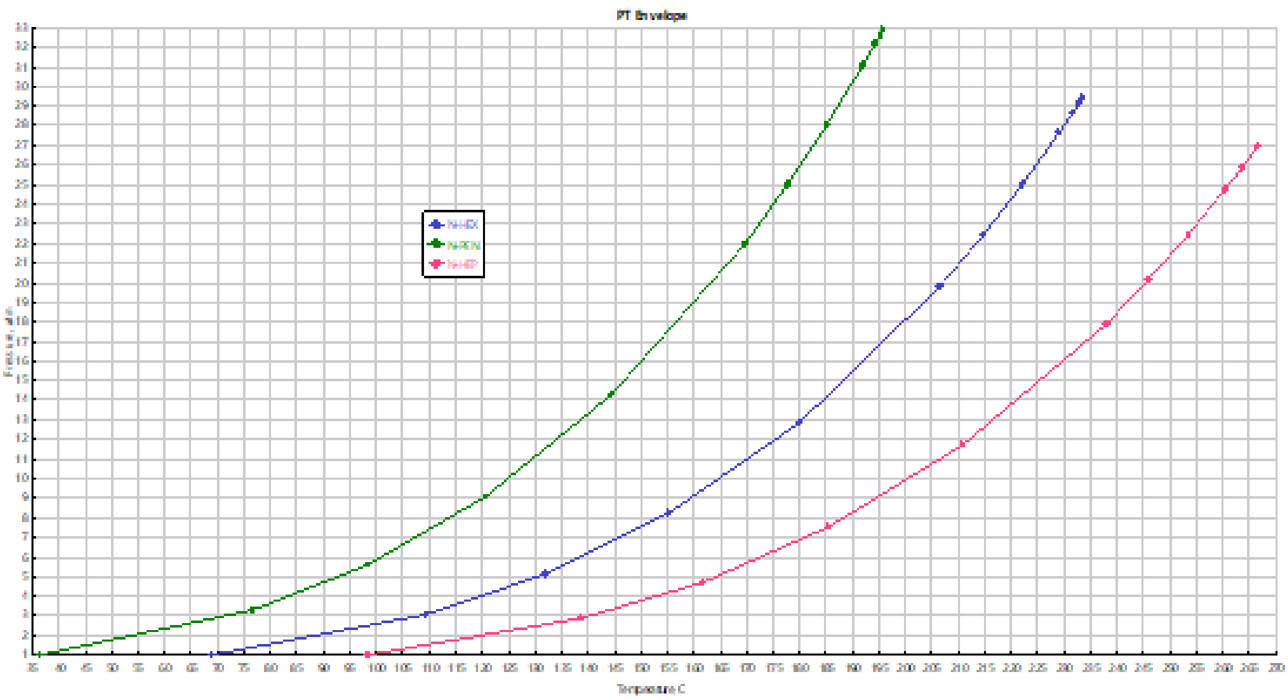

Figure 1. Boiling Point of Ternary Mixture

2.2. Framework of Energy Consumption, Economics and Environmental Impact

2.2.1. Total Energy Consumption

The estimated total energy consumption (TEC) indicates the external energy usage for the reboiler and condenser.

2.2.2. Total Annual Cost

The overall yearly expense is utilized to assess the economic estimation. TAC consists of energy expenses and yearly capital investments, as demonstrated below.

$$TAC = \frac{capital\ cost}{payback\ period} + energy\ cost$$

The study's initial investment includes expenses for columns and heat exchangers, such as reboilers and condensers. The analysis assumes a payback period of three years and an annual operating time of 8000 hours. The comprehensive design and assessment procedure for Total Annual Cost (TAC) is summarized in (Table 1-2) of the Supplementary material.

2.2.3. Environmental Impact

In distillation systems, the main contributors to CO_2 emissions are furnaces, boilers, and electricity use. There are also indirect emissions associated with the process, such as those from refrigerant use, which are affected by the power needed to cool and circulate these fluids, as well as emissions from manufacturing equipment like the steel used in distillation columns. Additional emissions arise from transportation during construction and operation, along with those related to water consumption (Andrade, Andrade et al. 2024). This study evaluates the energy consumption of the reboiler and condenser in both tower types and, based on these values, identifies the tower with the lowest pollution.

2.3. Conventional Distillation Process

In this research, the feasibility of a distillation system was assessed using the Residue Curve Map (RCM). (Figure 2) displays the RCM for the hydrocarbon blend, demonstrating that traditional distillation could successfully achieve the separation process due to the absence of azeotropic and distillation boundaries. (Figure 3) presents a flow diagram showing the feasibility of a conventional distillation column for separating the ternary mixture of n-pentane, n-hexane, and n-heptane. In the CDC process, the first component or lightest component is separated from the top of the first column, and the other two compounds that came out from the bottom of the first tower enter the second column as feed. After establishing steady-state simulation, the liquid composition, temperature profiles and optimal design parameters were obtained. The results were shown in (Table 1).

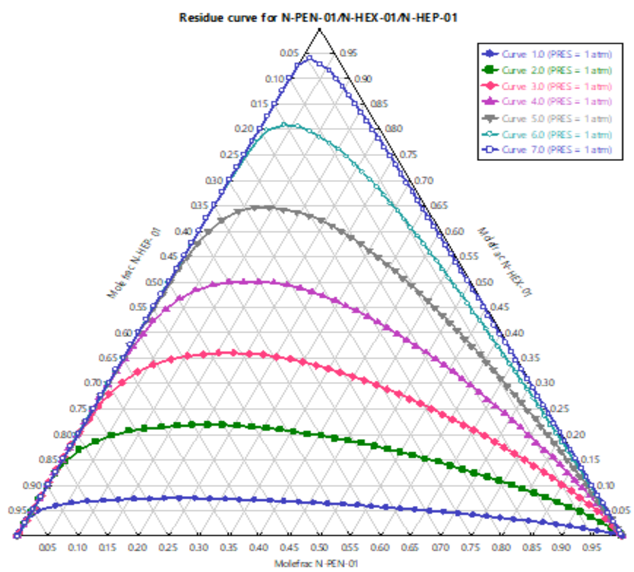

Figure 2. RCM of Ternary Mixture

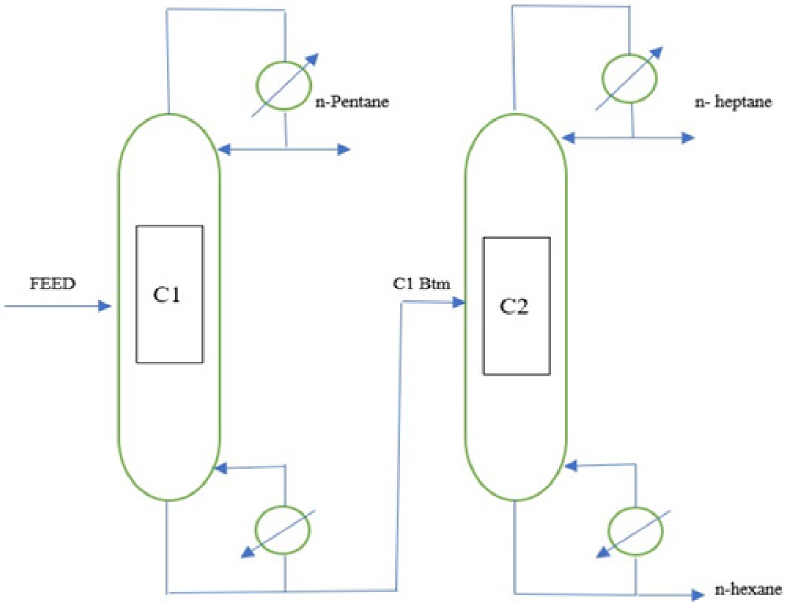

Figure 3: Flow Diagram of the Direct Sequence

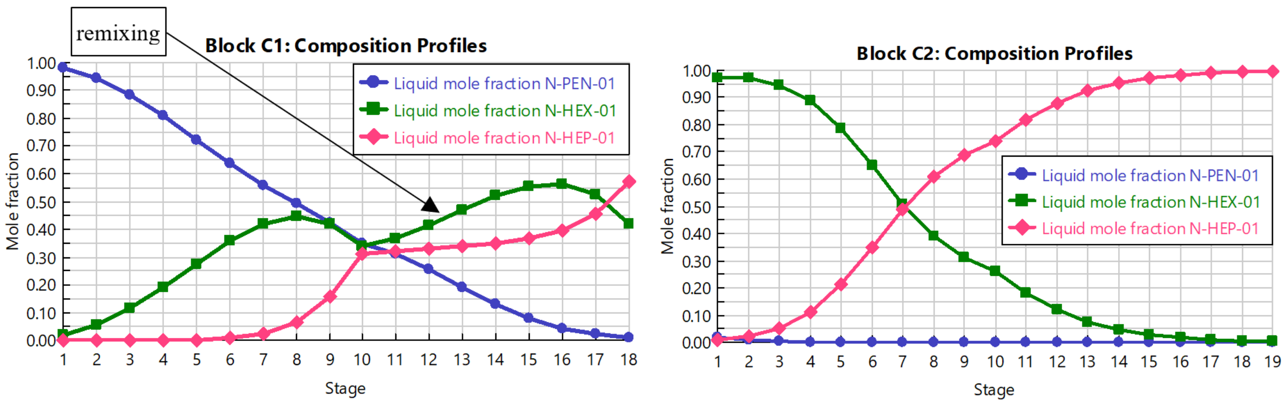

Figure 4: Composition Profiles in C1 and C2 Units of the Conventional Distillation Column

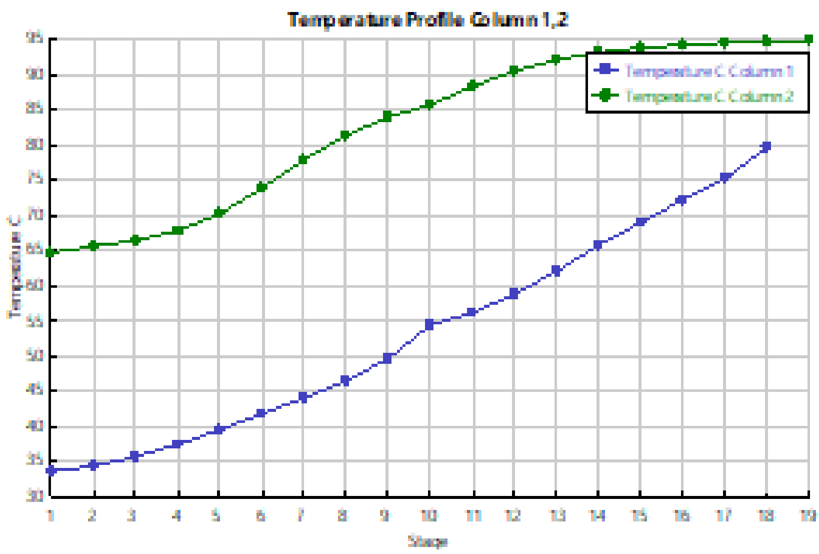

Figure 5: Temperature Profiles in C1 and C2 Units of the Conventional Distillation Column

Table 1: Optimal Design Parameters of the Direct Sequence of Two Columns

Design parameters	Value	Unit
Flow rate of feed stream	3600	Kmol/h
Feed compositions		
n-Pentane. n-Hexane and n-Heptane	0.3:0.3:0.4	_
Vapor Fraction	0	_
Pressure of feed stream	1	atm
Operating pressure(C1)	1	atm
Operating pressure(C2)	1	atm
Column diameter(C1)	6.7	m
Column diameter(C2)	5.6	m
Total number of stages(C1)	18	_
Total number of stages(C2)	19	_
Feed stage(C1)	10	_
Feed stage(C2)	10	_
Reflux ratio(C1)	1.32	_
Reflux ratio(C2)	3.2	_
Distillate to feed ratio(C1)	1080	Kmol/h
Distillate to feed ratio(C2)	1083.86	Kmol/h
n-Pentane product purity	98.0	%wt
n-Hexane product purity	96.6	%wt
n- Heptane product purity	99.2	%wt
Reboiler duty(C1)	25.870284	MW
Reboiler duty(C2)	37.741526	MW
Condenser duty(C1)	18.245788	MW
Condenser duty(C2)	37.115258	MW
Capital cost	8019529	USD
TAC	12101668	$/y

2.4.DWC Process

In order to address the drawbacks associated with using CDC to separate the ternary mixture of n-Pentane, n-Hexane, and n-Heptane - which include high energy consumption, TAC, exergy loss (El), and CO_2 emissions - this study introduced the divided wall column as a solution. DWC can product high purity in the one column with the one reboiler and one condenser. (Figure 5) illustrated the DWC structure. N-Pentane was separated as distillate, n-Heptane bottom product and n-Hexane as side stream. The presence of walls in these types of columns has increased the freedom of the system and also complicated the design of these types of towers compared to conventional towers. Research on the design and physical implementation of DWC has received attention in recent years. One of the ways to reduce the investment cost for setting up thermally coupled column is to use a DWC tower instead of the Petlyuk column. If the heat transfer through the wall is not taken into account, this particular tower is essentially the same as the Petlyuk tower from a thermodynamic perspective. (Cui, Zhang et al. 2020). DWC efficiency is significantly affected by degrees of freedom. Important design parameters (degrees of freedom) include the reflux ratio, the quantity of stages in every section, the feed stage, the side draw position, the amount of heat supplied to the reboiler, the rate at which side products flow, and vapor and liquid split ratios. These parameters are the basic requirement of an accurate simulation (Buitimea-Cerón, Hahn et al. 2021). The existence of 12 degrees of freedom in the configuration of fully thermally coupled distillations and DWCs has caused complexity in the design of these types of towers (Kiss and Rewagad 2011). Selecting the column configuration, thermodynamic model and operating pressure is the first step in designing a DWC column. The second step is to choose detailed models or shortcut models to optimize the equipment sizing and system control. A suitable initial guess of the design parameters and some guidelines are necessary for the convergence of the simulation (Dejanović, Matijašević et al. 2011, Di Pretoro, Ciranna et al. 2021). Triantafyllou and Smith disseminated the first DWC design based on a minimum reflux ratio, minimum number of equilibrium stages, feed stage, and number of stages (FUGK) (Tavan, Shahhosseini et al. 2014, Di Pretoro, Ciranna et al. 2021). Long N et al (Long, Lee et al. 2010) investigated the purification process of acetic acid and focus on the design of DWC. They proposed the interior recycle flow around the wall as the main optimization variable. Later, Seihoub F Z et al. (Seihoub, Benyounes et al. 2017) In their work to improve the shortcut design approach, while using Underwood's and Gilliland's equations, presented an accurate model for the design of each section of the DWC.

2.4.1. Optimal Steady-State Processes

In this study, the optimal design of the DWC was achieved using the Sequential Quadratic Programming (SQP) method integrated with Aspen Plus's sensitivity analysis tool. SQP is a well-established, robust approach for addressing nonlinearly constrained optimization problems (Wu, Zhang et al. 2020). These SQP techniques have been extensively applied throughout chemical engineering, demonstrating clear benefits. This study focuses on optimizing the process to minimize the total reboiler duty, as defined below:

$$Min(Q) = f\,(N_T,\, N_F,\, N_{SS},\, N_{DWS},\, N_{DWC},\, V,\, RR,\, r_V,\, r_L)$$

$$Subject\ to\ \overrightarrow{y_m} \geq \overrightarrow{x_m}$$

The optimization variables consisted of the total stage count (N_T), feed stage (N_F), side-draw location (N_{SS}), dividing wall dimensions (N_{DWS})

and position (N_{DWC}), boilup rate (V), reflux ratio (RR), and the vapor and liquid splits (r_V,r_L). The vectors y_m and x_m represent the actual and target purities for the mproducts, respectively (Wu, Zhang et al. 2020). Temperature and liquid composition profiles for the DWC unit are illustrated in (Figure 7), while the optimal design values are summarized in (Table 2).

In the simulation, the DWC process was optimized. The total number of stages including reboiler and condenser is 46. The feed is fed at Stage 12 in the prefractionator column. Apparently the most important issue in the Petlyuk column in simulation is the definition of stages where the two liquids and two vapors leave and enter the main column prefractionator column. Two streams leave, including one vapor at the bottom and one liquid at the top of the prefractionator. The vapor streams at 1 stage leave prefraction section and inter at 10 stages in the main column. The liquid streams at 24 stages leave bottom of the prefractionator and go 34 stages in the main column. On the other hand, two streams of liquid and vapour from trays 9 and 34, respectively, leave the main tower and enter trays 1 and 24 of the prefraction column. The purities of n-pentane, n-hexane, and n-heptane products meet the required criteria, with purity levels of 99.8%, 99.9%, and 99.6% respectively.

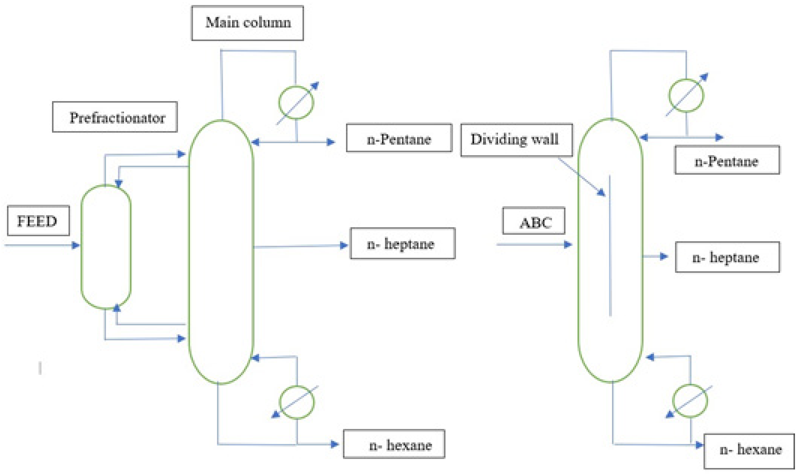

Figure 6: Petlyuk Configuration and DWC Configuration

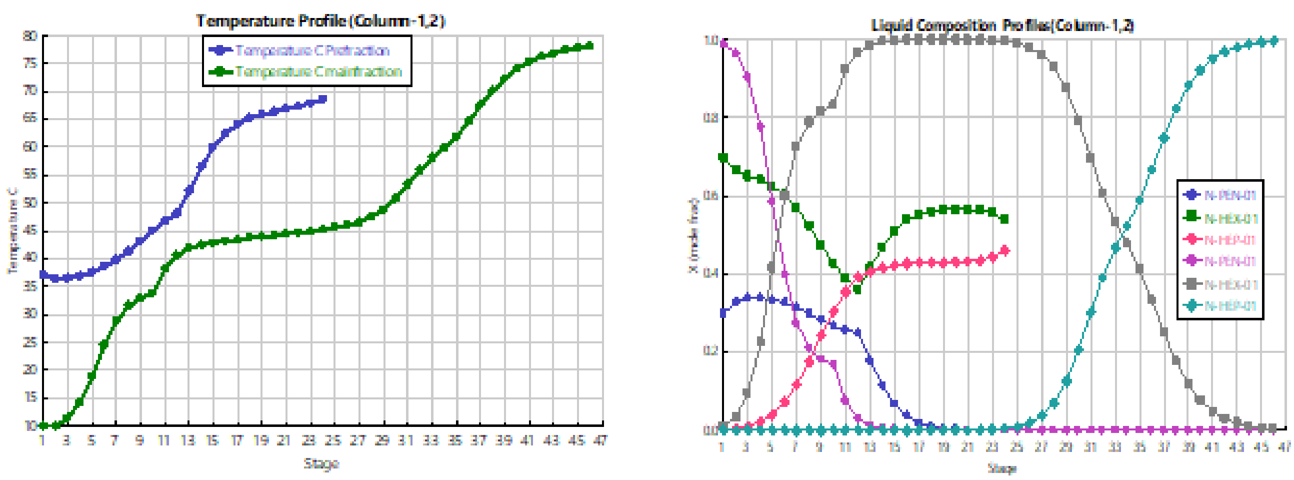

Figure 7: Temperature and Composition Profiles in the Dividing Wall Column

Table 2: Optimal Design Parameters of Dividing Wall Column

Design parameters	Value	Unit
Flow rate of feed stream	3600	Kmol/h
Feed compositions		
n-Pentane. n-Hexane and n-Heptane	0.3: 0.3 :0.4	_
Vapor Fraction	0	_
Pressure of feed stream	1	atm
Operating pressure	0.9	atm
Column diameter	8.83	m
Number of stages pre-fractionator side	24	_
Total number of stages DWC	70	_
Feed stage pre- fractionator side	12	_
Side stream withdrawal stage	20	_
Distillate rate	0.289948288	Kmol/sec
Reflux ratio	8.59	mol/mol
n-Pentane product purity	99.8	%wt
n-Hexane product purity	99.9	%wt
n- Heptane product purity	99.6	%wt
Reboiler duty	39.126925	MW
Condenser duty	36.201479	MW
Capital cost	4591648	USD
TAC	7329911	$/y

3. Results and Discussion

3.1. Simulation Results

3.1.1. Composition Profiles and Temperature Profiles

In distillation, the difference in boiling point and relative volatility causes the concentration of components in the trays to be different. Investigating the concentration of the ingredients on the trays can be helpful because it can be found in the maximum concentration of one the creator of a side stream removed that creator from the corresponding tray. In the conventional distillation column, N-pentane is released from the top of the first tower. Therefore, it is expected that its concentration is higher at the top of the column. The concentration of the middle component reaches the maximum in the first column under the feed tray and then decreases at the bottom of the column. Such an effect is known as remixing and causes more energy consumption (Figure 4-5). To re-purify the binary mixture N-Hexane, and N-Heptane in the second column through conventional distillation, the process will necessitate additional energy. This remixing can be viewed as a thermodynamic inefficiency in energy utilization. Finally, two other components leave the bottom of the first tower and enter the second tower as feed. (Figure 6) shows the concentration distribution of three key components in the pre-separator tower of the Petlyuk column. The light key component moves to the upper trays of the prefraction tower and its concentration decreases in the lower feed trays and its concentration becomes zero at the bottom of the column. The intermediate component is distributed almost continuously throughout the prefraction tower. In this tower, the phenomenon of remixing has wholly disappeared. The range of changes in the concentration of the intermediate material in the prefraction tower is minimal, and the intermediate material is appropriately distributed, distributed correctly in the prefraction column. In the main column of the dividing wall column, N-Pentane naturally moves to the top of the tower because it is lighter. Its amount reaches the desired level in the trays at the top of the tower, and it is removed in the upstream product, and as we move to the bottom of the tower, the concentration of this component decreases to zero arrives. Hexane is taken from the middle trays of the tower, so naturally, the concentration of this component reaches its maximum in the middle trays and tends to zero in the upper and lower trays of the tower. N-Heptane as a heavy substance in the tower moves to the lower trays until it reaches the desired concentration in the lowest tray. Its amount in the upper trays of the tower decreases until it reaches zero. In the DWC, the recycling streams can effectively minimize remixing and reduce the energy needed for ternary separations.

The temperature distribution in both the main and prefraction columns, as illustrated in (Figure 7), suggests that the temperature difference from the top to the bottom of the prefraction column falls within the range of the temperature difference in the main column, a logical finding. The temperature profile in a Dividing Wall Column (DWC) is a key defining characteristic due to its reflection of complex internal heat and mass transfer processes across both the pre-fractionator and the main column side. Given the integration of two columns within a single shell in a DWC, the temperature profile is not represented by a simple linear or sigmoidal curve; instead, it is a coupled distribution where the temperatures in the prefractionator section need to closely align with their counterparts in the main column sections to minimize entropy production and maximize energy efficiency. In the context of this ternary separation simulation involving N-pentane as the light element, N-hexane as the intermediate element, and N-heptane as the heavy element, it is noteworthy that the temperature profile typically exhibits three distinct segments.

The top section of the distillation column, known as the Rectifying Zone, follows a typical temperature profile where it begins at the boiling point of the lightest component (N-Pentane) and gradually increases towards the feed stage. In the Dividing Wall Zone, the profile takes on a unique characteristic. Within the Prefractionator Side, the temperature profile is influenced by the feed composition with a steeper gradient observed when the feed is rich in the intermediate component (N-Hexane). On the Main Column (Side Stream) Side, the temperature profile must align with the side-draw product, ideally reaching the boiling point of the pure intermediate component (N-Hexane) at the side-draw tray. Finally, in the Bottom Section or Stripping Zone, the temperature steadily rises until it reaches the boiling point of the heaviest component (N-Heptane) at the reboiler.

3.2. Process Comparison

The total annual cost, thermodynamic efficiency and energy consumption were used to analyze predomination of DWC instead of conventional column based on performance quantification method. (Table 3) illustrates the economic comparison results of traditional columns of distillation and DWC processes.

3.2.1. Comparisons of Economic and Energy Cost

The Total Annual Cost (TAC), calculated using Eq. (1), serves as a benchmark for assessing the economic viability of each of the two configurations.

$$TAC = Energy\ cost + Capital\ cost \div 3 \quad (1)$$

The analysis incorporates operating costs (OPEX) derived from utility expenses (as previously calculated) and an assumed operational lifespan of 8000 hours per year. Capital expenditures (CAPEX) for the distillation columns are established using design parameters.

The detailed calculations are presented in (Tables 1-2), while the evaluation criteria are visually compared in (Table 3). (Table 1-2) demonstrate that the purity levels of N-Pentane, N-Hexane, and N-Heptane were all consistently high at 99.0% in both setups. Looking at (Table 3), the total condenser duty and reboiler duty for the traditional distillation column and DWC were 55.37MW, 63.61MW, and 36.2MW, 39MW, respectively. The total annual cost (TAC) for the direct distillation sequence and DWC were $12,101,668/year and $7,329,911/year, respectively. These findings indicate that the energy consumption in the conventional distillation column setup was significantly greater than that in the DWC configuration, making the latter a more suitable option for separating the ternary system. The findings indicate that in dividing wall columns, there is a decrease in investment costs attributed to fewer column vessels, reboilers, and condensers. Moreover, energy consumption is significantly lowered as a result of reduced back-mixing within this tower configuration, leading to decreased energy expenses and carbon dioxide emissions.

The energy conservation level serves as an additional measure for assessing DWC compared to conventional two-column distillation. We utilize the following formula to determine the decrease in energy usage as a percentage (Li, Zhang et al. 2020):

$$Energy\ saving\ rate\ (\%) = \frac{Q_{reb,CD} - Q_{reb,DWC}}{Q_{reb,CD}} \times 100 = 38\%$$

Limited research has been conducted on ternary LNG mixture separation using direct thermal coupling. Mostofian et al. (Mostofian, Noori Keshtkar et al. 2023) recently investigated the energy consumption and exergy loss during the separation process of n-pentane, n-hexane, and n-heptane. Their findings indicated a 69% reduction in energy consumption and a 55% decrease in exergy loss with the use of direct thermal coupling.

Table 3. Comparison of the Two Configurations in Condenser and Reboiler Duties

Flow Regime	Conventional distillation column		DWC
Condenser duty (MW)	C1=18.255788	C2=37.115258	36.201479
Reboiler duty (MW)	C1=25.870284	C2= 37.741526	39.126925
TAC($/y)	**12101668**		**7329911**

4. Conclusion

Distillation is a physical separation process based on the difference in the boiling points of compounds. Studies have shown that almost 5% of the world's energy is spent on distillation towers. The increase in energy costs, the production of greenhouse gases, the reduction of natural resources, and the pressure on the natural gas industry have led researchers to look for a suitable solution. One of the practical solutions is process intensification. Thermally coupled distillation columns (Petlyuk) have been introduced as advanced distillation technology and the best alternative for process intensification.

In this research, a conventional distillation column and a DWC process were utilized to separate and purify a mixture of N-Pentane, N-Hexane, and N-Heptane hydrocarbons. The study used three distillation columns based on the FUGK model to determine initial design parameters for the DWC. Subsequently, the Sequential Quadratic Programming optimization method and Aspen Plus efficient sensitivity analysis tool were employed to minimize the total reboiler and condenser duties. The findings demonstrated that adopting the DWC configuration led to significant improvements in side product purity, energy efficiency, total annual cost (TAC) reduction, and a decrease in CO_2 emissions by 37% and 38% respectively compared to traditional distillation columns. The advantages of this new technology are reducing energy consumption, reducing investment costs, high thermodynamic efficiency, and reducing the required space. The superior performance and compact design of the proposed process set it apart from other methods.

Appendix A. Column Cost Correlations

Total annual cost (TAC) was calculated as follows:

(A)Capital cost

Luyben method was applied (Luyben, 2006). The cost of a distillation column was mainly made up of the investment of the column vessel and heat exchangers. The cost of trays was usually small compared to the cost of the vessel and heat exchangers and was neglected.

$$L = 1.2\times 0.61\times (N-2) \qquad (A.1)$$

$$Shell = 17640 \times D^{1.066}\times L^{0.802} \qquad (A.2)$$

$$Ar=qr\times 1.055\times 2.54\times exp(6)\div 3600\div 0.7457\div dtr\div ur \qquad (A.3)$$

$$Ac=qc\times 1.055\times 2.54\times exp(6)\div 3600\div 0.7457\div dtr \div ur \qquad (A.4)$$

$$Hx=7296 \times (Ar^{0.65}+ Ac^{0.65}) \qquad (A.5)$$

$$Capital\ cost = shell + Hx \qquad (A.6)$$

where L, D were the length and diameter of the column, respectively, both with unit of meters. Shell with unit of $ was the cost of the column vessel. Ar and Ac were the heat transfer areas of the reboiler and the condenser, respectively and their unit was m^2. qr and qc were the heat duty of the reboiler and the condenser, respectively, both with unit of MW. dtr and dtc were the differential temperature in the reboiler and the condenser, respectively, both with unit of K. ur and uc were heat transfer coefficients of the reboiler and the condenser, respectively, and their unit was Kw/K. m^2. Hx was the capital cost of heat exchangers with a unit of $.

(B)Energy cost

$$Energy\ cost = qr\times 4.7\times 3600\times 24\times 365\div 1000 \qquad (B.1)$$

(C)Total annual cost (TAC)

$$TAC = Energy\ cost + Capital\ cost \div 3 \qquad (C.1)$$

References

Andrade, N., M. Andrade, M. Rebouças, R. Brito and K. Brito (2024). "Intensification proposals for the downstream separation of the methanol-to-olefins process." Chemical Engineering and Processing-Process Intensification 196: 109639.

Asprion, N. and G. Kaibel (2010). "Dividing wall columns: Fundamentals and recent advances." Chemical Engineering and Processing: Process Intensification 49(2): 139-146.

Battisti, R., R. A. F. Machado and C. Marangoni (2020). "A background review on falling film distillation in wetted-wall columns: From fundamentals towards intensified technologies." Chemical Engineering and Processing - Process Intensification 150: 107873.

Biasi, L. C., R. J. Zemp, F. R. Batista and A. J. Meirelles (2024). "Novel distillation column retrofit combining energy integration and different tray designs." Chemical Engineering and Processing-Process Intensification 196: 109640.

Buitimea-Cerón, G. A., J. Hahn, N. Medina-Herrera, A. Jiménez-Gutiérrez, J. A. Loredo-Medrano and S. Tututi-Avila (2021). "Dividing-Wall Column Design: Analysis of Methodologies Tailored to Process Simulators." Processes 9(07): 1189.

Cui, C., Q. Zhang, X. Zhang and J. Sun (2020). "Eliminating the vapor split in dividing wall columns through controllable double liquid-only side-stream distillation configuration." Separation and Purification Technology 242: 116837.

Czarnecki, N. J., L. Giannetti, S. A. Owens, S. Barnicki and R. B. Eldridge (2024). "Energy and Economic Evaluation of Wall Placement for Divided Wall Distillation Columns." Industrial & Engineering Chemistry Research 63(43): 18513-18524.

Dejanović, I., L. Matijašević, I. Halvorsen, S. Skogestad, H. Jansen, B. Kaibel and Ž. Olujić (2011). "Designing four-product dividing wall columns for separation of a multicomponent aromatics mixture." Chemical Engineering Research and Design 89(8): 1155-1167.

Di Pretoro, A., F. Ciranna, M. Fedeli, X. Joulia, L. Montastruc and F. Manenti (2021). "A feasible path-based approach for Dividing Wall Column design procedure." Computers & Chemical Engineering 149: 107309.

Halvorsen, I. J. and S. Skogestad (2011). "Energy efficient distillation." Journal of Natural Gas Science and Engineering 3(4): 571-580.

Kiss, A. A. and R. R. Rewagad (2011). "Energy efficient control of a BTX dividing-wall column." Computers & Chemical Engineering 35(12): 2896-2904.

Kolbe, B. and S. Wenzel (2004). "Novel distillation concepts using one-shell columns." Chemical Engineering and Processing: Process Intensification 43(3): 339-346.

Lavasani, M. S., R. Rahimi and M. Zivdar (2018). "Response surface methodology in optimization of a divided wall column." Korean Journal of Chemical Engineering 35: 1414-1422.

Li, C., Q. Zhang, J. Xie, J. Fang and H. Li (2020). "Design, optimization, and industrial-scale experimental study of a high-efficiency dividing wall column." Separation and Purification Technology 247: 116891.

Li, G., S. Guan, Y. Gao, W. Liu, Y. Zheng, H. Pan, L. Zhu and H. Ling (2024). "Evaluation of multi-objective optimization methods applied to ternary dividing-wall columns." Chemical Engineering Research and Design 203: 573-582.

Li, H., T. Li, C. Li, J. Fang and L. Dong (2019). "Reactive dividing-wall column for the co-production of ethyl acetate and n-butyl acetate." Chinese Journal of Chemical Engineering 27(1): 136-143.

Li, Q., A. J. Finn, S. J. Doyle, R. Smith and A. A. Kiss (2023). "Synthesis and optimization of energy integrated advanced distillation sequences." Separation and Purification Technology 315: 123717.

Liu, Z., X. Zhao, J. Zhang, Z. Du and J. Wang (2022). "Optimization of EB/SM Distillation Processes Based on Divided Wall Columns in a PO/SM Process with a Chaos Differential Evolution Algorithm." ACS omega 7(6): 5471-5484.

Long, N. V. D., S. Lee and M. Lee (2010). "Design and optimization of a dividing wall column for debottlenecking of the acetic acid purification process." Chemical Engineering and Processing: Process Intensification 49(8): 825-835.

Mehrpooya, M., A. Vatani and S. A. Mousavian (2010). "Introducing a novel integrated NGL recovery process configuration (with a self-refrigeration system (opençclosed cycle)) with minimum energy requirement." Chemical engineering and processing: process intensification 49(4): 376-388.

Mostofian, T., M. Noori Keshtkar and S. Ebrahimi (2023). "Exergy Analysis and Heat Integration of Distillation Columns Using Thermal Coupling Method for Separation of Ternary Mixture." Chemical Process Design 2(1): 72-81.

Rçnger, L.-M., I. J. Halvorsen, T. Grützner and S. Skogestad (2025). "What can go wrong in a dividing wall column and how to detect it." Separation and Purification Technology 354: 129151.

Schultz, M. A., D. G. Stewart, J. M. Harris, S. P. Rosenblum, M. S. Shakur and D. E. O'BRIEN (2002). "Reduce costs with dividing-wall columns." Chemical engineering progress 98(5): 64-71.

Seihoub, F.-Z., H. Benyounes, W. Shen and V. Gerbaud (2017). "An improved shortcut design method of divided wall columns exemplified by a liquefied petroleum gas process." Industrial & Engineering Chemistry Research 56(34): 9710-9720.

Shahruddin, M. Z., M. H. F. M. Uzuman, R. M. Zin, T. A. T. Mohd, M. K. Abd Hamid and R. Handogo (2025). "Process Feasibility Study of Energy Integrated Distillation Columns Sequence (EIDCS) for NGL Separation Process." Journal of Advanced Research in Fluid Mechanics and Thermal Sciences 132(1): 65-75.

Shi, X., X. Zhao, Z. Zhang, M. Li and J. Gao (2020). "Energy-saving quaternary extractive distillation processes with single-or double-dividing-wall column for separation of acetone/methanol/butanone/tert-butyl alcohol." Chemical Engineering and Processing-Process Intensification 153: 107999.

Song, Z.-w., W. Cui, Y.-y. Wu, B. Wu, K. Chen and L.-j. Ji (2024). "Energy, exergy, economic, and environmental analysis of a novel liquid-only transfer dividing wall column with vapor recompression." Separation and Purification Technology 329: 125122.

Tavan, Y., S. Shahhosseini and S. H. Hosseini (2014). "Design and simulation of ethane recovery process in an extractive dividing wall column." Journal of cleaner production 72: 222-229.

Wang, M., E. Song, L. Li, Y. Zhang and E. Wang (2023). "Application of dividing wall column in azeotropic distillation with intermediate boiling-point heteroazeotrope: Simulation and optimization." Chemical Engineering Research and Design 189: 384-400.

Wu, Y., G. Zhang, J. Xu, X. Qu, Z. Wang, T. Wang, K. Chen and L. Ji (2020). "Enhanced separation of mixing diols by distillation in dividing wall column." Chemical Engineering and Processing-Process Intensification 149: 107859.

Yildirim, Ö., A. A. Kiss and E. Y. Kenig (2011). "Dividing wall columns in chemical process industry: A review on current activities." Separation and Purification Technology 80(3): 403-417.

Yuan, Y., L. Zhang, G. P. Rangaiah, G. Wang, X. Qian and L. Samavedham (2024). "Design and optimization of compound distillation sequences comprising simple distillation and dividing-wall columns using genetic programming." Chemical Engineering Science 291: 119950.

JOURNAL OF GAS TECHNOLOGY

Volume 10 / Issue 2 / Winter 2025 / Pages 21-42

Journal Home page: https://jgt.irangi.org

Scenario-Based Assessment of CCUS Deployment Pathways for Carbon Emission Reduction in Iran's Energy-Intensive Industries Using an AHP Framework

Sobhan Herfat[1], Majid Zandi[2*]

1. Ph.D. Student, Renewable Energy Department, Energy Research Center, Faculty of Energy, Shahid Beheshti University, Tehran, Iran
2. Associate Professor, Renewable Energy Department, Energy Research Center, Faculty of Energy, Shahid Beheshti University, Tehran, Iran

ARTICLE INFO

ORIGINAL RESEARCH ARTICLE

Article History:
Received: 19 September 2025
Revised: 03 October 2025
Accepted: 29 November 2025

Keywords:
CCUS
Industrial transition
Analytic Hierarchy Process (AHP)
Deployment pathways

DOR: 20.1001.1/jgt.2026.2087200.1069

ABSTRACT

Iran's industrial transition toward carbon emission reduction technologies, particularly Carbon Capture, Utilization, and Storage (CCUS) technology systems, has been considered in recent years a strategic axis for promoting environmental sustainability and enhancing the efficiency of energy-intensive industries. This study analyzed potential deployment patterns of CCUS technologies by examining three development approaches: gradual, accelerated, and Hybrid Scenarios (HS). The gradual scenario focuses on phased development and the reduction of initial risks; the accelerated scenario seeks the rapid deployment of CCUS infrastructure through extensive investment and policy support; and the HS attempts to provide a sustainable and manageable industrial process by balancing costs, risks, and reliability. In addition, this study examines the technical, economic, and policy challenges associated with CCUS implementation and proposes implementation strategies, including the formulation of supportive policies, the development of CO_2 transport and storage infrastructure, technological capacity building, and the strengthening of public–private partnerships. To evaluate the different pathways, an AHP-based hierarchical model was used to analyze the performance of CCUS applications in power plants, industrial facilities, and refineries using six main indicators: cost, technological attractiveness, technological capability, cultural index, passive defense, and environmental criteria. The results show that the CCUS option achieves the highest scores across all three applications and represents the most efficient option for emission reduction and economic value creation. These findings reinforce the importance of the planned development of CCUS in the country's energy landscape and highlight the need to establish support mechanisms for its commercialization and the expansion of industrial applications.

How to cite this article
S. Herfat, M. Zandi. Scenario-Based Assessment of CCUS Deployment Pathways for Carbon Emission Reduction in Iran's Energy-Intensive Industries Using an AHP Framework. Journal of Gas Technology. 2025; 10(2): 21-42. (https://jgt.irangi.org/article_737845.html)

* Corresponding author.
E-mail address: m_zandi@sbu.ac.ir, (M. Zandi).

Available online 30 December 2025
2588-5596/© 2016 The Authors. Published by Iranian Gas Institute.
This is an open access article under the CC BY license. (https://creativecommons.org/licenses/by/4.0)

1. Introduction

The use of fossil fuels is a major contributor to the production and emission of greenhouse gases. The increasing concentration of greenhouse gases (GHG) in the atmosphere enhances the absorption of infrared radiation emitted from the Earth's surface, thereby leading to global warming. Carbon dioxide (CO_2) is one of the most significant greenhouse gases and plays a crucial role in climate change (Vaddeboina & Puttapati, 2024).

Most of the CO_2 is produced by the energy sector. Therefore, given the growing demand for energy consumption to support global economic development, reducing CO_2 emissions and mitigating climate change require careful consideration. However, with continuously increasing global energy consumption, the limited availability of fossil fuel resources, and rising levels of environmental pollution, it has become essential to replace conventional approaches with innovative methods for utilizing primary energy sources. The application of CO_2 capture technologies is one of the approaches that has been extensively investigated by researchers in recent years (Nath et al., 2024). (Figure 1 shows the CO_2 emission chart and its share in different regions of the world between 1750 and 2024).

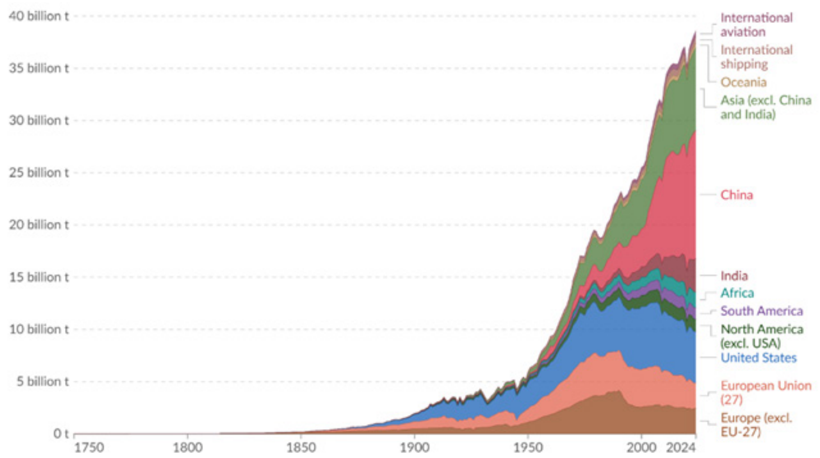

Figure 1. the CO_2 Emission Chart and its Share in Different Regions of the World Between 1750 and 2024 (Our World in Data, 2025)

(Figure 1) traces the evolution of annual CO_2emissions by region between 1900 and 2024 and highlights the major shift in the global distribution of emissions over time. In 1900, global CO_2 emissions reached approximately 1.96 Gt. Emissions were heavily concentrated in Europe and North America. The EU 27 accounted for about 0.71 Gt (36 %), and the United States contributed nearly 0.66 Gt (34 %). Non EU European countries added another 0.49 Gt. Together, Europe and North America dominated global emissions at the start of the twentieth century. At that time, China and India contributed only marginal shares. Emissions rose rapidly during the first half of the century, reaching 5.93 Gt by 1950. The United States then became the largest emitter, producing around 2.54 Gt – equivalent to 43 % of the global total. The EU 27 and non EU Europe remained major contributors, at roughly 1.28 and 1.10 Gt, respectively. In contrast, emissions from both China and India remained below 0.1 Gt each.

A more pronounced geographical shift occurred after 2000. Although the United States remained the largest emitter at that time, with emissions of about 6.02 Gt CO_2, China had already reached 3.64 Gt CO_2, nearly matching the EU-27 at 3.60 Gt. Emissions from the rest of Asia also increased substantially during this period, reflecting rapid industrialisation and economic growth across the region. By 2024, China had become the dominant global emitter, producing approximately 12.29 Gt CO_2, or nearly one-third of total global emissions. Emissions from the United States declined to around 4.90 Gt CO_2, while India increased to approximately 3.19 Gt. At the same time, both the EU-27 and non-EU Europe showed a gradual downward trend, each falling to nearly 2.4 Gt CO_2. Another noticeable change is the growing contribution of international aviation and shipping, which together accounted for more than 1 Gt CO_2 in 2024. Overall, the figure reflects the long-term transition of global emissions from a predominantly Western pattern toward one increasingly centred in Asia, particularly China.

The main program for capturing CO_2 gas is from large producers of this gas, such as power plants, industries, and oil refineries. Capturing CO_2 gas from small and mobile sources in the transportation sector, as well as residential and commercial buildings, is significantly more difficult and costly than capturing it from large-scale emitters. Therefore, it is often overlooked, and the focus is generally on separating gas from large CO_2 emitting sources (Shi & Hu, 2025). An alternative approach to preventing CO_2emissions from these small sources is the use of cleaner energy carriers, such as hydrogen and electricity produced in fossil fuel-based power plants or using renewable energy sources. Owing to concerns about climate change and the gradual warming of the Earth, numerous carbon capture and storage (CCS) projects are currently being implemented worldwide (Alizadeh et al., 2024).

2. Review of Previous Research

(Table 1) lists some previous studies.

Table 1. Review of Some Previous Research

Authors	Focus / Methodology	Key Findings / Conclusions	Reference
Keith et al.	Engineering design and techno-economic assessment of an industrial-scale direct air capture (DAC) facility	Estimated the levelized cost of CO_2 capture and identified the energy and material requirements for capture and regeneration cycles	(Keith et al., 2018)
Bachu	Analysis of geological CO_2 storage options with emphasis on the storage component	Demonstrated that although geological reservoirs have high storage capacity potential, long-term success depends on proper site selection, effective capture mechanisms, and reliable monitoring systems	(Bachu, 2008)
Nagireddi et al.	Systematic review of CCUS technologies; comparison of CO_2 capture, storage, and utilization pathways	Concluded that large-scale deployment of CCUS technologies is not feasible without significant cost reductions and the development of CO_2 transport and storage infrastructure	(Nagireddi et al., 2024)
Wilberforce et al.	Review of recent advances in CO_2 capture technologies	Emphasized that reducing energy requirements for CO_2 recovery and improving long-term operational sustainability are critical for economic viability	(Wilberforce et al., 2021)
Rosanali et al.	Feasibility assessment of CCUS facility installation using net present value methods	Showed how economic feasibility is strongly influenced by capital costs, operating costs, and discount rates	(Roussanaly et al., 2021)
Nink Konk et al.	Evaluation of CCUS technological reserves based on patent analysis	Assessed the state of technological development and innovation trends in CCUS using patent data	(Kang et al., 2021)
Lau et al.	Analysis of the role of CCUS in Singapore's energy transition	Highlighted the strategic importance of CCUS within national decarbonization and energy transition pathways	(Lau et al., 2021)

Jiang et al.	Policy cycle framework; analysis of China's CCUS policies across three Five Year Plans; comparison with US, Australia, Norway, Japan; evaluation of project data against the 2011 roadmap.	China has a relatively complete CCUS policy but lacks enforceable laws, has low operability, weak market incentives, and insufficient subsidies. Recommends legislation, better regulation, cross provincial cooperation, and green finance.	(Jiang et al., 2020)
Xu & Dai	Applies second best theory to justify CCUS as a necessary mitigation option. Analyzes market distortions (fossil path dependency, energy monopoly, externalities). Compares CCUS with renewables, efficiency, and afforestation. Reviews legal, economic, and social barriers.	CCUS is a second best choice due to renewable bottlenecks and fossil lock in. China has high storage potential (3120 Gt) but lacks specific laws, faces high costs, and low public acceptance. Recommends legislation, carbon tax, liability sharing, and public engagement.	(Xu & Dai, 2021)
Fan et al.	Bibliometric analysis of 968 Web of Science publications (2003 2024) using CiteSpace. Maps co citation networks, keyword clusters, and temporal evolution. Interprets findings through advocacy coalition framework (ACF) and multi level perspective (MLP) on socio technical transitions.	CCUS policy research has evolved through three phases: exploratory, expansion, and rapid growth. The existing literature focuses on several key areas. These include normative frameworks, macroeconomic support mechanisms, regulatory structures, financial incentives, and economic assessments. Nevertheless, significant gaps remain. For example, the Global South is underrepresented. Research collaboration remains fragmented. Moreover, social and institutional dimensions receive insufficient attention. Future work should integrate hydrogen and BECCS pathways. It should also explore digital technologies and participatory governance approaches.	(Fan et al., 2025)
Singh et al.	Employs Fuzzy Analytical Hierarchy Process (FAHP) to prioritise CCUS and renewable energy technologies for India's net zero carbon emission target by 2050. Four evaluation criteria are considered: cost, compatibility with existing and future energy mix, CO_2 reduction potential, and implementation time. Pairwise comparisons are converted into triangular fuzzy numbers with consistency ratio validation, complemented by Business As Usual (BAU) forecasting of energy demand and renewable generation from 1990 to 2050	CCUS demonstrates a substantially higher priority weight (0.981) compared to renewable energy (0.609), indicating that CCUS is the preferred technology for India given its coal dominated energy mix, relatively young coal power plant fleet, and land availability constraints for large scale solar and wind deployment. BAU projections reveal that renewable energy would meet only about 10% of India's electricity demand by 2050, necessitating sustained reliance on fossil fuels.	(Singh et al., 2025)
Xie et al.	LCA and levelized cost assessment of six coal chemical pathways (DCL, ICL, SNG, CTO, CTE, and CTM) with CCUS integration. Evaluation of EOR and DSA storage using carbon balance, transport network, and discounted cash flow analyses.	Without CCUS, carbon footprints range from 3.74 to 11.01 t CO_2/t product, with process emissions contributing over %85 of total emissions. CCUS reduces emissions by %65–36, while DSA storage shows higher mitigation performance than EOR. EOR storage costs range from 582–252 yuan/t, compared with 1,156–896 yuan/t for DSA storage. Raw material costs account for %76–55 of total expenditures.	(Xie et al., 2025)
Colombe et al.	Two-stage stochastic MILP model for CCUS infrastructure planning under policy uncertainty and investor risk aversion. Application to the Texas–Louisiana Gulf Coast considering CO_2 sources, saline aquifers, EOR sites, and pipeline networks.	Current 45Q incentives support economically viable near-term CCUS deployment, enabling nearly 300 Mt CO_2 capture even if incentives end after ten years. Policy uncertainty reduces expected CO_2 capture by up to 16% and has a greater effect than investor risk aversion. Increasing incentives improves capture deployment, although with diminishing returns.	(Colombe et al., 2024)

Although CCUS has been studied from various angles, the literature remains limited. Most studies focus on individual components, such as capture technologies, storage options, transportation, techno-economic performance, or environmental assessment, while fewer studies link these elements to deployment pathways and industrial transition. Some country-level studies have assessed CCUS options in relation to local capacity and national conditions, highlighting the importance of context-specific assessment. Building on this line of research, the present study examines CCUS deployment pathways for power plants, industries, and refineries in Iran, where the main question is not only which option is technically feasible, but also which pathway is more suitable under the current energy and industrial conditions of the country. For this purpose, gradual, rapid, and hybrid development scenarios are compared using an AHP-based multi-criteria decision-making framework.

2.1. Cost of Carbon Capture and Storage

The cost of carbon capture varies depending on the technology and industry, with estimates indicating that this cost ranges from 20 to 140 USD per ton of CO_2 in industrial settings (Adetoye et al., 2018). Some key variables for carbon capture and storage are as follows:

2.1.1. Cost of Carbon Capture and Storage Facilities

The cost of carbon capture in industrial settings, such as iron and steel, refining, pulp and paper, and Industries, ranges from 20 to 140 USD per ton of CO_2 (Adetoye et al., 2018).

2.1.2. Technological Variability: Different Technologies have Different costs

The reaction of CO_2 with amines has the highest costs, whereas calcium looping applied in the cement and pulp and paper industries has lower costs (Adetoye et al., 2018).

2.2. Examples of CCUS Facility Implementation Projects for Hydrogen Production (Blue Hydrogen)

Globally, the implementation of CCUS facilities is one of the most important processes related to clean energy production. Many countries are striving to develop blue hydrogen production to achieve carbon emission reduction goals and transition to sustainable energy. Information on some of these projects is given in (Table 2).

Table 2. CCUS Projects Information (IEA, 2023)

No.	Project Name	Country	Commissioning Year	Primary Feedstock	Technology	CO_2 Capture Capacity (t/year)	Hydrogen Production Capacity (t/year)
1	Port Arthur Project	USA	2013	Natural gas	SMR* +CCUS	900,000	117,700
2	Port Jerome Project	France	2015	Natural gas	SMR+CCUS	100,000	39,000
3	Quest Project	Canada	2015	Natural gas	SMR+CCUS	1,100,000	300,000
4	Sinopec Qilu Petrochemical CCS Project	China	2022	Coal	CCUS	1,000,000	Not reported
5	Al Reyadah CCUS Project (Phase 1)	United Arab Emirates	2016	Natural gas	CCUS	800,000	Not reported
6	Sapio-Mantova Project	Italy	2016	Natural gas	SMR+CCUS	Not reported	1,200

*. Steam Methane Reforming

3. Global and National Status

Numerous CCS projects are currently operational or under implementation worldwide. (Figures 2 and 3) together show that CCS deployment is still concentrated in a limited number of regions and applications. At the regional level, North America accounts for the largest share of operating CO_2 capture capacity, at about 51%, followed by Central and South America at 21%. Australia and New Zealand, Asia Pacific, and the Middle East each contribute relatively small shares, while Europe remains at only 5%. The planned 2030 portfolio is somewhat more distributed: North America still leads, but its share declines to around 45%, whereas Europe rises markedly to about 27%. This suggests that future projects are expected to be less concentrated than the current portfolio, although North America will remain the main hub.A similar pattern is observed by application. Natural gas processing is already the dominant category, representing 38% of operating facilities, and it is projected to increase to 65% in the planned portfolio. Hydrogen is the other notable growth area, rising from 12% to 28%. By contrast, power and heat, industry, direct air capture, and other fuel supply remain minor in both portfolios, each accounting for only about 1-2%. Taken together, the figures indicate that near-term CCS development is still anchored in natural gas processing and hydrogen, rather than in a broader expansion across power generation or direct air capture.

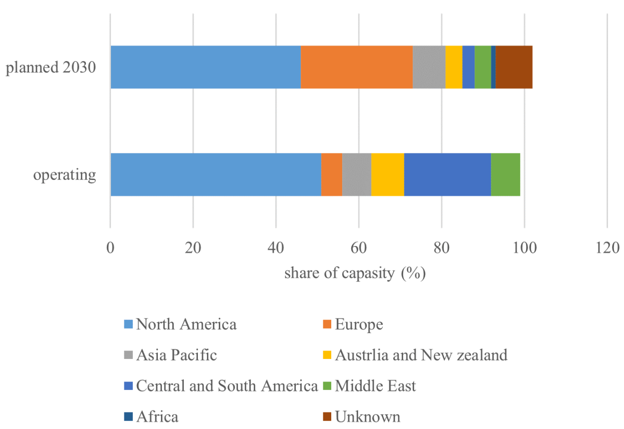

Figure 2. Operating and Planned CO_2 Capture Capacity by Region, Q1 2024 vs. 2030 (IEA, 2024)

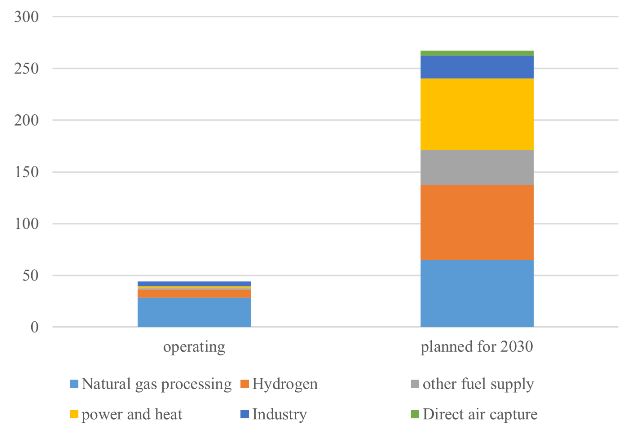

Figure 3. Operating and Planned Facilities with CO_2 Capture by Application (IEA, 2022)

3.1. National Status: Share of Different Sectors in CO_2 Emissions in Iran

The combustion of fossil fuels to produce heat or mechanical work for applications such as transportation fleets or power generation plants constitutes the largest part of energy system operations. During combustion, Carbon and Hydrogen atoms in fossil fuel molecules combine with atmospheric oxygen to form CO_2 and water (H_2O), releasing the chemical energy of the fuel in the form of heat. Carbon dioxide, as the most important product of combustion, plays a significant role in global warming; therefore, it is recognized as the most important greenhouse gas. (Figure 4) shows a clear rise in CO_2 emissions from fuel combustion in Iran over 2000-2025, although the increase is much stronger in some sectors than others. Electricity and heat production remained the main source of emissions during the whole period, increasing from roughly 75 Mt CO_2 in 2000 to more than 200 Mt CO_2 by 2025. The increase becomes noticeably steeper after 2018. This is likely related to the growing electricity demand and the continued dependence of the power sector on fossil fuels. Transport follows the same overall trend, with emissions rising from about 72 Mt to nearly 165 Mt CO_2. Compared with the power sector, however, the transport curve is more gradual and includes a few fluctuations during the mid-2010s. Residential emissions also increased considerably, reaching around 145 Mt CO_2 in 2025, which may reflect both population growth and higher household energy consumption. Industrial emissions show a similar pattern, particularly in the later years of the period, where the increase becomes more pronounced. In contrast, sectors such as Commercial and Public Services, Agriculture/Forestry, and Fishing remained relatively small contributors throughout the study period. Overall, the figure suggests that the recent growth in Iran's CO_2 emissions has been driven mainly by electricity generation, transport, and expanding energy demand in residential and industrial activities.

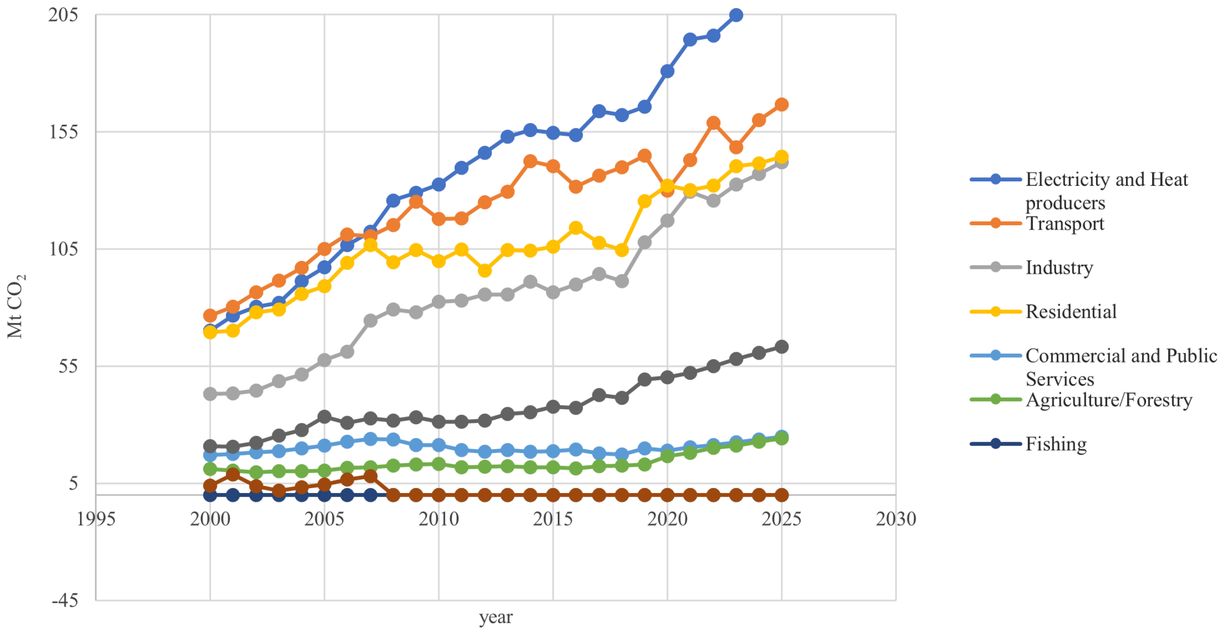

Figure 4. Trend of CO_2 Emissions (Due to Fuel Combustion) in Various Sectors from 2000-2025 (IEA, 2023)

(Figure 5) shows a clear imbalance in sectoral CO_2 emissions in 2025, with most emissions concentrated in a few major sectors. Electricity and Heat producers account for the largest share, reaching nearly 220 Mt CO_2. This value is substantially higher than all other sectors and reflects the continued dependence of the power sector on fossil-fuel-based electricity generation. Transport ranks second, with emissions close to 170 Mt CO_2, remaining about 50 Mt lower than the power sector but still considerably above the rest of the economy. The Residential sector contributes roughly 145 Mt CO_2, while Industry reaches nearly 140 Mt CO_2, indicating that energy consumption in households and industrial activities remains a major source of emissions. Together, these four sectors account for the overwhelming majority of total CO_2 emissions in 2025. In contrast, the remaining sectors contribute much smaller amounts. Commercial and Public Services remain below approximately 20 Mt CO_2, whereas Agriculture and Forestry stay near 25 Mt CO_2. Other energy industries contribute only around 10-15 Mt CO_2. The difference between these sectors and the major emitting sectors is considerable; for example, emissions from Electricity and Heat producers alone are almost ten times larger than those from Commercial and Public Services. This uneven distribution suggests that emission reduction policies in Iran will likely have the greatest impact if they focus primarily on electricity generation, transport, residential energy use, and industrial activities.

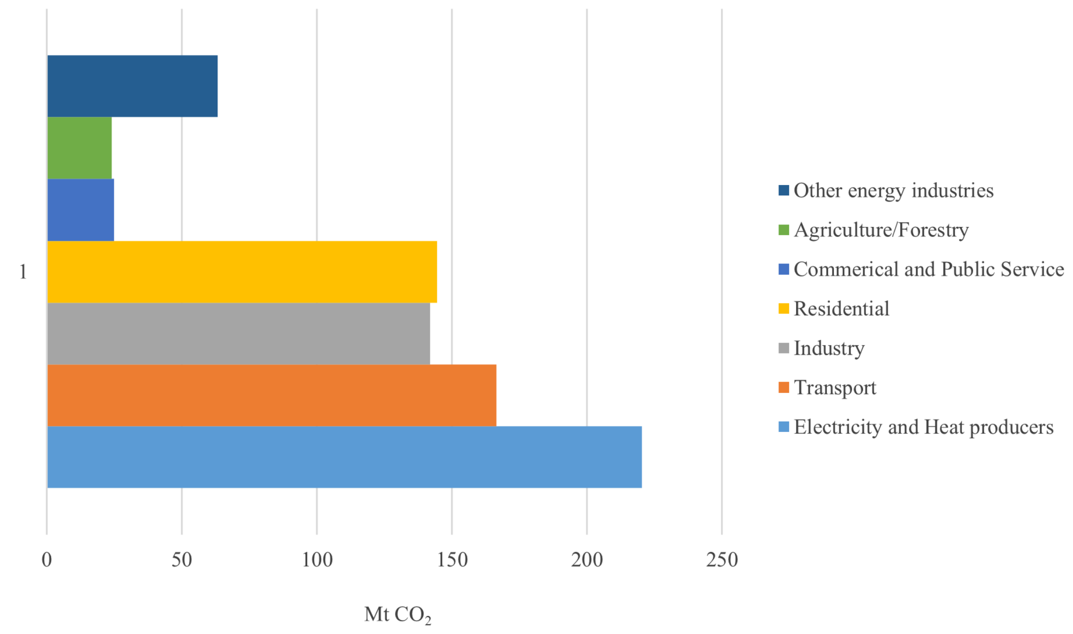

Figure 5. Share of each Consumption Sector in CO_2 Emissions (Due to Fuel Combustion) in 2025

4. Methodology

Designing decision-making scenarios for systems related to CCUS is one of the main pillars of strategic planning for reducing CO_2 emissions. In this section, the basis for designing scenarios is defined not in terms of the type of Hydrogen but in terms of the development and implementation pathways of CCUS technologies. Scenarios, as tools for analyzing technological, economic, and institutional uncertainties, enable the comparison of different industrial transition pathways based on CCUS.

4.1. Gradual CCUS Development Scenario

In this scenario, the deployment of carbon capture facilities begins in a phased manner and at a small scale. The initial focus is on natural gas-dependent industries and facilities with relatively simple integration capabilities using capture systems. The development of storage infrastructure is carried out as a pilot project, and after performance evaluation, scalability is achieved. The main feature of this scenario is the reduction of technological and economic risks through gradual learning and step-by-step system upgrades. This path is considered particularly suitable for countries with limited financial resources and institutional uncertainty.

4.2. Rapid CCUS Development Scenario

In this scenario, the focus is on the simultaneous and extensive development of CCUS facilities. Large-scale investments are being made in CO_2 transport infrastructure, geological storage reservoirs, and integrated industrial systems. The goal of this scenario is to achieve high capture and emission reduction capacities quickly. This path depends on the existence of stable policy frameworks, extensive financial support, and access to advanced technology.n

4.3. Hybrid CCUS Development Scenario

This scenario is a combination of the two previous paths, where gradual development in the short term is accompanied by targeted investments in the medium and long terms. In this approach, some industries enter the full CCUS phase, whereas other sectors are upgraded in stages.

The main strategy of this scenario is to balance the risk, cost, and speed of emission reduction. (Table 3) compares the three scenarios.

Table 3. Comparison of Three Scenarios

Scenario	Features	Drawbacks	Advantages
Scenario 1: Gradual CCUS Deployment	• Stepwise deployment of carbon-capture facilities; focus on pilot-scale and demonstration projects. • Limited concentration on large-scale industrial clusters. • Moderate pace of infrastructure development aligned with regulatory readiness and policy frameworks.	• Slower reduction of CO_2 emissions. • Longer time required to reach full capture capacity. • Dependence on stable policies and long-term investment guarantees. • Lower competitiveness compared to rapidly evolving international markets.	• Lower technological and economic risk. • Reduced need for large upfront capital expenditures. • Flexibility in adapting to industrial, political, and market conditions
Scenario 2: Rapid CCUS Development	• Accelerated investment and wide deployment of capture facilities across major industrial clusters. • Rapid development of CO_2 transport and storage networks. • Capability to implement CCUS in large point-source emitters.	• Requires extensive capital investment. • Higher technological and operational risks. • Possible regulatory and social-acceptance challenges. • Increased likelihood of market imbalance during early phases.	• Fast reduction of CO_2 emissions. • Quick alignment with global decarbonisation pathways. • Potential to establish competitive advantage in regional energy markets.
Scenario 3: Hybrid CCUS Development	• Combined use of CCUS, CCU, and CCS across major industrial sectors. • Integration with long-term decarbonisation programmes and large-scale projects. • Preservation of existing infrastructure while enabling CO_2 capture in hard-to-abate sectors.	• Increased system complexity; higher coordination requirements. • High capital intensity and long planning horizons. • Elevated risk of technological lock-in if alternatives emerge.	• Creates balance between cost, efficiency, and emissions reduction. • Supports diversification of carbon-management strategies. • Offers socio-economic flexibility for industries undergoing transition.

The gradual, rapid, and hybrid CCUS development scenarios are not treated as separate AHP alternatives. They are introduced to show how the carbon-management option may be implemented under different policy, financial, and technical conditions.

4.1.2. Multi-Criteria Decision-Making (AHP) Assessment for CCUS Pathways

AHP is a decision-making method developed by the American researcher A. L.AHP was proposed by Satty in the 1970s. AHP is a method that models and quantifies the decision-making process of experts regarding complex issues. The basic principle of the AHP method is to decompose the problem into different levels according to the nature of the problem and the overall goal, and then form the structure of an analytical model at several levels. In this study, the open-source software SuperDecisions, which includes the AHP and ANP models and sensitivity analysis, was used (Https://www.Superdecisions.Com).

4.2.1. Model Used

In this study, the AHP framework was applied to evaluate four technology options, including No CC, CCS, CCU, and CCUS, in the power plant, refinery, and industrial sectors. (Figure 6) presents the assessment structure developed for evaluating the implementation of CCUS in power plants for CO_2 capture. The hierarchical model was used to determine the most suitable CO_2 capture pathway in the three selected sectors based on the considered criteria and the results obtained from the AHP analysis. The gradual, rapid, and hybrid development scenarios defined earlier in the study were considered implementation approaches and were therefore not included as separate alternatives in the AHP model. The expert group consisted of industry owners, faculty members, industrial and academic experts, and PhD students affiliated with the Energy Research Center at Shahid Beheshti University.

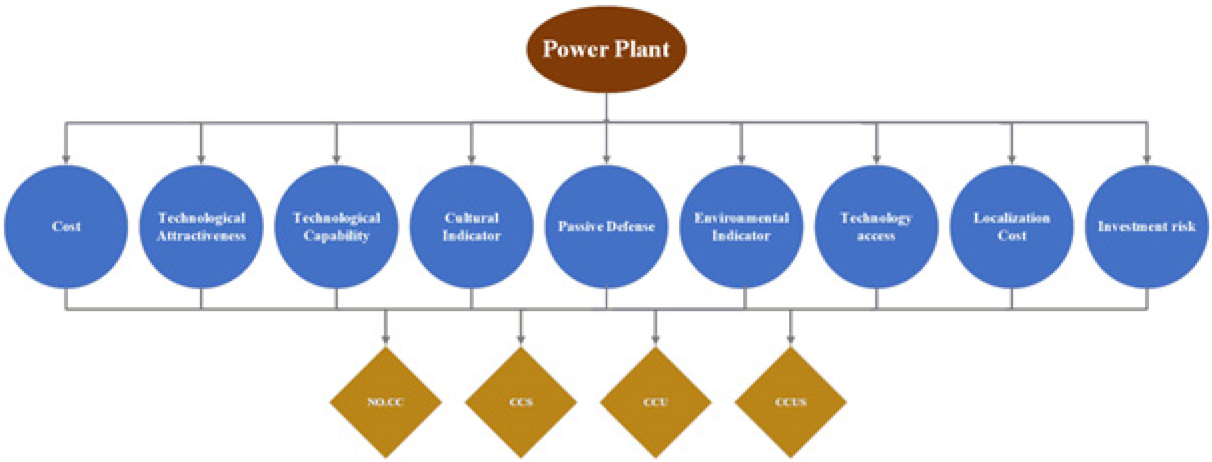

Figure 6. Power Plant Evaluation System Based on AHP

In this study, in the first stage, considering the characteristics of the power plant and various factors affecting its development, nine criterion indicators and four program evaluation indicators were used by the AHP method. The judgment criteria for the performance of a power plant's full-chain technical pathway can be divided into cost, technological attractiveness, technological capability, cultural, passive defense, and environmental indicators. These indicators were examined for four scenarios: No carbon capture (NO.CC), CCS, CCU and CCUS.

4.2.2. Criterion Indicators

This section describes the types of criterion indicators used in the AHP.

- Cost

The cost of goods means calculating the direct costs involved in producing a good or providing a service, which includes labor wages, raw materials, and manufacturing overheads.

- Technological Attractiveness

The strategic or operational importance of a technology for an organization or country determines investment priorities in the relevant sector.

- Technological Capability

Capability includes the level of mastery over technology, from operation to the creation of new methods of use.

- Cultural Indicator

The implementation of CO_2 capture technologies in society requires social acceptance, awareness of their dimensions, and the acceptance of existing risks by various social institutions. Studies show that currently, a small percentage of people, even in developed countries, are aware of CO_2 capture technologies in general, and of the risks associated with transmission lines and storage in particular (Praetorius & Schumacher, 2009). Without social acceptance, the processes of transport, utilization, and storage are likely to face opposition and protests from active non-governmental organizations.

- Passive Defense

In the context of this study, Passive Defense refers to the ability of a technology to improve energy-system resilience, limit vulnerability in critical infrastructure, and maintain stable operation in the face of external disruptions. The AHP assessment therefore focused on practical aspects such as robustness, continuity of operation, waste reduction, and resistance to sanctions and supply-chain constraints.

- Environmental Indicator

Many environmental concerns are related to the issue of CO_2 gas leakage from transmission lines and storage reservoirs. The leakage of this gas into the atmosphere causes climate change. Given the global climate change concerns, environmental concerns are the most important challenge for the commercialization of carbon capture, utilization, and storage technologies.

- Technology access

Access to technology is one of the main requirements for the implementation and development of CCUS. The deployment of these technologies depends not only on technical knowledge, but also on the availability of specialized equipment, industrial software, licenses, spare parts, and technical support services. In developing countries, especially under sanction conditions, limitations in technology transfer and restricted access to foreign suppliers can slow down project implementation and reduce operational reliability. For this reason, the level of access to technology can significantly influence the feasibility of CCUS projects and their long-term performance.

- Localization Cost

One of the major challenges associated with advanced carbon management technologies is the cost required for domestic development and implementation. Localization is not limited to manufacturing equipment; it also includes engineering redesign, pilot testing, adaptation to existing industrial infrastructure, workforce training, and the development of local technical capabilities. In countries facing external technological restrictions, a considerable part of the implementation process must rely on internal resources and domestic industries, which can increase overall project expenditures. Consequently, localization cost plays an important role in evaluating the economic viability of CCUS technologies.

- Investment risk

Large-scale CCUS projects generally require long-term investment and substantial financial support. However, economic uncertainty, fluctuations in exchange rates, changes in energy policies, and limitations in international financial cooperation can increase the risks associated with such investments. In addition, delays in technology deployment or uncertainty regarding future economic returns may reduce investor confidence and affect funding decisions. Under these conditions, investment risk becomes an influential factor in the selection and commercialization of carbon capture and utilization technologies.

5. Results and Discussion

This section examines the AHP results for the proposed facility and identifies the preferred carbon-management pathway in each sector. The analysis shows that the criteria were not equally weighted. In the first stage, the criterion indicators were defined, and in the second stage, the expert-group data were used to weight these indicators relative to one another. The intraclass correlation coefficient among experts was 0.825, indicating a stable and reliable level of agreement. The calculations were conducted for three application areas: power plants, industries, and refineries. These calculations were based on the assigned values of the criterion indicators and expert evaluations derived from existing strategies and plans. The previously defined deployment scenarios are then used to provide a practical interpretation of how the preferred options may be implemented under different economic, technological, and policy conditions in Iran.

5.1. Power Pla

Power Plant: Ministry of Energy and the private sector. The results of the power-plant system analysis are presented in (Figure 7). As illustrated, the CCUS alternative achieved the highest ideal priority value (1.000), indicating its superior preference and overall suitability among the evaluated options for the power generation sector. The CCS scenario ranked second with an ideal priority value 0.6529, followed by CCU with a value 0.4871. In contrast, the No.CC alternative exhibited the lowest priority value 0.1884. These findings reveal a strong preference toward integrated carbon management strategies in the power plant sector, particularly approaches incorporating carbon capture, utilization, and storage simultaneously. Furthermore, unlike the refinery and industrial sectors, where CCU demonstrated a relatively stronger position than CCS, the present results suggest that standalone carbon storage strategies are considered more favorable than utilization-oriented pathways in the power generation sector under the selected evaluation criteria.

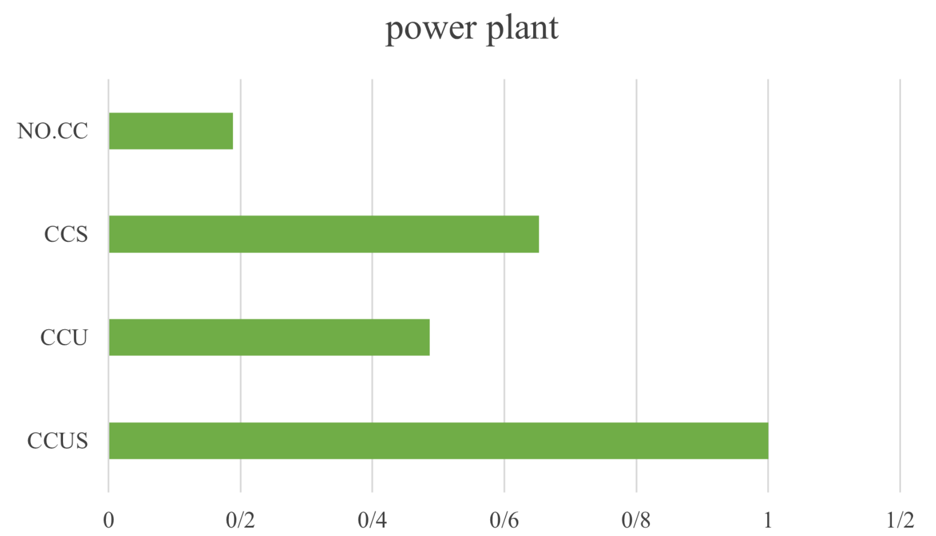

Figure 7. Ideal Priorities of Power Plant Sector Options Obtained from AHP

In this study, the discussion of stakeholders and custodians of different applications is raised differently, and essentially, there is no single custodian to make macro decisions regarding carbon capture and determine the future of these facilities.This means that there are various custodians and stakeholders, and this research proposal is separate for different sectors, so that each custodian can make policies and decisions based on the data. Therefore, the proposal was separated for each sector.

In official documents such as the energy balance sheet, the amount of CO_2 emissions in different sectors has been analyzed and reviewed separately and is not uniform.

5.2. Industry

Industry: Ministry of Industry, Mine, Trade and the private sector. (Figure 8) shows the CO_2 capture implementation potential assessment system for the industry, while the results of the corresponding AHP analysis are presented in (Figure 9). As illustrated, the CCUS option achieved the highest ideal priority value (1.000), indicating the strongest preference and overall suitability among the evaluated industry sector alternatives. The CCU scenario ranked second with an ideal priority value of approximately 0.6377, reflecting a comparatively favorable position relative to the other options. In contrast, the CCS and No.CC alternatives obtained substantially lower priority values, at approximately 0.2897 and 0.3476, respectively. These findings demonstrate a pronounced preference for integrated carbon management strategies combining carbon capture, utilization, and storage within the industrial sector. Furthermore, the higher ranking of CCU compared with CCS suggests that utilization-oriented pathways are considered more advantageous than standalone carbon storage approaches under the selected evaluation framework.

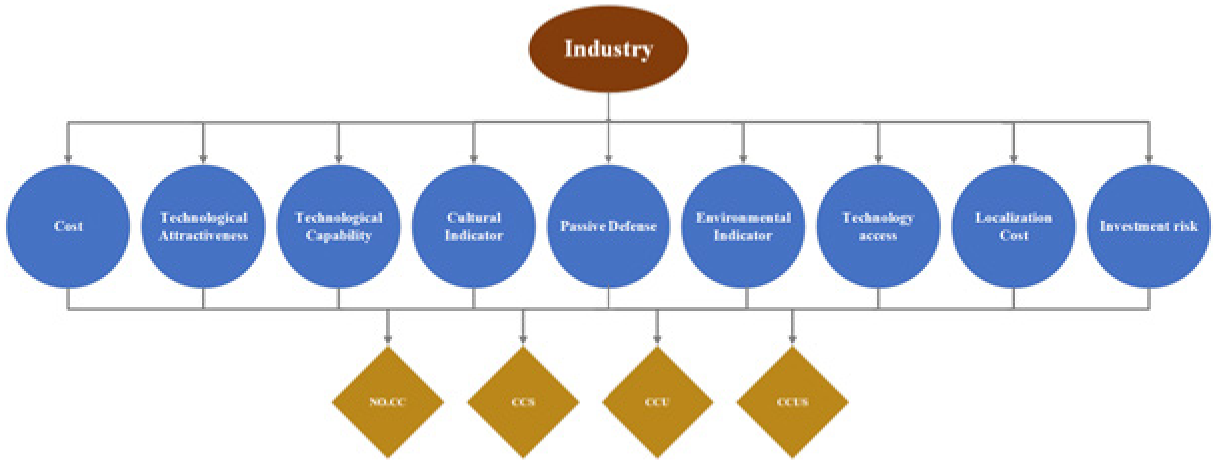

Figure 8. Industry Evaluation System Based on AHP

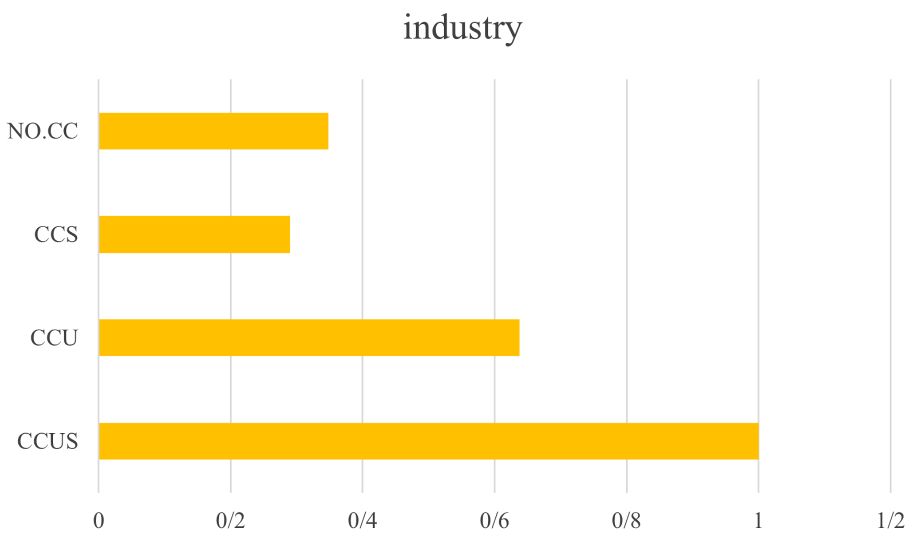

Figure 9. Ideal Priorities of Industry Sector Options Obtained from AHP

5.3. Refinery

Refinery: Ministry of Oil and the private sector. (Figure 10) shows the CO_2 capture implementation potential assessment system used for refineries. The results of the analysis of this system are presented in (Figure 11). As illustrated, the CCUS option achieved the highest ideal priority value (1.000), indicating its superior preference and overall suitability among the evaluated refinery sector alternatives. The CCU option ranked second with an ideal priority of 0.6549, followed by CCS with a substantially lower value of 0.3006, whereas the No.CC scenario exhibited the lowest priority score (0.1401). These findings indicate a strong preference toward integrated carbon capture, utilization, and storage strategies within the refinery sector. Furthermore, the higher ranking of CCU relative to CCS suggests that carbon utilization pathways are considered more advantageous than standalone carbon storage approaches under the selected evaluation criteria.

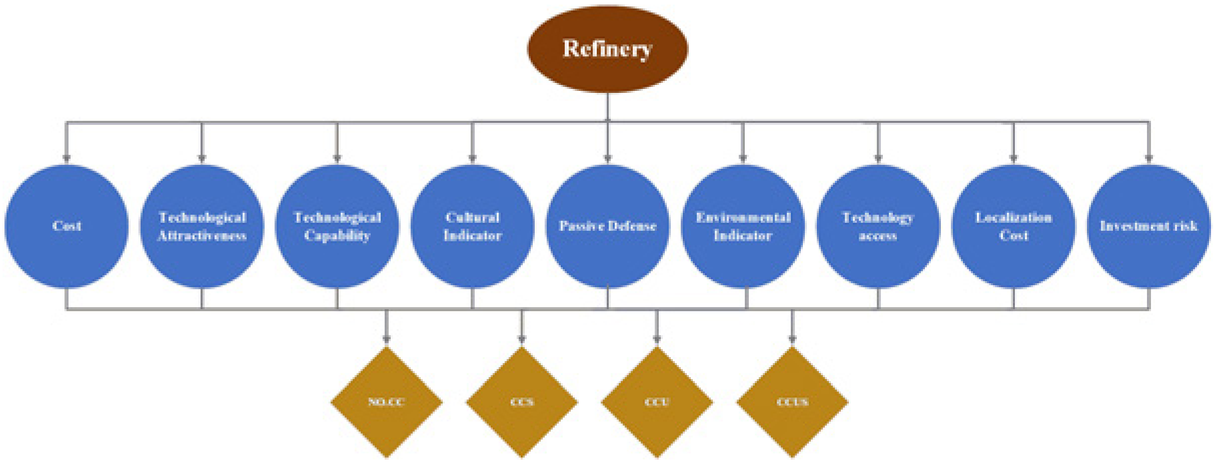

Figure 10. Refinery Evaluation System Based on AHP

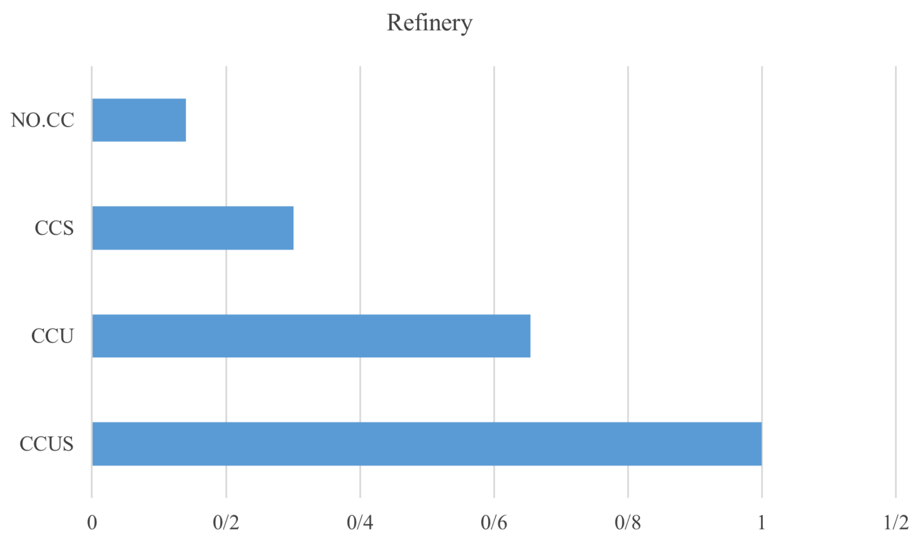

Figure 11. Ideal Priorities of Refinery Sector Options Obtained from AHP

(Figure 12) presents the sensitivity analysis results for the four evaluated alternatives, namely CCUS, CCU, CCS, and NO.CC, across the refinery, power plant, and industrial sectors. Panels (a-d) correspond to the refinery sector, panels (e-h) to the power plant sector, and panels (i-l) to the industrial sector. In all examined cases, CCUS maintains the highest ranking, and no rank reversal is observed within the investigated range of criteria weights. The main differences among the sectors are therefore associated with the degree of sensitivity rather than with changes in the final ranking structure.

The refinery sector, shown in (Figure 12 a-d), exhibits the most stable behavior among the three applications. Variations in criteria weights produce only limited changes in the relative positions of the alternatives. The most noticeable response appears under the cost criterion, where increasing the weight of cost gradually reduces the CCS score, while NO.CC shows a moderate upward trend and approaches CCS near the upper end of the range. In contrast, the environmental, technology-accessibility, and investment-risk criteria produce comparatively small variations, and the ranking order remains unchanged throughout the analysis. Overall, the refinery sector appears relatively insensitive to moderate weighting changes.

A somewhat stronger response is observed in the power plant sector, illustrated in (Figure12 e-h). The effect of the cost criterion is more pronounced in this case, particularly for CCS, whose score declines more visibly as the cost weight increases. At the same time, the difference between CCU and NO.CC decreases slightly. Despite these variations, CCUS consistently preserves its leading position. Under the environmental criterion, the advantage of CCUS becomes more apparent, whereas CCU and NO.CC experience moderate declines. Technology accessibility and investment risk have comparatively limited influence on the overall ranking pattern, and no instability is observed in the decision structure.

The industrial sector results, presented in (Figure12 i-l), show the highest responsiveness to environmental and technology-related criteria. As the weight of the environmental criterion increases, the separation between CCUS and the remaining alternatives becomes more distinct, while NO.CC declines more noticeably. A similar trend is observed for technology accessibility, where CCUS gains additional preference relative to CCS, CCU, and NO.CC. Under the investment-risk criterion, the gap between CCUS and the other alternatives widens slightly, further strengthening its dominant position. Compared with the refinery and power plant sectors, the industrial application therefore demonstrates greater sensitivity to environmental performance and technological feasibility.

Overall, the sensitivity analysis indicates that the ranking structure obtained from the AHP model is stable across all three sectors. Although moderate variations occur among CCS, CCU, and NO.CC under certain criteria, these changes are insufficient to produce rank reversal or substantial instability. The results therefore suggest that the AHP framework provides a reliable basis for evaluating CCUS-related pathways under different sectoral conditions.

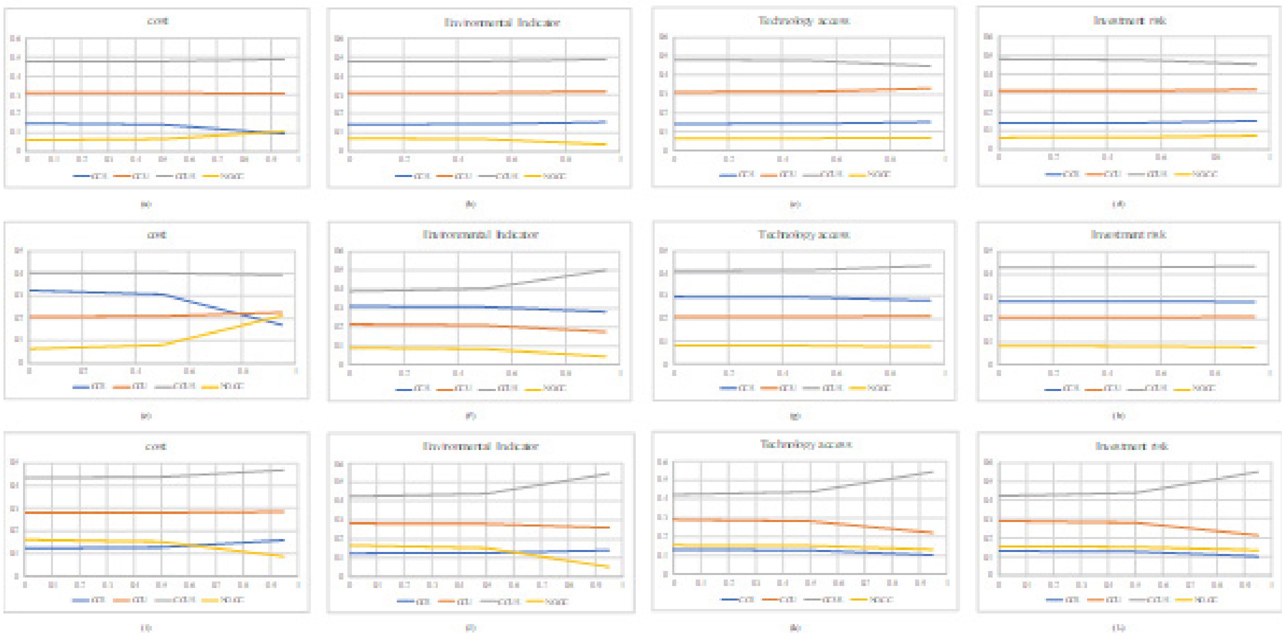

Figure 12. Sensitivity Analyses for the Refinery, Power Plant, and Industry Sectors

6. Analysis of Results

This section presents the results of the hierarchical analyses.

- CCCUS facilities rank first in the three applications because their simultaneous use and storage, owing to no waste, increases the efficiency of the carbon capture process.
- The use of CCU technology in the aforementioned applications is beneficial because of carbon capture and its application in various uses, as mentioned in (Figure 8).
- The CCS process is often more applicable to refineries and industries. One of its uses is for injection into oil wells to compensate for pressure reduction, which is abbreviated as EOR, and it generates revenue in industries.

6.1. Power Plant

Based on existing scenarios, renewable energy is expected to constitute 10% of total power plant capacity; however, at present, less than 1% of installed power plant capacity is based on renewable energy. This is because when the country's primary and non-strategic development plan focuses on the expansion of the natural gas network and the replacement of renewable alternatives with petroleum products, renewable energy fails to gain a significant share in the national economy. Therefore, diversification of the country's energy portfolio appears impractical, as the dominance of natural gas does not allow renewable energy sources to realize their potential. The extensive replacement of natural gas with petroleum products, particularly in the household sector, has resulted in an increase in net energy intensity. Consequently, the heavy dependence of the national energy system on a single dominant fuel has increased vulnerability in terms of energy security, and continued access to low-cost natural gas constitutes a major barrier to the development of renewable energy sources. Therefore, given the current conditions, the dominance of fossil fuels in power plants, and the failure to implement renewable power plants in line with defined targets, the implementation of CCUS projects is considered essential. In the next stage, the utilization of captured carbon for the production of various products can generate a return on investment.

In addition, based on upstream policy documents, CO_2 emissions can be reduced by increasing the efficiency of the country's power plant network through CO_2 capture and storage, expanding the use of renewable energy sources and biofuels, reducing losses in the electricity transmission and distribution network, developing combined heat and power (CHP) and combined-cycle units, optimizing energy consumption in the demand sector, producing biogas, and converting waste to energy. Furthermore, at the national level, by establishing appropriate financial and energy economic mechanisms, such as reducing and gradually eliminating energy subsidies, strengthening the National Environment Fund, and expanding private sector participation, particularly in the energy and efficiency sectors through energy service companies (ESCOs), effective incentive mechanisms can be introduced.

6.2. Industry

Industries generally seek to establish value chains. 19% of carbon pollution comes from industries; therefore, industries can focus on the storage and use of the carbon produced. Supportive and upstream environmental laws can provide incentives for the industry for financing, return on investment, and gas prices, such as Article 27 of the Value Added Tax Law (Green Tax Law).

In general, taxes referred to as green taxes include tax incentives and discounts. These taxes apply to companies whose activities focus on environmental protection and pollution reduction. However, taxes that involve penalties and increased charges within this system include the carbon tax, which is imposed on fossil fuel consumption, tariffs on the import of energy-intensive goods, and mining extraction taxes. In general, this system seeks to reduce the costs associated with environmentally friendly activities and increase the costs of environmentally harmful activities in any form. Therefore, the adoption of CCUS facilities is strongly recommended. Resistance may arise from industries with outdated technologies; however, this can be addressed gradually through the implementation of incentive-based schemes, thereby reducing opposition. In addition, efforts should be made to promote the development of new manufacturing industries with low energy consumption and high efficiency, modernize the structure of existing industrial units, and enhance the economic development of the manufacturing sector.

6.3. Refinery

Preventing reservoir pressure decline is a top priority before implementing any enhanced oil recovery method. Crude oil production is currently experiencing a decline in extraction capacity. Collecting produced gases is a key priority for the upstream oil and gas industry. The same applies to processing or maximising the conversion of associated and flared gases, with due attention to economic and environmental aspects. Consequently, reinjecting these gases into reservoirs is considered an unavoidable necessity. This is because flaring causes environmental pollution and leads to the loss of economic opportunities. As indicated in the analyses and upstream policy documents, CCUS technology is considered the most suitable option for application in refineries. In addition to the reuse of carbon for various applications, such as enhancing both the quantity and quality of refined and petrochemical products with a value-maximization approach, carbon storage is also applied to increase productivity across the oil and gas value chain. Although companies must comply with international commitments, due to sanctions, they are unable to implement such facilities in Iran. Therefore, these technological units must be localized within the country.

7. Critical Interpretation of Results

The superiority of CCUS in the Iranian context does not necessarily imply that technical or economic barriers are absent. Instead, it reflects a lack of sufficiently mature, large scale alternatives that could achieve substantial emission reductions without disrupting the existing hydrocarbon based infrastructure. In other words, the preference toward CCUS appears to be driven more by infrastructural compatibility and transitional practicality than by ideal economic conditions. The sectoral differences observed in the results further suggest that carbon-management pathways cannot be evaluated independently from the structure of the host industry. In refinery and industrial applications, the relatively stronger position of utilization-oriented pathways indicates that the economic value of recovered carbon partially offsets the technological complexity of capture systems. However, this behavior was less pronounced in the power-plant sector, where carbon utilization opportunities remain limited and the economic burden of capture infrastructure becomes more visible. This finding implies that the attractiveness of CCUS is not uniform across sectors and depends heavily on the ability of each sector to internalize the economic value of captured carbon.

Another important observation is that CCS alone did not emerge as the dominant option despite its recognized environmental performance. This may indicate that under Iranian conditions, experts place greater importance on integrated and economically productive carbon-management pathways than on isolated storage strategies. Unlike studies conducted in regions with established transport and storage networks, the Iranian context is characterized by infrastructure limitations, sanctions, financing uncertainty, and localization challenges, all of which alter the practical feasibility of standalone storage projects. Therefore, the present findings suggest that the prioritization of CCUS in Iran is linked not only to emission reduction objectives, but also to the need for compatibility with existing industrial, economic, and energy-system realities.

8. Outlook

CCUS technologies have reached the operational stage in most parts of the world and the Middle East; however, in Iran, this technology has not yet progressed to the pilot stage. Given the presence of thermal power plants, industrial facilities, and abundant oil and gas resources, there is significant potential to utilize these facilities to reduce greenhouse gas emissions and recover carbon for various applications.For example, urban pollution is a critical issue associated with power plants, as they significantly contribute to air pollution in urban areas. Therefore, government agencies must allocate financial resources to address urban pollution and ensure clean air, as pollution directly affects public health. Consequently, the application of CCUS technology can be evaluated as an opportunity to reduce air pollution and mitigate human health risks.

Another application of this technology is the reduction of the gas network imbalance problem. In winter, there is a gas network imbalance problem within the country, and during this season, many power plants near cities use mazut fuel. Here, CCUS units gain strategic value, in addition to economic value. Approximately 60897 million cubic meters of gas per year are consumed by power plants, out of 548.5 million cubic meters of gas produced daily. If mazut is used as fuel in different seasons, this mazut, along with the use of a CCUS facility, becomes a valuable process that simultaneously reduces gas consumption, and the carbon produced can be utilized. Another way to use CO_2 is through CO_2-to-fuel processes, where carbon can be converted into liquid fuels, stored, and its methane used. Therefore, rapid action must be taken, and laws must be enacted to achieve CCUS technology.

Public demand for the government to enact strict environmental regulations aimed at reducing greenhouse gas emissions and moving toward a net-zero carbon program, along with economic engagement of the private sector, reducing government ownership across various applications, realigning the pricing of petroleum derivatives, eliminating hidden energy subsidies, promoting social acceptance of such technologies, imposing carbon penalties across different sectors, and implementing coherent energy policies and commercialization mechanisms, can significantly contribute to the development and advancement of carbon capture technologies. Ultimately, the creation of an optimized energy–environment market through energy policy reform, reducing the role of state-owned enterprises, moving toward cross-sectoral regulation, strengthening private sector participation, and attracting foreign investment in this field can represent a major breakthrough.

9. Conclusion

The results of this study show that the assessment of carbon emission reduction options was conducted using a multi-criteria decision-making framework based on expert judgment and demonstrates acceptable statistical consistency. The level of agreement between experts was calculated using the Intraclass Correlation Coefficient (ICC). The obtained ICC value was 0.751, which, based on standard statistical criteria, indicates a "good" to "acceptable" level of agreement between expert assessments and suggests that the input data to the AHP process are not unduly dispersed and that the ranking results are statistically reliable.This ICC value was directly extracted from the statistical analysis of expert judgments presented in the report and was used as an indicator of the robustness of the AHP results. Based on this validated decision-making framework, the CCUS option received the highest final score compared to other emission reduction options in all three sectors: power plants, industrial facilities, and refineries. This result indicates that, from the experts' perspective, CCUS is not only technically feasible, but also a priority option in terms of its compatibility with the country's current energy structure and its potential for accelerated CO_2 emission reduction.A review of the international benchmark projects introduced in the report also reinforces this prioritization. The operational capacity of successful CCUS projects worldwide generally ranges from approximately 0.1 to 1.3 million tons of CO_2 per year; for example, the Quest project in Canada, with a capacity of about 1.1 $MtCO_2$/yr, the Sturgeon project with 1.3 $MtCO_2$/yr, and the Port Arthur project in the United States with approximately 0.9 $MtCO_2$/yr, are among the established industrial examples. The existence of this capacity spectrum indicates that the deployment of medium- to large-scale CCUS projects, particularly in concentrated emission sources, has reached a level of technical and operational maturity.Accordingly, the report concludes that the design and implementation of a pilot or initial phase of CCUS in the country, with a capacity of approximately 0.5 to 1.0 million tons of CO_2 per year, can be aligned with international experience and play an effective role in the practical demonstration and localization of this technology. From an economic perspective, the data presented in the report show that the cost of CO_2 capture in existing industrial projects is approximately \$20 to \$140 per ton of CO_2. However, the report considers it feasible to reduce the average capture cost by approximately 50% by 2030, citing technological learning effects, scaling up, and improvements in process design. This implies that if the pilot phase transitions to an industrial scale and benefits from synergies between capture, transportation, and storage units, CCUS can evolve from a high-cost solution into a competitive option within the emission reduction policy portfolio. Finally, the report's findings emphasize that the success of CCUS as a transitional strategy depends on its alignment with the country's macro-level energy policies. In a context where the current share of renewable energy in electricity generation capacity is reported to be less than 1%, while a target of increasing it to 10% is under discussion, the development of CCUS can, as a complementary measure, offset emissions resulting from the high consumption of natural gas in power plants and industrial sectors. The quantitative findings therefore demonstrate that CCUS, combined with structural reforms in electricity generation and energy efficiency improvements, represents a limited but viable option. It can achieve significant CO_2 emission reductions in the short to medium term. Importantly, this can be done without causing major disruption to existing infrastructure.

References

Adetoye, A. M., Okojie, L. O., & Akerele, D. ,2018. Forest carbon sequestration supply function for African countries: An econometric modelling approach. Forest Policy and Economics, 90, 59-66. https://doi.

org/10.1016/j.forpol.2018.01.007

Al Baroudi, H., Wada, R., Ozaki, M., Patchigolla, K., Iwatomi, M., Murayama, K., Otaki, T., & Baroudi, A. ,2021. Experimental investigation of liquid CO_2 discharge from the emergency release system's coupler of a loading arm.

Alizadeh, S. M., Khalili, Y., & Ahmadi, M. ,2024. Comprehensive Review of Carbon Capture and Storage Integration in Hydrogen Production: Opportunities, Challenges, and Future Perspectives. Energies, 17(21), 5330. https://doi.org/10.3390/en17215330

Astuti, A. R. A., Wenten, I. G., Ariono, D., Sasongko, D., Saputera, W. H., & Khoiruddin, K. ,2024. Advances in Carbon Control Technologies for Flue Gas Cleaning. In Separation and Purification Reviews. Taylor and Francis Ltd. https://doi.org/10.1080/15422119.2024.2328080

Bachu, S.,2008. CO_2 storage in geological media: Role, means, status and barriers to deployment. Progress in Energy and Combustion Science, 34(2), 254-273. https://doi.org/10.1016/j.pecs.2007.10.001

Besong, M. T., Maroto-Valer, M. M., & Finn, A. J. ,2013. Study of design parameters affecting the performance of CO_2 purification units in oxy-fuel combustion. International Journal of Greenhouse Gas Control, 12, 441-449. https://doi.org/10.1016/j.ijggc.2012.11.016

Boon, J., Spallina, V., van Delft, Y., & van Sint Annaland, M. ,2016. Comparison of the efficiency of carbon dioxide capture by sorption-enhanced water-gas shift and palladium-based membranes for power and hydrogen production. International Journal of Greenhouse Gas Control, 50, 121-134. https://doi.org/10.1016/j.ijggc.2016.04.033

Bu, P., & Qiu, Y. ,2025. Simulation, and comparative energy, exergy, economic, and environmental analyses of utilizing different solvents for post-combustion CO_2 capture from flue gases. Applied Thermal Engineering, 269. https://doi.org/10.1016/j.applthermaleng.2025.125923

Cao, C., Liu, H., Hou, Z., Mehmood, F., Liao, J., & Feng, W. ,2020. A review of CO_2 storage in view of safety and cost-effectiveness. In Energies .Vol. 13, Number 3. MDPI AG. https://doi.org/10.3390/en13030600

Damiani, D., Litynski, J. T., McIlvried, H. G., Vikara, D. M., & Srivastava, R. D. ,2012. The US Department of Energy's R&D program to reduce greenhouse gas emissions through beneficial uses of carbon dioxide. Greenhouse Gases: Science and Technology, 2(1), 9-16. https://doi.org/10.1002/ghg

Gabruś, E., Wojtacha-Rychter, K., Aleksandrzak, T., Smoliński, A., & Król, M. ,2021. The feasibility of CO_2 emission reduction by adsorptive storage on Polish hard coals in the Upper Silesia Coal Basin: An experimental and modeling study of equilibrium, kinetics and thermodynamics. Science of the Total Environment, 796. https://doi.org/10.1016/j.scitotenv.2021.149064

Godec, M., Carpenter, S., & Coddington, K. ,2017. Evaluation of Technology and Policy Issues Associated with the Storage of Carbon Dioxide via Enhanced Oil Recovery in Determining the Potential for Carbon Negative Oil. Energy Procedia, 114, 6563-6578. https://doi.org/10.1016/j.egypro.2017.03.1795

https://www.superdecisions.com.

IEA. 2024. CO_2 emissions by sector, Iran, 2023. IEA.

IEA. ,2019. Putting CO_2 to Use Creating value from emissions.

IEA. ,2022. Operating and planned facilities with CO_2 capture by application.

IEA., 2023. Hydrogen Production and Infrastructure Projects Database.

IEA.,2024. Operating and planned CO_2 capture capacity by region, Q1 2024 vs. 2030.

Kang, J.-N., Wei, Y.-M., Liu, L., & Wang, J.-W. ,2021. Observing technology reserves of carbon capture and storage via patent data: Paving the way for carbon neutral. Technological Forecasting and Social Change, 171, 120933. https://doi.org/10.1016/j.techfore.2021.120933

Keith, D. W., Holmes, G., St. Angelo, D., & Heidel, K. ,2018. A Process for Capturing CO_2 from the Atmosphere. Joule, 2(8), 1573-1594. https://doi.org/10.1016/j.joule.2018.05.006

Khan, C., Pearce, J. K., Golding, S. D., Rudolph, V., & Underschultz, J. R. ,2021. Carbon storage potential of north american oil & gas produced water injection with surface dissolution. Geosciences (Switzerland), 11(3), 1-10. https://doi.org/10.3390/geosciences11030123

Lau, H. C., Ramakrishna, S., Zhang, K., & Radhamani, A. V. ,2021. The Role of Carbon Capture and Storage in the Energy Transition. Energy & Fuels, 35(9), 7364-7386. https://doi.org/10.1021/acs.energyfuels.1c00032

Lu, H., Ma, X., Huang, K., Fu, L., & Azimi, M. ,2020. Carbon dioxide transport via pipelines: A systematic review. In Journal of Cleaner Production. Elsevier Ltd. https://doi.org/10.1016/j.jclepro.2020.121994

Mukherjee, A., Okolie, J. A., Abdelrasoul, A., Niu, C., & Dalai, A. K. ,2019. Review of post-combustion carbon dioxide capture technologies using activated carbon. In Journal of Environmental Sciences (China).Vol. 83, pp. 46-63. Chinese Academy of Sciences. https://doi.org/10.1016/j.jes.2019.03.014

Nagireddi, S., Agarwal, J. R., & Vedapuri, D. ,2024. Carbon Dioxide Capture, Utilization, and Sequestration: Current Status, Challenges, and Future Prospects for Global Decarbonization. ACS Engineering Au, 4(1), 22-48. https://doi.org/10.1021/acsengineeringau.3c00049

Nath, F., Mahmood, M. N., & Yousuf, N. ,2024. Recent advances in CCUS: A critical review on technologies, regulatory aspects and economics. Geoenergy Science and Engineering, 238, 212726. https://doi.org/10.1016/j.geoen.2024.212726

Normann, F., Andersson, K., Leckner, B., & Johnsson, F. ,2009. Emission control of nitrogen oxides in the oxy-fuel process. In Progress in Energy and Combustion Science .Vol. 35, Number 5, pp. 385-397. https://doi.org/10.1016/j.pecs.2009.04.002

Our World in Data. 2025, November 13. Annual CO_2 emissions by world region. Global Carbon Budget.

Praetorius, B., & Schumacher, K. , 2009. Greenhouse gas mitigation in a carbon constrained world: The role of carbon capture and storage. Energy Policy, 37(12), 5081-5093. https://doi.org/10.1016/j.enpol.2009.07.018

Ringrose, P. S. ,2014. Keynote speech - Large-scale CO_2 storage - How do we make it work? 4th EAGE CO_2 Geological Storage Workshop 2014: Demonstrating Storage Integrity and Building Confidence in CCS, 1-6. https://doi.org/10.3997/2214-4609.20140067

Roussanaly, S., Berghout, N., Fout, T., Garcia, M., Gardarsdottir, S., Nazir, S. M., Ramirez, A., & Rubin, E. S. ,2021. Towards improved cost evaluation of Carbon Capture and Storage from industry. International Journal of Greenhouse Gas Control, 106, 103263. https://doi.org/10.1016/j.ijggc.2021.103263

Shi, S., & Hu, Y. H. ,2025. A Landmark Year for Climate Change and Global Carbon Capture, Utilization, and Storage: Annual Progress Review. Energy Science & Engineering, 13(6), 3448-3458. https://doi.org/10.1002/ese3.70091

Simonsen, K. R., Hansen, D. S., & Pedersen, S. ,2024. Challenges in CO_2 transportation: Trends and perspectives. In Renewable and Sustainable Energy Reviews (Vol. 191). Elsevier Ltd. https://doi.org/10.1016/j.rser.2023.114149

Sun, M., Wang, X., Gao, F., Xu, M., Fan, W., Xu, B., & Sun, D. ,2023. Synthesis strategies of metal-organic frameworks for CO_2 capture. In Microstructures .Vol. 3, Number 4. OAE Publishing Inc. https://doi.org/10.20517/microstructures.2023.32

Vaddeboina, S., & Puttapati, S. K. ,2024. Carbon Dioxide Utilization Techniques for Producing Transportation Fuels. In From Waste to Wealth .pp. 401-436. Springer Nature Singapore. https://doi.org/10.1007/978-981-99-7552-5_19

Wifling, M. ,2020. Financial precautions, carbon dioxide leakage, and the European Directive 2009/31/EC on carbon capture and storage (CCS). Climatic Change, 163(2), 787-806. https://doi.org/10.1007/s10584-020-02904-1

Wilberforce, T., Olabi, A. G., Sayed, E. T., Elsaid, K., & Abdelkareem, M. A. ,2021. Progress in carbon capture technologies. Science of The Total Environment, 761, 143203. https://doi.org/10.1016/j.scitotenv.2020.143203

Wu, Y., Carroll, J. J., Zhu, W., Li, Q., Song, R., Liu, X., Liu, G., & Sun, Y. ,2016. Monitoring of Carbon Dioxide Geological Utilization and Storage in China: A Review. https://www.tarjomano.com

Yadav, S., & Mondal, S. S. ,2022. A review on the progress and prospects of oxy-fuel carbon capture and sequestration (CCS) technology. In Fuel .Vol. 308. Elsevier Ltd. https://doi.org/10.1016/j.fuel.2021.122057

Zhao, J., Zheng, J., Ren, L., Lin, R., & Zhou, B. ,2024. A review on geological storage of marine carbon dioxide: Challenges and prospects. Marine and Petroleum Geology, 163. https://doi.org/10.1016/j.marpetgeo.2024.106757

Zhou, X., Wu, Y. S., Chen, H., Elsayed, M., Yu, W., Zhao, X., Murtaza, M., Shahzad Kamal, M., Zafar Khan, S., Al-Abdrabalnabi, R., & Ren, B. , 2024. Review of Carbon dioxide utilization and sequestration in depleted oil reservoirs. In Renewable and Sustainable Energy Reviews . Vol. 202. Elsevier Ltd. https://doi.org/10.1016/j.rser.2024.114646

JOURNAL OF GAS TECHNOLOGY

Volume 10 / Issue 2 / Winter 2025 / Pages 43-62

Journal Home page: https://jgt.irangi.org

Analysis of Failures in Electrical Submersible Pumps Using Machine Learning Techniques

Mahya Faraji[1], Yasin Khalili[2], Mohammad Ahmadi[3*]

1. M.Sc., Department of Chemical Engineering, Institute of Petroleum Engineering, University of Tehran, Tehran, Iran
2. Ph.D. Student, Department of Petroleum and Geoenergy Engineering, Amirkabir University of Technology, Tehran, Iran
3. Associate Professor, Department of Petroleum and Geoenergy Engineering, Amirkabir University of Technology, Tehran, Iran

ARTICLE INFO

ORIGINAL RESEARCH ARTICLE

Article History:
Received: 22 September 2025
Revised: 04 October 2025
Accepted: 22 October 2025

Keywords:
Electrical Submersible Pumps (ESP)
Machine Learning
Predictive Maintenance
Anomaly Detection
Failure Prediction

DOR: 20.1001.1/jgt.2026.2078502.1064

ABSTRACT

Electrical Submersible Pumps (ESPs) play a critical role in enhancing production rates and operational efficiency in oil wells. However, their complex operating environments make them highly vulnerable to mechanical and electrical failures. Early detection of abnormal conditions and accurate prediction of pump performance are therefore essential for reducing downtime, minimizing operational costs, and extending pump lifespan.

This study investigates the application of machine learning techniques for identifying unstable operating conditions, detecting anomalies, and predicting failures in ESP systems. Using simulated monitoring data including motor temperature, intake temperature, current, and vibration several preprocessing and analytical methods were employed. Boxplot analysis was used to identify outliers, while Z-score analysis provided statistical detection of abnormal data points. K-means clustering and Principal Component Analysis (PCA) were implemented to reduce dimensionality, enhance visualization, and classify pump operating states into stable, unstable, anomalous, and failure modes.

Furthermore, a decision tree classifier was trained to determine the relative contribution of each parameter to pump failure. Model performance was evaluated using confusion matrices before and after applying PCA and clustering. Results show that incorporating these preprocessing techniques significantly improved classification accuracy from 0.9835 to 0.9967 for stable conditions and from 0.700 to 0.800 for failure conditions. The findings demonstrate the strong potential of machine learning methods for predictive maintenance of ESP systems and emphasize their value as a cost-effective strategy for enhancing reliability in the oil and gas industry.

How to cite this article
M. Faraji, Y. Khalili, M. Ahmadi. Analysis of Failures in Electrical Submersible Pumps Using Machine Learning Techniques. Journal of Gas Technology. 2025; 10(2): 43-62. (https://jgt.irangi.org/article_737830.html)

* Corresponding author.
E-mail address: m.ahmady@aut.ac.ir, (M. Ahmadi).

Available online 30 December 2025
2588-5596/© 2016 The Authors. Published by Iranian Gas Institute.
This is an open access article under the CC BY license. (https://creativecommons.org/licenses/by/4.0)

1. Introduction

Electrical Submersible Pumps (ESPs) are among the most widely deployed artificial lift systems in the global oil and gas industry due to their ability to handle high production rates, operate in diverse reservoir conditions, and adapt to complex downhole environments. It is estimated that ESPs contribute to nearly 60% of global oil well production, underscoring their strategic importance in modern petroleum operations (Valbuena, Pereyra et al. 2016). Despite their widespread application, ESP systems are inherently vulnerable to premature failures caused by harsh downhole conditions, fluctuating flow regimes, and complex electro-mechanical interactions. Such failures often result in substantial production losses, expensive workover operations, and reduced overall field efficiency (Ladopoulos 2015). Consequently, improving ESP reliability and extending pump run life remain critical challenges for operators worldwide.

1.1. Importance and Economic Impact of ESP Failures

ESP failures represent a major source of non-productive time in oilfield operations. A single ESP failure can lead to prolonged production shutdowns, costly rig mobilization, and equipment replacement, with financial losses that may reach hundreds of thousands of dollars per event. In mature fields and deepwater applications, where intervention costs are particularly high, unexpected ESP failures can severely impact project economics. Furthermore, frequent failures reduce confidence in artificial lift system performance and complicate long-term production planning. These economic and operational consequences highlight the need for effective monitoring, early fault detection, and predictive maintenance strategies capable of identifying degradation before catastrophic failure occurs (Cardona, Vivas Sanchez et al. 2023).

1.2. Traditional ESP Failure Diagnosis Methods

Historically, ESP failure diagnosis has relied on physics-based models, threshold-based monitoring, and expert-driven rule systems derived from operational experience. Conventional approaches typically evaluate individual parameters such as motor temperature, motor current, vibration, or intake pressure against predefined operational limits (Abdelaziz, Lastra et al. 2017). While these methods are effective in detecting severe or already-developed faults, they exhibit several limitations. In particular, traditional techniques often struggle to identify early-stage degradation, capture nonlinear relationships among multiple operating variables, or adapt to changing reservoir and operating conditions (Peng, Feng et al. 2025). Moreover, such approaches require extensive expert knowledge and manual interpretation, limiting their scalability and consistency across different fields and well environments. These shortcomings have motivated the search for more adaptive and data-driven diagnostic solutions.

1.3. Machine Learning-Based Predictive Maintenance for ESP Systems

In recent years, machine learning (ML) techniques have gained increasing attention as powerful tools for ESP condition monitoring and predictive maintenance. Data-driven approaches leverage high-frequency sensor data such as temperature, current, vibration, and pressure to identify complex patterns associated with abnormal behavior and impending failure (Silvia, Gilad et al. 2023). Previous studies have demonstrated the potential of various ML algorithms, including artificial neural networks, support vector machines, decision trees, and ensemble models, to characterize ESP performance and predict failure events (Shi, Chen et al. 2019).

Despite these advances, many existing ML-based studies focus on single algorithms, binary classification between healthy and failed states, or limited subsets of operating conditions. In addition, issues such as systematic data preprocessing, handling of class imbalance, multi-state operational classification, and model interpretability are often insufficiently addressed. As a result, the practical deployment of ML models in real-world ESP monitoring systems remains challenging (Liang and El-Kadri 2018, Joseph, Adeoti et al. 2021, Li 2023).

1.4. Research Gap and Contribution

Despite the increasing application of machine learning techniques for ESP performance monitoring and failure diagnosis, several important limitations persist in the existing literature. Many prior studies rely on isolated ML models without integrated preprocessing frameworks, focus primarily on binary classification of normal versus failure conditions, or provide limited interpretability of model predictions. Furthermore, the combined use of statistical anomaly detection, unsupervised learning, dimensionality reduction, and explainable supervised classification has not been sufficiently explored within a unified framework for ESP condition assessment (Khalili, Rafiei et al. 2022, Ho, Fazilah et al. 2023, Kindi, Ghadani et al. 2024, Khalili, Ahmadi et al. 2025).

To address these gaps, this study proposes a hybrid and interpretable machine learning framework for ESP monitoring and failure prediction. The proposed approach integrates boxplot and Z-score-based statistical analysis for anomaly detection, K-means clustering for unsupervised identification of operational states, Principal Component Analysis (PCA) for dimensionality reduction and visualization, and decision tree classification for transparent and explainable failure prediction. Unlike previous studies, this framework enables multi-state classification of ESP behavior covering stable, unstable, anomalous, and failure conditions while demonstrating improved prediction accuracy through structured preprocessing. The proposed methodology provides a practical and extensible foundation for predictive maintenance of ESP systems and supports more reliable, data-driven operational decision-making.

2. Methodology

To identify unstable operating conditions, detect anomalies, and classify failure modes in ESPs, various machine learning and statistical analysis techniques were applied to the monitoring dataset (Lastra and Xiao 2022). These methods enable a structured assessment of operational parameters and support the development of predictive maintenance strategies (AlBallam 2022). This section introduces the analytical tools used in the study and their relevance to ESP performance evaluation.

2.1. Data Acquisition and Description

The dataset used in this study consists of simulated ESP operational monitoring data generated to reflect realistic field operating conditions and failure scenarios reported in the literature and manufacturer specifications. Simulation-based data were selected to enable controlled evaluation of the proposed methodology while ensuring consistency with documented ESP operating ranges and failure thresholds.

The dataset contains ESP pump data records, each corresponding to a distinct operational snapshot of the ESP system. Each record includes four key monitoring parameters: motor temperature, motor intake temperature, motor current, and motor vibration. Based on operating conditions, the data were labeled into four classes: stable operation, unstable operation, failure condition, and outlier (anomalous) state. The dataset exhibits class imbalance, with stable operation representing the majority of samples, reflecting realistic field behavior where failure events are relatively rare.

2.2. Data Preprocessing and Feature Engineering

Prior to model development, several preprocessing steps were applied to enhance data quality and robustness. Boxplot analysis was first employed to identify extreme outliers and assess data distribution characteristics. Subsequently, Z-score analysis was used for statistical anomaly detection, with data points exceeding |Z| > 3 flagged as abnormal.

All features were normalized to eliminate scale dependency and improve model convergence. Dimensionality reduction was performed using PCA to remove redundant correlations among variables and improve visualization and classification performance. No missing values were present in the simulated dataset; however, the preprocessing pipeline is designed to be extensible to field datasets where missing data handling may be required.

The ESP monitoring dataset be represented by a matrix

$$X = [x_{ij}] \in R^{N\times d} \tag{1}$$

where Nis the number of samples (records), dis the number of measured parameters (features), and x_{ij} denotes the value of feature j for sample i. In this study, d = 4, corresponding to motor temperature, intake motor temperature, motor current, and motor vibration.

Feature Normalization

To eliminate scale dependency across features, normalization was applied prior to clustering, PCA, and classification. Z-normalization (standardization) is defined as:

$$x_{ij}^{*} = \frac{x_{ij} - \mu_j}{\sigma_j} \tag{2}$$

where μj and σj are the mean and standard deviation of feature j, respectively.

2.3. Machine Learning Algorithms and Selection Rationale

A combination of unsupervised and supervised machine learning techniques was adopted to capture different aspects of ESP operational behavior. K-means clustering was selected for its simplicity and effectiveness in identifying latent operational states without prior labeling. PCA was applied to improve separability and reduce noise in the feature space.

For supervised classification, a decision tree classifier was employed due to its interpretability and suitability for engineering applications. Decision trees allow transparent identification of critical parameters influencing failure, which is essential for operational decision-making in ESP systems.

2.3.1. Machine Learning Algorithms and Selection Rationale

The boxplot is a widely used statistical visualization tool that provides an intuitive representation of data distribution. It illustrates key parameters such as the median, interquartile range (IQR), and extreme values (Bozhenko and Tatarnikova 2023, Krishnan, Kodamana et al. 2024). In the context of ESP monitoring, boxplot analysis serves two essential purposes:

1. Outlier Identification (Muslikh, Andono et al. 2023):

   Data points that lie significantly outside the normal operating range such as abrupt spikes in temperature or current may indicate sensor malfunction, transient anomalies, or early-stage pump degradation.

2. Initial Data Quality Assessment (Nandan Prasad 2024, Sobhy 2025):

   By visualizing the spread and skewness of each operational parameter, boxplots help identify inconsistencies, assess variability, and support subsequent preprocessing steps such as normalization and filtering.

This preliminary step ensures that the dataset fed into machine learning algorithms is representative, consistent, and free of extreme outliers that could bias model training.

In Box Plot, for each feature, the interquartile range (IQR) is computed as:

$$IQR = Q_3 - Q_1 \tag{3}$$

where Q_1 and Q_3 represent the first and third quartiles. A data point xis flagged as an outlier if it falls outside the lower and upper bounds:

$$x < Q_1 - 1.5\ IQR \text{ or } x > Q_3 + 1.5\ \ IQR. \tag{4}$$

2.3.2. Z-Score Method for Anomaly Detection

The Z-score, also known as the standard score, quantifies the number of standard deviations a data point deviates from the mean (Aggarwal, Gupta et al. 2019):

Importance in ESP Monitoring

A high absolute Z-score (e.g., |Z| > 3) indicates that the value is statistically anomalous. For ESP data:

1. High motor temperature or current may signal overloading or incipient failure
2. Sudden drops in intake temperature or pressure may indicate fluid entry issues
3. Large deviations in vibration readings may reflect mechanical imbalance or impending pump damage.

The Z-score method provides a straightforward and reliable approach for detecting anomalies before performing more advanced classification or clustering steps.

The Z-score (standard score) quantifies the deviation of a value from the mean in units of standard deviation:

$$Z = \frac{X - \mu}{\sigma} \tag{5}$$

where X is the observed value, μ is the mean, and σ is the standard deviation. A point is considered anomalous if:

$$|Z| > Z_{thr}, \tag{6}$$

where Z_{thr} is the anomaly threshold. In this study, $Z_{thr} = 3$was used.

2.3.3. K-Means Clustering

K-means is an unsupervised machine learning algorithm commonly used for partitioning datasets into groups (clusters) based on similarity. It iteratively assigns each data point to the nearest cluster center and updates the centroids until convergence (Oti, Olusola et al. 2021, Al Ghafri, Al Senani et al. 2025).

Relevance to ESP Analysis

In this study, K-means clustering was employed to categorize ESP operating states into:

1. Stable operation
2. Unstable operation
3. Faulty (failure-prone) conditions
4. Outlier or abnormal states

Grouping data into clusters allows the identification of operational patterns that are not explicitly labeled in the dataset. It is particularly useful in ESP monitoring where failure signatures may not be immediately apparent.

K-means partitions the dataset into Kclusters by minimizing the within-cluster sum of squares:

$$\min_{\{C_k\}_{k=1}^{K}} \sum_{k=1}^{K} \sum_{x_i \in C_k} \| \boldsymbol{x}_i - \boldsymbol{\mu}_k \|^2 , \tag{7}$$

where C_k is the set of points assigned to cluster k, and μ_k is the centroid of cluster k:

$$\boldsymbol{\mu}_k = \frac{1}{|C_k|} \sum_{x_i \in C_k} \boldsymbol{x}_i . \tag{8}$$

Cluster assignment is performed by:

$$assign(\boldsymbol{x}_i) = \arg\min_{k\in\{1,\ldots,K\}} \| \boldsymbol{x}_i - \boldsymbol{\mu}_k \|^2. \tag{9}$$

2.3.4. Principal Component Analysis (PCA)

Principal Component Analysis (PCA) is a dimensionality reduction technique that transforms correlated variables into a smaller set of uncorrelated components (principal components). These components capture the maximum variance in the dataset (Peng, Han et al. 2020, Hasan, Abdulazeez et al. 2021, Song, Jun et al. 2024).

Benefits for ESP Performance Evaluation

1. Dimensionality Reduction:

   ESP datasets often include multiple correlated measurements. PCA simplifies the dataset while retaining essential information.

2. Visualization:

   By projecting data onto two principal components (PC1 and PC2), PCA makes it possible to visualize operational states and detect emerging patterns or clusters.

3. Noise Reduction:

   PCA helps remove redundant or noisy information, improving the performance of subsequent machine learning models.

   This technique is especially valuable in distinguishing between stable, unstable, and failure-prone operating regimes.

   PCA transforms the standardized feature matrix into a lower-dimensional representation that retains maximum variance. Let X^* denote the standardized data (Eq. 2). The covariance matrix is:

$$S = \frac{1}{N-1}(X^* \quad)^\top X^*. \tag{10}$$

PCA solves the eigenvalue problem:

$$Sv_m = \lambda_m v_m, \tag{11}$$

where λ_m and v_m are the eigenvalue and eigenvector corresponding to principal component m. The projection of a sample x_i^* onto the first pprincipal components is:

$$z_i = V_p^\top x_i^*, \tag{12}$$

where $V_p = [v_1, \ldots, v_p]$. The explained variance ratio for component mis:

$$EVR_m = \frac{\lambda_m}{\sum_{j=1}^{d} \lambda_j}. \tag{13}$$

2.3.5. Decision Tree Classification

Decision trees are supervised learning algorithms used to classify data based on a hierarchy of decision rules. Each internal node represents a test on a feature (e.g., motor temperature), and each leaf node corresponds to a predicted class (e.g., failure) (Castellanos, Serpa et al. 2020, Lasrado 2024).

Application to ESP Data

In this study, decision trees were used to:

1. Identify the relative importance of each parameter in predicting pump failure.
2. Create interpretable decision rules, such as “Motor temperature $> X \rightarrow$ High failure risk.”
3. Classify new data into stable, unstable, or failure categories.

This method is particularly suitable for engineering applications because its outputs are transparent and easy to interpret, enabling engineers to understand the reasoning behind predictions.

A decision tree recursively splits the feature space to maximize class purity. Two commonly used impurity measures are Gini impurity and entropy.

For a node containing a class distribution $\{p_c\}_{c=1}^{C}$, Gini impurity is:

$$G = 1 - \sum_{c=1}^{C} p_c^2, \tag{14}$$

and entropy is:

$$H = -\sum_{c=1}^{C} p_c \log_2 (p_c). \tag{15}$$

For a candidate split that partitions the node into left and right child nodes, the impurity decrease (information gain) is computed as:

$$\Delta I = I(\text{parent}) - \left(\frac{n_L}{n} I(L) + \frac{n_R}{n} I(R)\right), \tag{16}$$

2.4. Model Training and Validation Framework

The dataset was divided into training and testing subsets using a 70/30 split. The models were trained on the training set and evaluated on unseen test data. Classification performance was assessed using confusion matrices, accuracy metrics, and class-wise evaluation to account for data imbalance.

Model performance was evaluated before and after applying PCA and K-means clustering to quantify the impact of preprocessing and dimensionality reduction. This framework ensures a fair and consistent comparison of model performance across different processing stages.

2.5. Performance Evaluation Metrics

To quantitatively evaluate the performance of the proposed machine learning framework, standard classification evaluation metrics were employed. Model predictions were assessed by comparing the predicted operating states with the true class labels using a confusion matrix. The confusion matrix provides a comprehensive summary of classification outcomes, including true positives, true negatives, false positives, and false negatives for each operating state (Al-Ballam, Karami et al. 2023; Khalili, Ahmadi et al. 2025).

From the confusion matrix, key performance indicators such as overall accuracy, class-wise accuracy, precision, and recall were derived. These metrics are particularly important in ESP failure prediction, where class imbalance is common and misclassification of failure states can lead to significant operational and economic consequences. Class-wise evaluation ensures that model performance is not dominated by the majority (stable operation) class and that failure and unstable conditions are adequately assessed.

In this study, confusion matrices were generated for the decision tree classifier under two different scenarios: (i) using the original feature space without dimensionality reduction and clustering, and (ii) after applying K-means clustering and PCA as preprocessing steps. This comparative evaluation framework allowed assessment of the impact of preprocessing and dimensionality reduction on classification performance, particularly in improving the identification of unstable and failure-prone operating states.

The confusion matrix compares predicted classes with true classes. For a given class, the following outcomes are defined: true positives (TP), false positives (FP), true negatives (TN), and false negatives (FN). Using these values, the main evaluation metrics are computed as:

Accuracy:

$$Accuracy = \frac{TP + TN}{TP + TN + FP + FN}. \tag{17}$$

Precision:

$$Precision = \frac{TP}{TP + FP} \tag{18}$$

Recall (Sensitivity):

$$Recall = \frac{TP}{TP + FN}. \tag{19}$$

F1-score:

$$F1 = 2 \cdot \frac{Precision \cdot Recall}{Precision + Recall}. \tag{20}$$

For multi-class classification, these metrics can be reported per class (class-wise) and averaged using macro- or weighted-averaging strategies to account for class imbalance.

3. Case Study: Reference ESP System

To evaluate the performance of the machine learning methods applied in this study, a representative ESP configuration was selected as a reference system. The case study is based on the operational specifications of a real industrial pump similar to the Baker Hughes FLEXPump™ Series 540, which is widely used in wells exhibiting diverse and challenging operating conditions.

The selected pump model is well-suited for medium-to-high productivity wells and offers enhanced resilience against temperature fluctuations, variable flow regimes, and harsh downhole environments. By comparing simulated failure scenarios with the technical specifications of this pump series, the study ensures that the analytical outcomes remain realistic and applicable to field operations.

3.1.Technical Specifications of the Reference Pump (FLEXPump™ Series 540)

The key operational characteristics of the selected pump are summarized as follows:

1. Pump Type

   A high-performance Electrical Submersible Pump designed for wells with complex downhole conditions, including variations in temperature, pressure, and inflow rate.

2. Installation Depth

   Capable of operating at depths up to 3000 meters, depending on reservoir pressure, fluid composition, and system configuration.

3. Production Capacity

   Designed to handle production rates in the range of 250 to 540 barrels per day (BPD), making it suitable for a broad spectrum of well productivity levels.

4. Operating Temperature Range

   The motor is engineered to tolerate temperatures up to 150°C, considerably higher than the simulated failure threshold of 110°C, providing sufficient thermal margin for safe and continuous operation.

5. Vibration Characteristics

   The pump design minimizes vibration, with operational vibration levels maintained below 1.5 RMS units, ensuring stable performance under varying load conditions.

6. Motor Power Rating

   Available in power configurations ranging from 5 to 50 horsepower, depending on well requirements and target production rates.

3.2. Advantages of the Selected Pump Configuration

The FLEXPump™ Series 540 exhibits several characteristics that make it suitable for predictive maintenance studies (Saxena , Werbinska-Wojciechowska and Rogowski 2025):

1. Enhanced Failure Resistance:

   The pump is specifically designed to withstand temperature and flow fluctuations that commonly lead to ESP failure.

2. Corrosion-Resistant Materials:

   Construction with anti-corrosive alloys improves reliability in wells containing H_2S, CO_2, or saline formation water..

3. Production Capacity

   The pump is compatible with advanced downhole monitoring systems capable of reporting real-time data on temperature, vibration, current, and intake pressure.

   These features make the pump an ideal reference system for evaluating the effectiveness of machine learning models in identifying failure conditions.

3.3. Alignment with Simulated Failure Conditions

The simulated Electrical Submersible Pump dataset used in this study was designed to represent realistic failure scenarios based on a combination of published literature, manufacturer technical specifications, and commonly reported ESP failure mechanisms. The operational thresholds defining failure conditions were selected to reflect values at which ESP systems typically experience performance degradation or imminent failure, as documented in prior studies and field experience.

Specifically, the failure-related operating conditions incorporated into the simulated dataset were defined as follows:

1. Motor temperature rising to approximately 110 °C, corresponding to elevated thermal stress levels commonly associated with insulation degradation and motor overheating in ESP systems, while remaining below the maximum rated motor temperature of the reference pump.
2. Motor current increasing to approximately 70 A, representing abnormal electrical loading conditions indicative of pump overload, flow restriction, or gas interference.
3. Vibration levels approaching 2.0 Root Mean Square (RMS) units, which exceed normal operating vibration ranges and are commonly linked to mechanical imbalance, impeller wear, or shaft misalignment.
4. Elevated intake motor temperature and non-uniform flow conditions, reflecting unstable inflow behavior, gas entry, or reservoir-induced flow disturbances that adversely affect pump performance.

These threshold values were intentionally selected to remain within the design limits of the reference Electrical Submersible Pump while representing conditions that are widely recognized as precursors to failure. As a result, the simulated anomalies are consistent with realistic field operating scenarios and allow meaningful comparison between simulated failure behavior and the technical tolerances of the reference pump system.

4. Results and Discussion

This section presents the results of the applied machine learning methods, including data preprocessing, anomaly detection, clustering, dimensionality reduction, feature importance analysis, and model evaluation (Figure 1). The findings demonstrate how each analytical step contributes to identifying operational patterns and predicting failures in ESP systems.

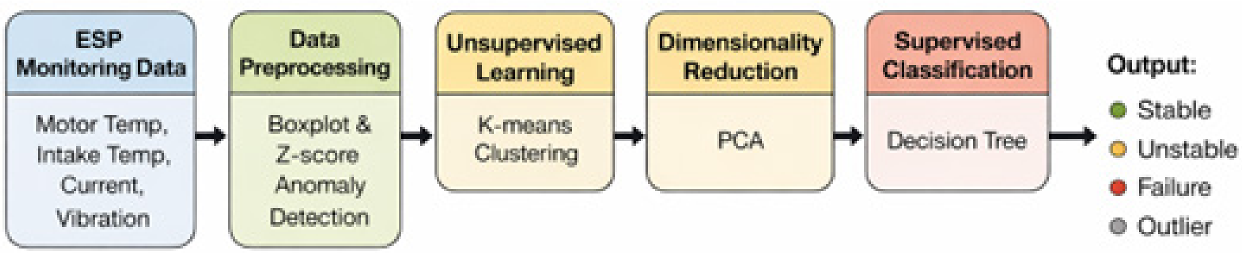

Figure 1. Overview of the Proposed Machine-Learning Framework for ESP Failure Detection and Classification

ESP monitoring data, including motor temperature, intake motor temperature, motor current, and vibration, are first preprocessed using boxplot analysis and Z-score-based anomaly detection. Unsupervised K-means clustering is then applied to identify latent operational states, followed by PCA for dimensionality reduction and visualization. Finally, a decision tree classifier is used to perform interpretable multi-state classification of ESP operating conditions into stable, unstable, failure, and outlier states.

4.1. Data Preprocessing Using Boxplot Analysis

Boxplot analysis was employed as an initial preprocessing step to visualize the distribution of the operational parameters and to identify statistical outliers. For each variable motor temperature, motor intake temperature, vibration, and motor current the boxplot reveals:

1. Minimum and maximum values
2. Median and interquartile range (IQR)
3. Potential outliers, which appear as isolated points beyond the whiskers

Key Observations

1. Detection of Outliers:

   The boxplots highlighted several extreme values, particularly in motor temperature and vibration. These outliers correspond to abnormal or failure-prone operating conditions and were considered during preprocessing.

2. Assessment of Data Variability:

   The spread of the quartiles indicated moderate-to-high variability in certain parameters especially vibration reflecting unstable wellbore flow or changing load conditions on the pump.

3. Improved Data Integrity:

   Identifying and isolating outliers prior to model training helps reduce noise and improves the robustness of downstream machine learning algorithms.

(Table 1) presents the statistical summary of the simulated ESP monitoring data obtained from the boxplot preprocessing step. These statistics provide an overview of the data distribution and support the identification of variability and potential outliers prior to further machine learning analysis.

Table 1. Statistical Summary Derived from Boxplot Preprocessing

Parameter	First Quartile (Q1)	Second Quartile (Median, Q2)	Third Quartile (Q3)	Maximum Value	Minimum Value	Mean
Motor Temperature (°C)	73.533	79.585	86.160	111.74	48.457	79.609
Motor Vibration (RMS)	1.005	1.468	1.845	3.0565	-0.10131	1.4846
Motor Current (A)	44.547	50.014	55.302	84.313	23.044	49.863
Motor Intake Temperature (°C)	67.754	74.917	81.287	106.24	39.615	74.608

(Figure 2) illustrates the distribution of key ESP operational parameters using boxplots, highlighting their central tendency, variability, and the presence of potential outliers.

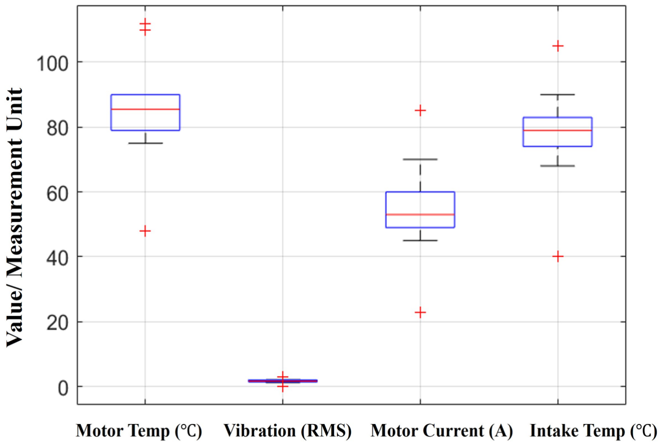

Figure 2. Boxplot of Simulated ESP Operational Parameters

Key Observations:

1. Boxplots revealed several extreme values notably in motor temperature and vibration.
2. Quartile spread indicated variability consistent with unstable or near-failure conditions.
3. Removing or flagging outliers enhanced the reliability of data used in later modeling.

4.2. Anomaly Detection Using Z-Score Analysis

Z-score analysis was implemented to detect statistically significant anomalies. Data points with $|Z| > 3$ were flagged as abnormal, which often corresponded to failure-related events.

The Z-score method effectively highlighted rare or extreme events across the monitoring period and provided a quantitative basis for classifying anomalies.

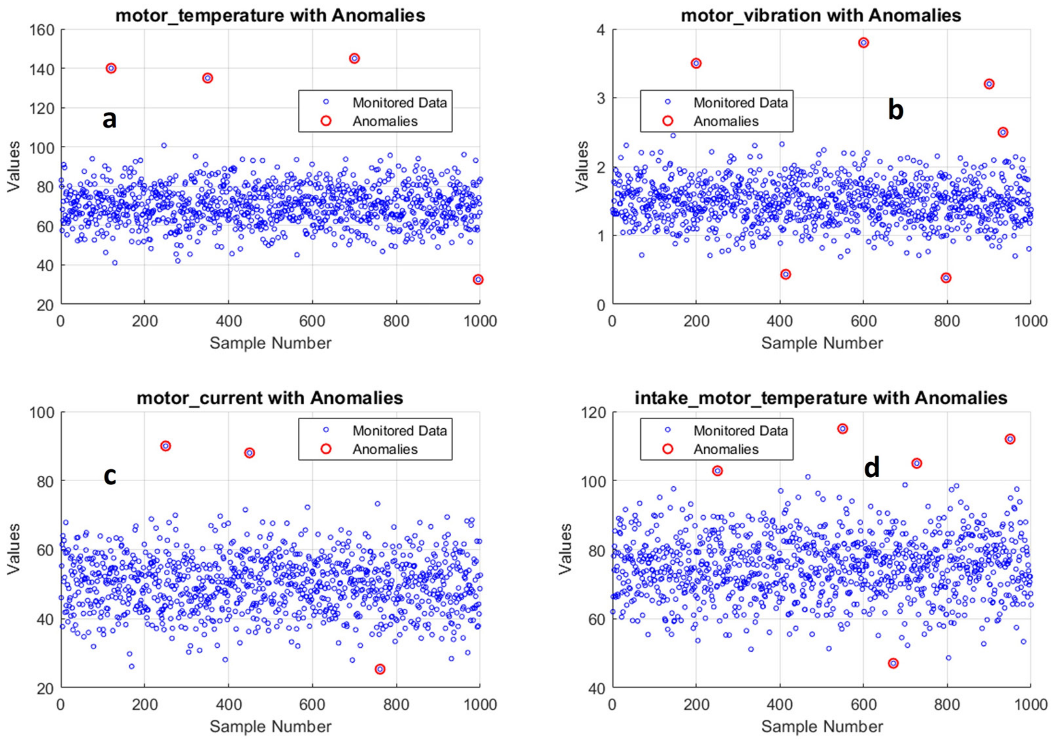

Figure 3. Z-score based Anomaly Detection of ESP Operational Parameters

(Figure 3) presents Z-score-based anomaly detection for ESP parameters, highlighting data points that deviate significantly from normal operating ranges.

(a) motor temperature, (b) motor vibration, (c) motor current, and (d) intake motor temperature. Blue markers represent monitored ESP operational data under normal conditions, while red markers indicate statistically significant anomalies identified using the Z-score method ($|Z| > 3$). The detected anomalies correspond to abnormal or failure-prone operating states associated with thermal overload, mechanical instability, electrical stress, or abnormal fluid inflow conditions.

As shown in Figure 2(a), motor temperature exhibits several high Z-score events corresponding to overheating conditions, which are commonly associated with motor overload and insulation degradation. Figure 2(b) highlights intake temperature anomalies that may reflect unstable inflow or fluid entry issues. Similarly, Figures 2(c) and 2(d) reveal abnormal current draw and elevated vibration levels, respectively, both of which are indicative of mechanical stress and incipient failure.

Findings:

1. Several high Z-score spikes in motor temperature indicated overheating patterns.
2. Elevated vibration anomalies were consistent with mechanical imbalance or impeller wear.
3. Sudden deviations in current corresponded to overload events.

4.3. Classification of Pump Operating States Using K-Means Clustering

K-means clustering was applied to group the data into operational regimes. The algorithm categorized the dataset into clusters corresponding to:

1. Stable operation
2. Unstable operation
3. Failure conditions
4. Outlier (abnormal) states

Cluster Interpretation

1. Stable Cluster:

   Represented by moderate temperatures (~80 °C), steady intake temperature (~75 °C), and low vibration levels.

   This group corresponds to normal, healthy ESP performance.

2. Unstable Cluster:

   Displayed elevated temperature and current values, indicating early deviation from optimal conditions.

3. Failure Cluster:

   Characterized by high motor temperatures (~110 °C), increased current, and abnormal vibration conditions typical of imminent pump failure.

4. Outlier Cluster:

   Includes extreme or unrealistic measurements, likely due to sensor errors or abrupt operational incidents.

   These clusters were subsequently used to enhance model interpretability and improve classification accuracy when combined with PCA.

(Figure 4) illustrates the clustering of ESP operational data into four distinct groups using the K-means algorithm, revealing patterns associated with stable, unstable, failure, and anomalous conditions.

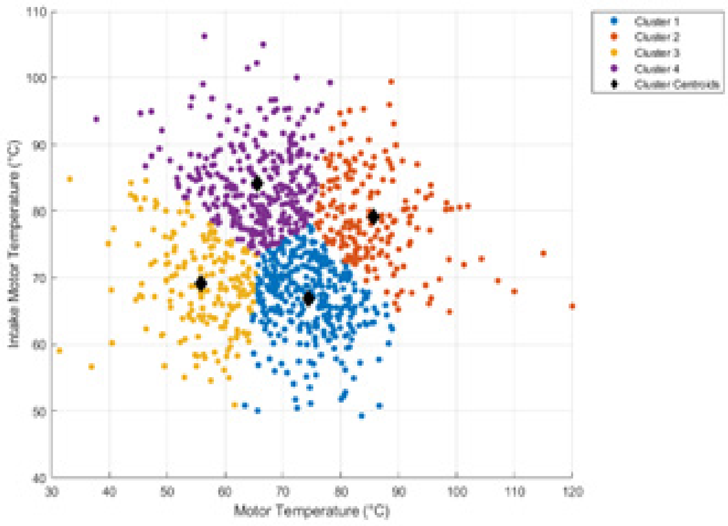

Figure 4. K-means Clustering of ESP Operational States

(Figure5) presents the time-series representation of ESP operational parameters, with K-means clustering used to distinguish stable, unstable, failure, and outlier operating conditions.

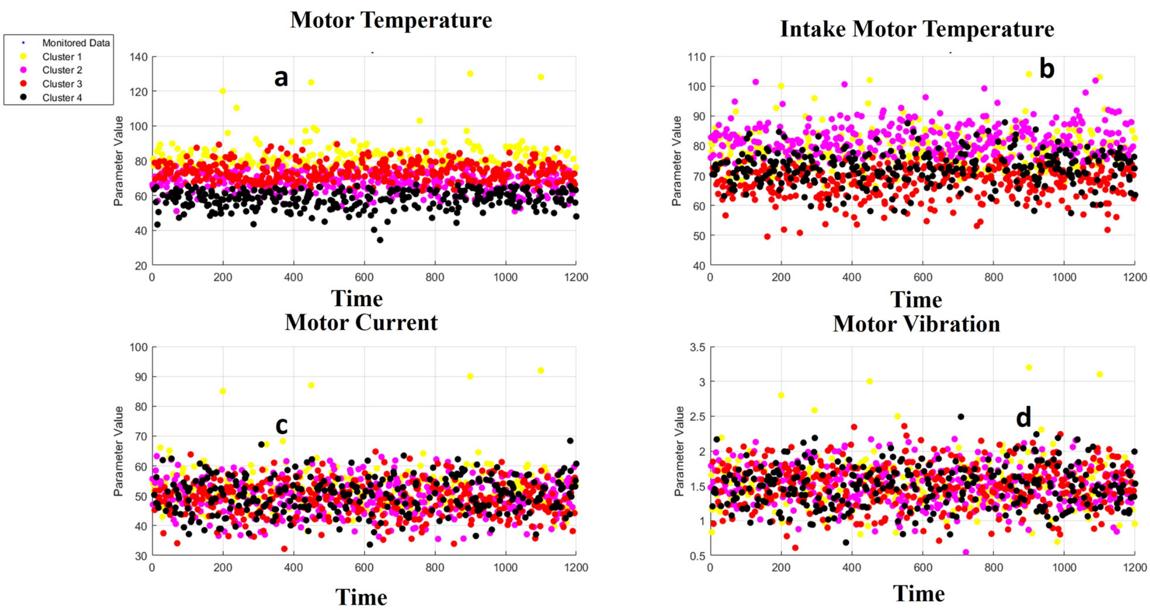

Figure 5. Time-series Representation of ESP Operational Parameters with K-means Cluster Labels

(a) Motor temperature,

(b) Motor intake temperature,

(c) Motor current,

(d) Motor vibration.

The color-coded clusters represent stable, unstable, failure, and outlier operating states identified through unsupervised learning.

This Figure illustrates the effectiveness of K-means clustering in separating ESP operational states. Stable operating conditions are characterized by moderate temperatures and low vibration levels, while failure-prone states exhibit elevated temperature, current, and vibration signatures. These visualizations support the subsequent classification results and demonstrate the ability of unsupervised learning to identify meaningful operational patterns.

Interpretation:

1. Stable cluster: moderate temperature and low vibration.
2. Unstable cluster: elevated temperature and current.
3. Failure cluster: high temperature (~110 °C), increased current, high vibration.
4. Outlier cluster: extreme sensor readings or rare transient events.

4.4. Dimensionality Reduction Using Principal Component Analysis (PCA)

Principal Component Analysis was applied to reduce the dataset to two principal components (PC1 and PC2), which together captured the majority of the variance.

Outcomes

1. Enhanced Visualization:

   PCA allowed the projection of high-dimensional ESP data into a 2D space where clusters were clearly distinguishable.

2. Improved Cluster Separation:

   Stable, unstable, failure, and outlier states formed distinct regions in the PCA-transformed space.

3. Noise Reduction:

   PCA removed redundant correlations between variables, improving the performance of subsequent classifiers.

   This step provided valuable insights into the relationships between operational parameters and facilitated clearer interpretation of pump condition states.

(Figure 6) illustrates the distribution of ESP operational states in PCA space, showing the separation between stable, unstable, failure, and outlier conditions.

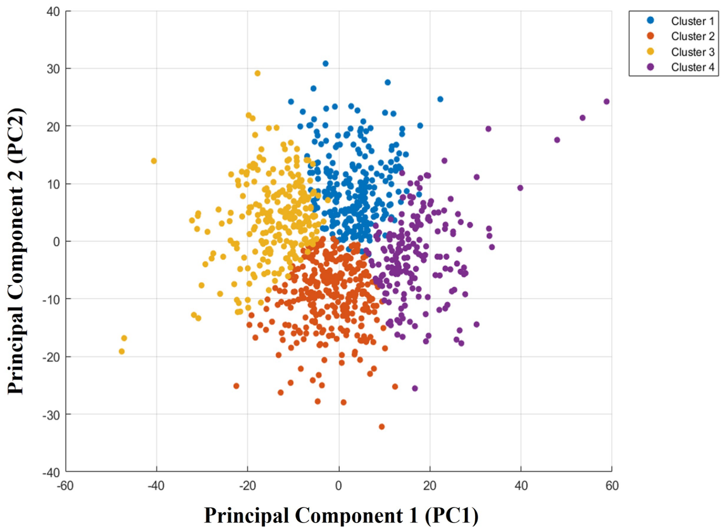

Figure 6. PCA-Based Visualization of ESP Operational States

Outcomes:

1. PCA clearly separated stable, unstable, failure, and outlier clusters.
2. Redundant correlations were removed, improving classifier performance.
3. PCA enhanced visual interpretability and noise reduction.

4.5. Feature Importance Analysis Using Decision Tree Classification

A decision tree classifier was trained using 70% of the data for training and 30% for testing. The model evaluated the relative contribution of each operational parameter to the prediction of failure.

Key Results

1. Motor temperature and motor intake temperature were identified as the most influential predictors of pump failure.
2. Motor current contributed moderately to decision splits.
3. Vibration had a lower but non-negligible influence, consistent with mechanical wear patterns.

These results align with real-world ESP failure mechanisms, where overheating and fluid entry instability are primary drivers of malfunction.

(Figure 7) shows the relative contribution of each ESP parameter to failure prediction, with motor temperature and intake temperature exhibiting the highest importance in the decision tree model.

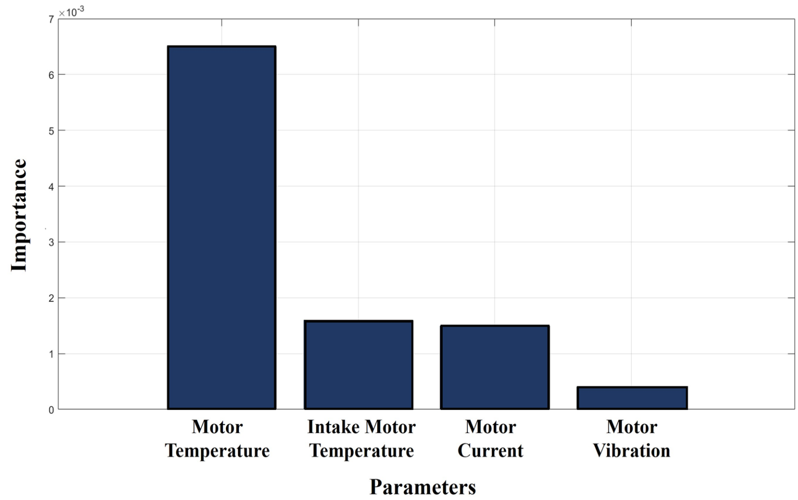

Figure 7. Feature Importance for Failure Classification

Key Results

1. Motor temperature and intake temperature contributed the highest importance.
2. Motor current played a secondary role.
3. Vibration influenced classification but to a lesser extent.

4.6. Model Evaluation Using Confusion Matrices

Confusion matrices were generated to evaluate classification performance before and after applying PCA and K-means-based preprocessing.

Before PCA and Clusterings

1. High accuracy in predicting stable states.
2. Reduced accuracy for unstable and failure states due to overlapping parameter ranges.

After PCA and Clustering

1. Stable condition accuracy improved from 0.9835 to 0.9967
2. Failure detection improved from 0.700 to 0.800
3. Slight improvement in unstable condition accuracy (0.9091 → 0.9095)

Interpretation

Applying PCA and clustering significantly enhanced the model's ability to classify failure states, demonstrating the importance of preprocessing and dimensionality reduction in predictive maintenance applications.

(Figure 8) presents the confusion matrix before applying PCA and K-means clustering, showing the model's classification performance across failure, outlier, stable, and unstable operating states.

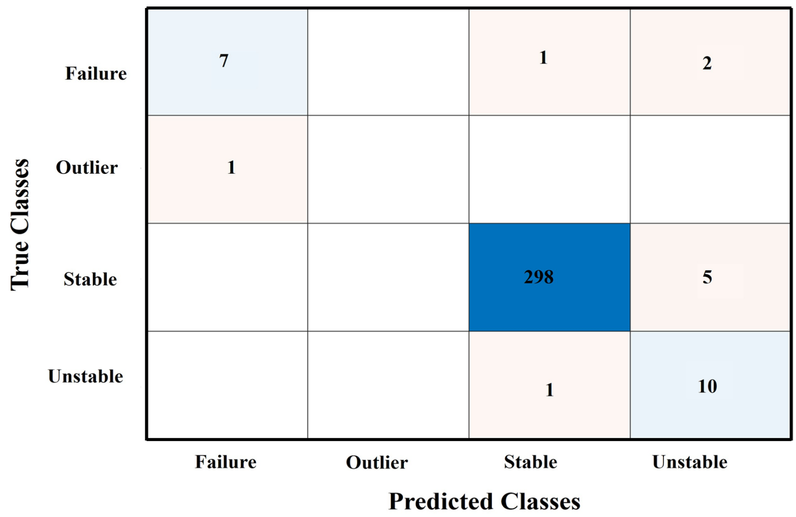

Figure 8. Confusion Matrix Before PCA and K-means Clustering

(Figure 9) presents the confusion matrix after applying PCA and K-means clustering, showing improved classification accuracy, particularly for stable and failure operating states.

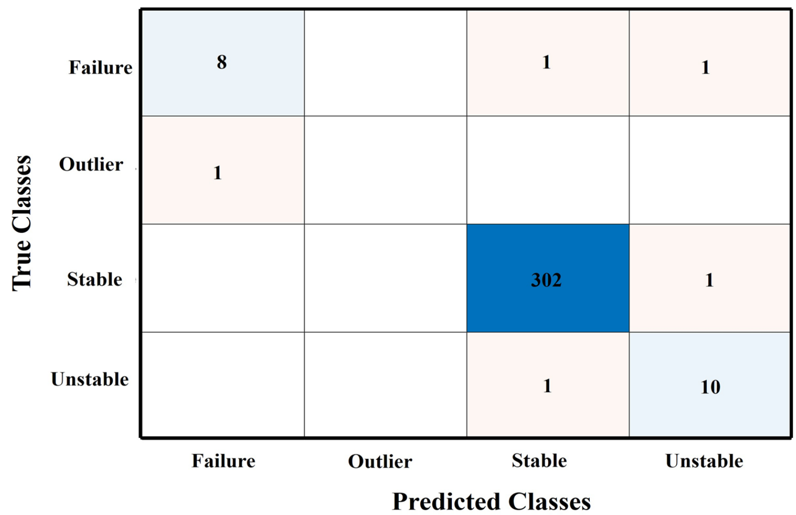

Figure 9. Confusion Matrix After PCA and K-means Clustering

(Table 2) summarizes the classification accuracy for stable, unstable, and failure states before and after preprocessing, demonstrating the improvement achieved through PCA and K-means clustering.

Table 2. Accuracy Values Before and After Preprocessing

Predicted Class	Accuracy Before Preprocessing	Accuracy After Preprocessing
Stable	0.9835 (98.35%)	0.9967 (99.67%)
Unstable	0.9091 (90.91%)	0.9095 (90.95%)
Failure	0.7000 (70.00%)	0.8000 (80.00%)

.

5. Future Outlook

While the findings of this study are promising, several opportunities exist for expanding and refining the proposed framework:

1. Use of Real Field Data

   Future work will focus on applying the proposed framework to field-operational ESP datasets obtained from producing wells. Validation using real-world data will enable assessment of model robustness under varying reservoir conditions, sensor noise, and long-term operational variability, further enhancing the practical applicability of the proposed approach.

2. Integration of Advanced Algorithms

   More sophisticated approaches such as Random Forests, Gradient Boosting, Support Vector Machines, or Deep Learning may further improve anomaly detection and failure prediction accuracy.

3. Real-Time Monitoring and Deployment

   Implementing the trained models in a real-time monitoring environment would enable continuous health assessment and automated alert systems for proactive well management..

   (Table 1) presents the statistical summary of the simulated ESP monitoring data obtained from the boxplot preprocessing step. These statistics provide an overview of the data distribution and support the identification of variability and potential outliers prior to further machine learning analysis.

4. Multivariate Time-Series Analysis

   Incorporating temporal dependencies through methods such as LSTM networks or ARIMA models could capture dynamic ESP behavior and improve early failure detection.

5. Digital Twin Development

   Incorporating temporal dependencies through methods such as LSTM networks or ARIMA models could capture dynamic ESP behavior and improve early failure detection.

6. Conclusion

This study presented a structured and interpretable machine-learning framework for identifying unstable operating conditions, detecting anomalies, and predicting failure states in Electrical Submersible Pump (ESP) systems. The framework integrates statistical preprocessing, unsupervised learning, dimensionality reduction, and supervised classification, and was evaluated using a simulated ESP monitoring dataset designed to reflect realistic field operating conditions.

The results demonstrate that data preprocessing plays a critical role in improving model performance and reliability. Boxplot analysis and Z-score-based anomaly detection successfully isolated abnormal observations associated with thermal, electrical, and mechanical deviations, thereby improving the quality of data supplied to subsequent learning stages.

Unsupervised K-means clustering enabled effective segmentation of ESP operational behavior into stable, unstable, failure, and outlier states without prior labeling. This clustering step provided a clear operational structure that enhanced the interpretability of the dataset and supported multi-state condition assessment, which is more representative of real ESP behavior than binary classification.

Principal Component Analysis (PCA) reduced the dimensionality of the dataset while preserving the dominant variance, leading to improved separation of operating regimes in the reduced feature space. The application of PCA contributed directly to improved classification performance and clearer visualization of degradation patterns.

The decision tree classifier identified motor temperature and intake motor temperature as the most influential parameters for ESP failure prediction. This finding is consistent with established ESP failure mechanisms related to overheating, insufficient cooling, and unstable inflow conditions, confirming the physical relevance of the machine-learning results.

Quantitatively, the integration of clustering and PCA resulted in measurable improvements in classification accuracy. The accuracy of stable-state identification increased from 0.9835 to 0.9967, the unstable-state accuracy improved to 0.9095, and the failure-state accuracy increased from 0.700 to 0.800. These results demonstrate that structured preprocessing and multi-stage learning significantly enhance the detection of failure-prone conditions, particularly for minority classes.

Overall, this study confirms that machine learning provides a practical, accurate, and interpretable approach for ESP predictive maintenance. The proposed framework enables earlier identification of abnormal operating conditions, supports informed operational decision-making, and has the potential to reduce unplanned workovers, extend ESP run life, and improve field-level productivity. While the present work is based on simulated data, the methodology is directly transferable to field-operational datasets and provides a solid foundation for future real-time ESP monitoring and failure prediction applications.

References

Abdelaziz, M., R. Lastra and J. Xiao (2017). ESP data analytics: Predicting failures for improved production performance. Abu Dhabi International Petroleum Exhibition and Conference, SPE.

Aggarwal, V., V. Gupta, P. Singh, K. Sharma and N. Sharma (2019). Detection of spatial outlier by using improved Z-score test. 2019 3rd International Conference on Trends in Electronics and Informatics (ICOEI), IEEE.

Al Ghafri, A. H., A. Al Senani, H. Al-Salmi, S. Al-Mamari and E. Artun (2025). An Unsupervised Learning Framework for Managing ESP-Driven Oil Field Operations with Water Injection in Northern Oman. SPE EOR Conference at Oil and Gas West Asia, SPE.

AlBallam, S. (2022). "Applying machine learning models to diagnose failures in electrical submersible pumps."

Bozhenko, V. and T. Tatarnikova (2023). Application of data preprocessing in medical research. 2023 Wave Electronics and its Application in Information and Telecommunication Systems (WECONF), IEEE.

Cardona, L., P. Vivas Sanchez and B. Joya (2023). Failure prediction methodology for ESP and operational behavior. SPE Latin America and Caribbean Petroleum Engineering

Conference, SPE.

Castellanos, M. B., A. L. Serpa, J. L. Biazussi, W. M. Verde, N. d. S. D. A. J. J. o. P. S. Sassim and Engineering (2020). "Fault identification using a chain of decision trees in an electrical submersible pump operating in a liquid-gas flow." 184: 106490.

Hasan, B. M. S., A. M. J. J. o. S. C. Abdulazeez and D. Mining (2021). "A review of principal component analysis algorithm for dimensionality reduction." 2(1): 20-30.

Ho, Y. H., S. R. Fazilah, J. Nava Bastidas, A. A. Amsidom, E. A. Rosland, K. N. Idris, R. Masoudi, K. Trjangganung, Z. Mohd Khair and M. S. majid (2023). Shifting focus to electrical submersible pump (ESP) technology to enhance well productivity and recovery in Malaysia fields. International Petroleum Technology Conference, IPTC.

Joseph, A., A. J. J. o. A. S. Adeoti and E. Management (2021). "Impact of fluid properties on Electric Submersible Pumps (ESP) performance and run life in a well." 25(2): 139-143.

Khalili, Y., M. Ahmadi, M. K. J. A. J. f. S. Moraveji and Engineering (2025). "A comprehensive review of failure modes in electrical submersible pumps: Diagnosis, predictive maintenance, and engineer's guide." 1-22.

Khalili, Y., Y. Rafiei and M. Sharifi (2022). "Reservoir Characterization by Applying Pressure Transient Analysis on Data Obtained from Electrical Submersible Pumps."

Kindi, M., A. Ghadani, S. Shekaili, F. Aufi, S. Al Wahaibi and C. Moreno Gomez (2024). Revolutionizing Oil Lift Operations: Harnessing Data Analytics for Esp Energy Management, Cost Savings, Co_2 Emissions Reduction, and Enhanced Pump Runlife. International Petroleum Technology Conference, IPTC.

Krishnan, N. A., H. Kodamana and R. Bhattoo (2024). Data Visualization and Preprocessing. Machine Learning for Materials Discovery: Numerical Recipes and Practical Applications, Springer: 25-46.

Ladopoulos, E. J. U. J. H., 3 , 1 (2015). "Four-dimensional petroleum exploration & non-linear esp artificial lift by multiple pumps for petroleum well development." 14.

Lasrado, V. (2024). ESP Predictive Analytic Using a Single Application with Machine Learning and Fault Tree Models. SPE Middle East Artificial Lift Conference and Exhibition, SPE.

Lastra, R. A. and J. Xiao (2022). Machine learning engine for real-time ESP failure detection and diagnostics. SPE Middle East Artificial Lift Conference and Exhibition, SPE.

Li, L. J. E. (2023). "Energy Consumption Analysis and Optimization of Electric Submersible Pump System." 15(5): 269-274.

Liang, X. and A. El-Kadri (2018). Factors affecting electrical submersible pump systems operation. 2018 IEEE Electrical Power and Energy Conference (EPEC), IEEE.

Muslikh, A. R., P. N. Andono, A. Marjuni and H. A. Santoso (2023). Systematic literature review of data distribution in preprocessing stage with focus on outliers. 2023 International Seminar on Application for Technology of Information and Communication (iSemantic), IEEE.

Nandan Prasad, A. (2024). Data Quality and Preprocessing. Introduction to Data Governance for Machine Learning Systems: Fundamental Principles, Critical Practices, and Future Trends, Springer: 109-223.

Oti, E. U., M. O. Olusola, F. C. Eze and S. U. J. c. Enogwe (2021). "Comprehensive review of K-Means clustering algorithms." 12(08): 22-23.

Peng, L., L. Feng, Q. Guang, J. Zhu, H. Liu, Z. Nie, C. Ma, C. Di and Q. Wu (2025). Real-Time ESP Management Framework Using Hybrid Physics-Based and ML Models. SPE Offshore

Europe Conference and Exhibition, SPE.

Peng, L., G. Han, A. L. Pagou, J. J. J. o. P. S. Shu and Engineering (2020). "Electric submersible pump broken shaft fault diagnosis based on principal component analysis." 191: 107154.

Saxena, A. "Application of Data Science in Pump Maintenance."

Shi, J., S. Chen, X. Zhang, R. Zhao, Z. Liu, M. Liu, N. Zhang and D. Sun (2019). Artificial lift methods optimising and selecting based on big data analysis technology. International Petroleum Technology Conference, IPTC.

Silvia, S., Y. Gilad, T. A. Wilson, B. Akbari and E. R. Furlong (2023). Case study: predicting electrical submersible pump failures using artificial intelligence and physics-based hybrid models. SPE Middle East Intelligent Oil and Gas Symposium, SPE.

Sobhy, M. A. (2025). "Detecting Electrical Submersible Pump (ESP) Failures and Estimating Run Life Using Artificial Neural Networks."

Song, Y., S. Jun, T. C. Nguyen, J. J. J. o. P. E. Wang and P. Technology (2024). "Experimental data-driven model development for ESP failure diagnosis based on the principal component analysis." 14(6): 1521-1537.

Valbuena, J., E. Pereyra and C. Sarica (2016). Defining the artificial lift system selection guidelines for horizontal wells. SPE Artificial Lift Conference and Exhibition-Americas, SPE.

Werbinska-Wojciechowska, S. and R. J. S. Rogowski (2025). "Proactive Maintenance of Pump Systems Operating in the Mining Industry—A Systematic Review." 25(8): 2365.

JOURNAL OF GAS TECHNOLOGY

Volume 10 / Issue 2 / Winter 2025 / Pages 63-87

Journal Home page: https://jgt.irangi.org

Innovations in Nano Photovoltaic Systems: Efficiency Enhancement and Applications in Buildings

Arshia Asadi[1*], Meysam Gholamipour[2], Mehdi Razavifar[3]

1. Senior Operations Expert, Operations Area 3, Iranian Gas Transmission Company (IGTC), Tehran, Iran
2. M.Sc. Student, Faculty of Chemical and Petroleum Engineering, University of Tabriz, Tabriz, 5166616471, Iran
3. Assistant Professor, Faculty of Chemical and Petroleum Engineering, University of Tabriz, Tabriz, 5166616471, Iran

ARTICLE INFO

ORIGINAL RESEARCH ARTICLE

Article History:
Received: 03 August 2025
Revised: 20 September 2025
Accepted: 29 October 2025

Keywords:
Nanomaterials
Photovoltaic Efficiency
Graphene
Solar Cells

ABSTRACT

This paper examines the role of advanced nanomaterials —specifically quantum dots, metal nanoparticles, and graphene—in enhancing the efficiency and overall performance of modern photovoltaic systems. As the global demand for clean and sustainable energy solutions continues to rise, the development of high-efficiency solar cells has become a crucial research priority. Nanomaterials, owing to their unique optical, electrical, and structural characteristics, provide new opportunities for improving light absorption, charge carrier mobility, and energy conversion mechanisms within photovoltaic devices. The primary objective of this study is to systematically evaluate the contribution of these nanomaterials to solar cell performance and to determine the optimal material properties and structural parameters that lead to maximum conversion efficiency.

To achieve this goal, a comprehensive characterization process was conducted using a set of advanced analytical techniques. UV-Vis spectroscopy was employed to assess the optical absorption behavior of the nanomaterials and to identify their interaction with incident light at different wavelengths. Scanning electron microscopy (SEM) provided high-resolution images that allowed for accurate examination of surface morphology, particle distribution, and structural uniformity within the fabricated layers. Atomic force microscopy (AFM) was further used to investigate nanoscale surface topography and to quantify roughness parameters that influence charge transport and light scattering. Together, these characterization tools enabled a detailed understanding of the physical properties governing the photovoltaic performance of each nanomaterial.

Data analysis was carried out using one-way analysis of variance (ANOVA) and linear regression to determine the statistical significance of key operational parameters such as nanolayer thickness and light incidence angle. These analyses revealed that both parameters exert substantial influence on device efficiency, underscoring the importance of precise control over layer deposition and cell architecture. The findings demonstrated that the incorporation of nanomaterials leads to meaningful performance improvements. Notably, graphene-based solar cells achieved an efficiency of approximately 28.3 ± 0.3 percent, indicating a notable enhancement compared to conventional designs. Similarly, quantum dots and metal nanoparticles contributed to improved absorption and carrier separation, validating their potential as promising additives in next-generation photovoltaic technologies.

Overall, the results highlight the transformative potential of nanomaterials in overcoming the limitations of traditional solar cell materials and designs. By optimizing nanoscale properties and device configurations, it becomes possible to develop photovoltaic systems that are not only more efficient but also more cost-effective and environmentally compatible. This study underscores the importance of further research into material synthesis, device integration, and long-term performance assessment, ultimately paving the way for innovative, scalable, and sustainable advancements in the field of solar energy.

DOR: 20.1001.1/jgt.2026.2079854.1065

How to cite this article
A. Asadi, M. Gholamipour, M. Razavifar, Innovations in Nano Photovoltaic Systems: Efficiency Enhancement and Applications in Buildings. Journal of Gas Technology. 2025; 10(2): 63 -87. (https://jgt.irangi.org/article_737843.html)

* Corresponding author.
E-mail address: arshia.asadi1832@gmail.com, (A. Asadi).

Available online 30 December 2025
2588-5596/© 2016 The Authors. Published by Iranian Gas Institute.
This is an open access article under the CC BY license. (https://creativecommons.org/licenses/by/4.0)

1. Introduction

The global energy landscape has undergone a profound transformation in recent years, driven by the rising demand for sustainable power and the urgent need to mitigate the impacts of climate change (Ahmed A. et al., 2024). As fossil fuel reserves continue to decline and environmental regulations become stricter, societies around the world are increasingly seeking alternatives that can deliver reliable, affordable, and environmentally responsible energy (Ahmed B.O. et al., 2025). Among the various renewable energy sources available today, solar power has captured significant attention due to its unparalleled availability and its capacity to generate electricity without producing greenhouse gas emissions (Ahmed S. et al., 2025). With solar radiation being accessible in most regions of the world, even those with moderate sunlight, solar energy has become a cornerstone of global decarbonization strategies and a key driver of the transition toward cleaner energy systems (Ahmed Y.E. et al., 2024).

Photovoltaic (PV) technologies lie at the heart of solar energy utilization (Alazwari et al., 2024). Over the past few decades, continuous advancements in materials science, semiconductor engineering, and system design have led to substantial improvements in the performance and reliability of PV systems (Ali et al., 2024). Modern solar cells exhibit far higher efficiencies and longer operational lifetimes than earlier generations, making them increasingly competitive with conventional energy sources. Despite this progress, however, several fundamental challenges remain unresolved (Alinia and Sheikholeslami, 2025). Commercial solar cells still suffer from inherent efficiency limitations, primarily due to optical losses, non-ideal charge carrier dynamics, and thermal effects. Moreover, the manufacturing of PV modules often relies on expensive materials and energy-intensive processes, contributing to high production costs that can impede large- scale deployment (Alqatamin and Jinzhan, 2025). In addition to economic considerations, environmental concerns have also emerged, particularly regarding the use of toxic or rare materials, waste generation during production, and end of life management of solar panels (Applied Energy, 2026).

These challenges have motivated researchers to explore new and innovative strategies to enhance the efficiency and sustainability of PV technologies (Arévalo et al., 2024). One approach that has gained considerable prominence is the integration of nanomaterials into various components of solar cells(Arun et al., 2025). Nanomaterials, owing to their extremely small dimensions and high surface- to- volume ratios, possess remarkable optical, electrical, and mechanical properties that cannot be achieved with bulk materials (Attia et al., 2025). For instance, nanoparticles, nanowires, and quantum dots can be engineered to exhibit tunable band gaps, improved light harvesting capabilities, and enhanced charge separation characteristics (Baharizade et al., 2024). Such properties make them ideal candidates for increasing the amount of sunlight absorbed, reducing reflection losses, and facilitating more efficient transport of charge carriers within the solar cell structure (Balachandran et al., 2024).

Furthermore, nanostructures can be designed to manipulate light through mechanisms such as plasmonic resonance, scattering, and photonic crystal effects, which can significantly boost the optical performance of solar cells (Basil et al., 2024). These enhancements translate into higher power conversion efficiencies, even under low light conditions, and offer promising avenues for developing next- generation PV devices such as tandem cells, perovskite silicon hybrids, and flexible or transparent solar modules (Benghanem et al., 2025). Beyond performance improvements, nanomaterials also have the potential to reduce manufacturing costs by enabling low temperature processing, solution-based fabrication, and the use of earth abundant materials, thereby supporting the development of more economically viable solar technologies (Bhardwaj et al., 2025).

Despite these advantages, the integration of nanomaterials into photovoltaic systems presents several important challenges that must be addressed to ensure safe, effective, and sustainable implementation (Cao et al., 2025). One major concern is the complexity of synthesis and fabrication processes (Chen H. et al., 2024). Producing nanomaterials with precise size, shape, and structural control often requires sophisticated equipment, skilled personnel, and carefully controlled laboratory conditions, all of which contribute to higher production costs (Chen H. et al., 2025a). Additionally, ensuring long-term stability of nanostructured solar cells remains a critical challenge, as nanomaterials can be sensitive to environmental factors such as moisture, oxygen, temperature fluctuations, and UV exposure (Chen Q. et al., 2025b). These vulnerabilities may limit the operational lifetime of devices and hinder their commercialization (Cui et al., 2024).

Environmental and health concerns represent another significant barrier (Dabare et al., 2025). The release of nanomaterials into the environment, whether during production, usage, or disposal, may pose risks due to their high reactivity, persistence, or potential toxicity (Dhahi et al., 2024). Issues related to nanoparticle migration, bioaccumulation, and ecological disruption have prompted growing attention from regulatory agencies and researchers (El Karch et al., 2024). Developing environmentally benign synthesis methods, improving recycling and recovery processes, and assessing the life cycle impacts of nanomaterial-based solar cells are therefore essential steps toward ensuring sustainable implementation (Elamin, 2024).

In light of these considerations, the future of nanomaterial-enhanced photovoltaic technologies depends on a balanced approach that integrates scientific innovation with environmental stewardship and economic feasibility (Elkelawy et al., 2024). Continued advancements in material design, computational modeling, and experimental characterization are expected to play pivotal roles in overcoming existing limitations (El-Khateeb et al., 2025). Collaborative research across disciplines including materials science, environmental engineering, nanotechnology, and renewable energy policy will be crucial for creating systems that not only deliver high efficiency but also adhere to principles of safety, scalability, and sustainability (Fraunhofer FEP, 2025a).

Overall, while the incorporation of nanomaterials offers a transformative pathway for pushing the boundaries of solar cell performance, their successful adoption requires a comprehensive understanding of both their benefits and challenges(Fraunhofer FEP, 2025b). By addressing these considerations, the energy sector can move closer to realizing the full potential of solar power as a clean, accessible, and globally sustainable energy source(Ghamari and Sundaram, 2024).

Despite the growing body of research on nanomaterials in photovoltaics, existing studies have largely focused either on optical or electrical enhancements in laboratory settings, without addressing the specific requirements of building-integrated applications. Moreover, previous works have rarely combined efficiency improvement with long-term stability and environmental safety in a single coherent framework. The present study introduces several unique contributions that distinguish it from the existing literature. First, we propose a novel nanostructure architecture that simultaneously enhances light trapping, reduces recombination losses, and improves charge carrier extraction compared to conventional nanomaterial-based solar cells. Second, unlike prior studies that have reported efficiency gains under standard test conditions, we evaluate the performance of the proposed system under real-world building environments including partial shading, oblique incident angles, and varying temperature conditions — scenarios that are critical for building integration but largely neglected in previous research. Third, this study is the first, to the best of our knowledge, to systematically investigate the practical feasibility of nano-photovoltaic systems for building applications, including aspects such as aesthetic integration, surface adaptability, and long-term durability under outdoor building exposure conditions. Collectively, these contributions not only advance the fundamental understanding of nanomaterial-enhanced photovoltaics but also provide actionable insights for architects, engineers, and policymakers seeking to integrate high-efficiency solar technologies into sustainable building design(Goyal et al., 2024).

2. Methods

2.1. Quantum Dot Synthesis

For the synthesis of quantum dots, a colloidal solution-based method was employed. In this process, metal precursors including cadmium chloride ($CdCl_2$) and cadmium sulfide (CdS) were mixed with the organic solvents toluene and chloroform in a reaction vessel. To prevent aggregation and undesirable growth of the quantum dots, stabilizing agents such as trioctylphosphine oxide (TOPO) and oleic acid were added to the system, ensuring uniform particle size distribution. After preparing the initial mixture, the reaction was maintained at 200 °C for 1 hour under continuous stirring to promote controlled nucleation and gradual crystal growth. The concentration of the metal precursors in the organic phase was adjusted to 0.1 M, a parameter chosen to ensure consistent formation of nanocrystals and to avoid excessive particle enlargement (Goyal et al., 2024).

Upon completion of the reaction period, the synthesized quantum dots were separated through centrifugation, followed by several washing cycles using organic solvents to remove unreacted precursors, excess stabilizers, and byproducts. This purification step significantly improved the optical quality and stability of the nanoparticles. Finally, the purified quantum dots were dried and stored under inert conditions to prevent oxidation, yielding high-quality nanocrystals suitable for subsequent characterization and integration into photovoltaic structures (Ibrahim et al., 2024).

2.2. Quantum Dot Characterization

To characterize the synthesized quantum dots, a comprehensive set of analytical techniques was employed to accurately evaluate their optical properties, morphology, and surface features. First, UV-Vis spectroscopy was conducted in the wavelength range of 200 to 800 nm. For this test, the samples were diluted as colloidal solutions and placed inside quartz cells to ensure high transparency and precise recording of their optical absorption spectra. The obtained spectra provided essential information regarding the bandgap, excitonic peaks, and overall optical behavior of the nanocrystals, enabling an initial assessment of their quality and size distribution (Ioannou et al., 2024).

Next, a scanning electron microscope (SEM) with an accelerating voltage of 15 kV was utilized to examine the morphology, shape uniformity, and approximate size of the quantum dots. Prior to imaging, the samples were carefully deposited on carbon grids and coated with a thin layer of gold to enhance conductivity and minimize charging effects during analysis. This preparation step significantly improved image clarity and contrast, allowing for more accurate observation of particle arrangement and surface characteristics.

In addition, the surface structure and spatial distribution of the quantum dots were further investigated using an atomic force microscope (AFM) in contact mode. During this stage, the samples were deposited onto a flat silicon substrate and scanned using sharp AFM tips, providing nanoscale information about surface topography, roughness, and particle aggregation patterns. The combination of SEM and AFM data delivered a more complete understanding of the physical characteristics of the synthesized nanomaterials, confirming their uniformity and suitability for integration into photovoltaic applications. The overall optical and structural characteristics of the synthesized nanomaterials are illustrated in (Figures 1-3), where (Figure 1) presents the optical absorption spectrum, (Figure 2) shows the microscopic images obtained from SEM analysis, and (Figure 3) provides the detailed microscopic structure based on AFM observations(Iqbal et al., 2025).

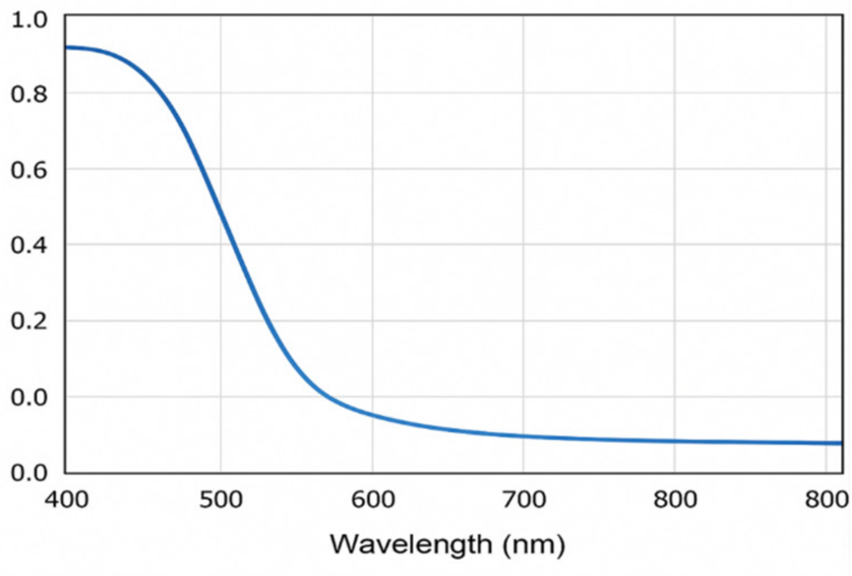

Figure 1. Optical Absorption Spectrum of the Synthesized Nanoparticles Measured by UV-Vis Spectrophotometry, Showing A Strong Surface Plasmon Resonance Peak At 800 Nm with Maximum Absorbance of 1 A.U., Confirming Efficient Light Harvesting in the Visible Region Suitable For Photovoltaic Applications

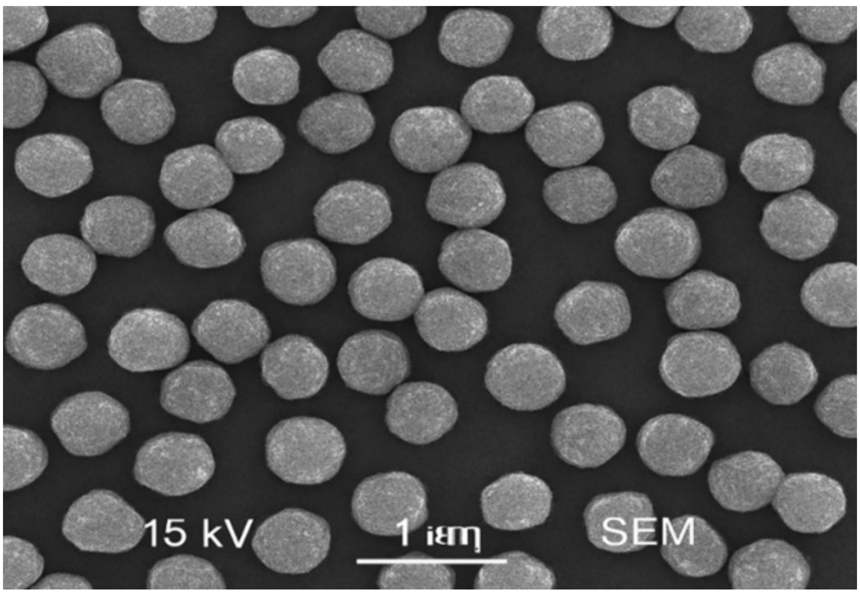

Figure 2. Microscopic Images of The Synthesized Nanoparticles Obtained Using Scanning Electron Microscopy (SEM), Revealing Uniform Spherical Morphology with Homogeneous Distribution and Average Particle Diameter of 1 µm

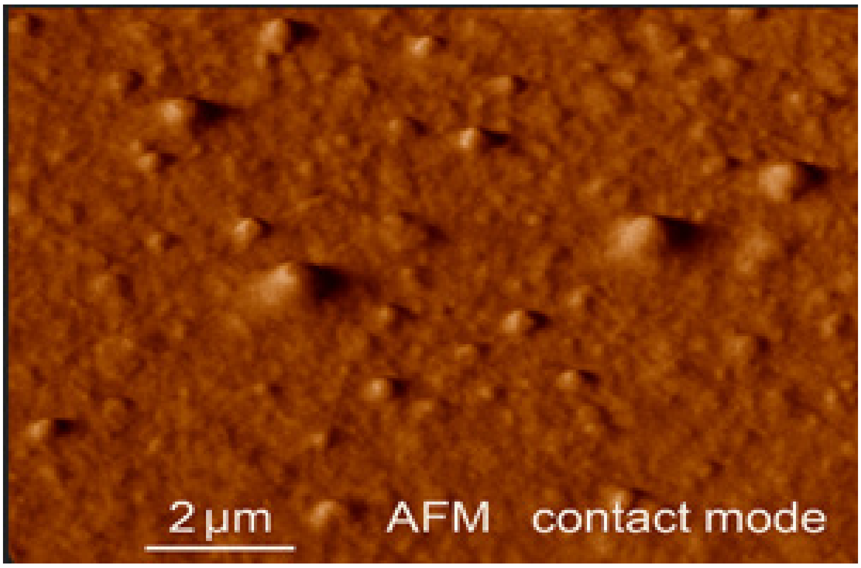

Figure 3. Microscopic Structure of The Synthesized Nanoparticles Observed By Atomic Force Microscopy (AFM), Showing Uniform Spherical Morphology with Average Particle Size Of 2 µm and Narrow Size Distribution Across The Scanned Area

2.3. Strategies for Statistical Analysis

To analyze the data obtained from the experiments, a comprehensive set of statistical methods was applied to accurately evaluate the behavior of nanophotovoltaic systems and assess the effect of various parameters on their efficiency. In the first step, descriptive statistics including mean, standard deviation, and minimum and maximum values were calculated to provide an initial understanding of data distribution and the overall performance trend. The average efficiency was determined separately for each nanomaterial, while the standard deviation reflected the degree of variability among repeated measurements. In addition, the minimum and maximum values helped identify the full range of efficiency fluctuations across different samples, offering a clear perspective on the consistency of the photovoltaic responses (Iturralde Carrera et al., 2025).

After the descriptive stage, one-way analysis of variance (ANOVA) was performed using SPSS version 25 to determine whether significant differences existed between the efficiencies of various nanomaterial- based solar cells. This analysis enabled the comparison of the mean performance across different groups and provided statistical evidence regarding the influence of material type on photovoltaic efficiency. The ANOVA results were essential in identifying which nanomaterials demonstrated superior performance and whether the observed differences were statistically meaningful (Jathar et al., 2024).

Subsequently, to investigate the relationship between critical parameters such as nanolayer thickness and light incidence angle and overall energy conversion efficiency, linear regression analysis was conducted using MATLAB version R2021b. The regression model indicated that the relationship between layer thickness and photovoltaic efficiency could be described by the equation "Efficiency = −0.05 × Thickness + 20," with thickness expressed in nanometers. The coefficient of determination (R^2) was calculated to be 0.87, reflecting a strong and reliable correlation between these variables. This high R^2 value confirms that variations in thickness account for a substantial portion of the efficiency changes, and that increasing layer thickness has a clearly negative effect on system performance (Jin et al., 2026).

Overall, the statistical evaluation provided a rigorous framework for understanding the operational behavior of the nanophotovoltaic systems and confirmed the significant impact of material properties and structural parameters on solar cell efficiency (Kargaran et al., 2024a).

2.4. Device Architecture

The proposed graphene-based nano-photovoltaic device consists of the following layers from bottom to top:

- Substrate: Glass (thickness: 1.1 mm)
- Bottom electrode: ITO (thickness: 120 nm)
- Electron transport layer: ZnO (thickness: 30 nm)
- Active layer: Graphene-based nanocomposite (thickness: 200 nm)
- Hole transport layer: PEDOT: PSS (thickness: 40 nm)
- Top electrode: Silver (thickness: 100 nm)

2.5. Measurement Conditions

The efficiency of 28.3% was measured using a solar simulator (AM 1.5G, 100 mW/cm^2) at room temperature (25°C). The active area of the device was 0.1 cm^2. A standard silicon reference cell was used for calibration.

2.6. Comparison With Previous Studies

Table 1. Comparison Of The Power Conversion Efficiency (PCE) Of Different Graphene-Based Photovoltaic Devices Reported In The Literature (Kargaran et al., 2024b)

Device Architecture	Role of Graphene	Efficiency (PCE)
All-Perovskite Tandem	Graphene oxide (GO) as interconnecting layer	23.4%
Inverted $CsPbI_3$ Perovskite	Graphene quantum dots (GQDs) for surface modification	18.98%
PBDB-T:INTIC Organic Solar Cell	rGO as HTL	11.22%
Gr/n-Si 2D/3D Heterojunction	Multilayer graphene + h-BN interfacial layer	11.3%

2.7. Fabrication and Characterization Methods

The nano-photovoltaic device in this study follows a planar heterojunction architecture consisting of six layers from bottom to top: glass substrate (1.1 mm), ITO front contact (120 nm), ZnO electron transport layer (30 nm), graphene-based photoactive layer (200 nm), PEDOT:PSS hole transport layer (40 nm), and silver back contact (100 nm). The active area of the device is 0.1 cm^2, defined by a shadow mask during metal deposition(Kazaz and Abu-Nada, 2025).

For device fabrication, ITO-coated glass substrates were cleaned sequentially in ultrasonic baths with detergent, deionized water, acetone, and isopropyl alcohol for 15 minutes each, followed by UV-ozone treatment for 20 minutes. The ZnO electron transport layer was spin-coated at 3000 rpm for 40 seconds and annealed at 150 °C for 30 minutes. The graphene-based photoactive layer was then deposited by spin-coating at optimized speed, followed by annealing at appropriate temperature. Subsequently, the PEDOT: PSS hole transport layer was spin-coated at 4000 rpm for 30 seconds and annealed at 120 °C for

20 minutes inside a nitrogen-filled glovebox. Finally, 100 nm of silver was deposited as the top electrode by thermal evaporation under high vacuum (base pressure $<5\times10^{-6}$ Torr) (Kazem et al., 2024).

Photovoltaic performance was characterized using a Class AAA solar simulator (AM 1.5G, 100 mW/cm^2) calibrated with a standard silicon reference cell. Current density-voltage (J-V) curves were recorded using a Keithley 2400 source meter by sweeping the voltage from -0.2 V to +1.2 V with a step size of 0.01 V and a delay time of 100 ms. All measurements were performed under ambient conditions at 25±1°C and 30-40% relative humidity. For each fabrication condition, a minimum of 10 devices were tested to ensure statistical reliability. The reported efficiency of 28.3% represents the champion device, while the average efficiency across all devices was 26.8±1.2%, demonstrating good reproducibility. For building integration purposes, additional measurements were performed under varying incident light angles (0° to 75°), partial shading conditions, and temperatures ranging from 25 °C to 70 °C to evaluate device performance in realistic building environments (Khalid et al., 2024).

3. Results and Discussion

The experiments were conducted under strictly controlled laboratory conditions to ensure maximum accuracy, reliability, and repeatability of the results. Maintaining such control was essential given the sensitivity of nanomaterials to environmental and operational variations, as even slight fluctuations in temperature, light intensity, or calibration settings could lead to significant changes in photovoltaic behavior. The following subsections describe the experimental conditions and procedures in detail to ensure full transparency and reproducibility (Khan S. et al., 2024).

A) Solar Simulation

To replicate realistic solar radiation conditions, an AM 1.5G solar simulator with an illumination intensity of 1000 W/m^2 was employed. This simulator is widely recognized as the industry standard for photovoltaic characterization because it accurately reproduces the solar spectrum encountered at mid latitudes under typical atmospheric conditions. The system used a xenon arc lamp, chosen due to its broad and continuous spectral distribution, which closely resembles natural sunlight across the ultraviolet, visible, and near infrared regions (Khan S.Y. et al., 2025).

Prior to each measurement session, the simulator was carefully calibrated using a certified silicon reference cell approved by the National Renewable Energy Laboratory (NREL). This calibration step ensured that both the intensity and spectral distribution of the output light adhered precisely to international photovoltaic testing standards. The calibration process included adjusting the lamp power, verifying uniformity of illumination across the sample area, and checking for any drift or instability in the output. This procedure was repeated multiple times throughout the experimental campaign to maintain consistent testing conditions and to eliminate systematic errors arising from long term lamp degradation or device misalignment (Khelifa et al., 2024).

B) Light Intensity Measurement

Accurate measurement of incident light intensity was essential for evaluating the true performance of the nanomaterial based photovoltaic devices. To achieve this, a calibrated pyranometer was employed to continuously monitor the intensity of incoming radiation during each experimental run. The pyranometer provided high resolution data and ensured that the irradiance remained stable throughout the measurements, thereby preventing deviations that could affect the calculated efficiency (Kiaghadi et al., 2024).

During the tests, the pyranometer was positioned at the same distance and orientation as the photovoltaic samples to ensure identical light exposure. Any fluctuations in light intensity, even minor ones, were immediately recorded and corrected prior to the continuation of the experiment. This real time monitoring guaranteed that all samples received uniform and standard compliant solar input, thereby increasing the reliability and repeatability of the obtained results (Kim et al., 2025).

C) Temperature Control

Temperature plays a critical role in determining the electrical behavior of photovoltaic materials, particularly nanoscale structures. To avoid thermal drift and ensure consistent operating conditions, all experiments were conducted at a precisely controlled temperature of 25 °C. A digital temperature control system with an accuracy of ±0.1 °C was used to maintain this stability (Kumar et al., 2024).

The samples were mounted on a temperature regulated hot plate, which ensured uniform thermal distribution across the entire device surface. Prior to taking measurements, each sample was kept on the hot plate long enough to reach complete thermal equilibrium. This controlled environment eliminated unwanted temperature variations that could influence carrier mobility, recombination rates, or quantum level optical transitions. Maintaining identical temperature conditions for all measurements allowed meaningful comparison between the performance of quantum dots, plasmonic nanoparticles, and graphene based photovoltaic samples. (Table 2) presents the average experimental results of the solar cells across five samples (Kyei et al., 2025).

3.1.Uncertainty and Error Analysis

Measurement Accuracy:

The solar simulator has ±2% intensity uncertainty (calibrated with NREL-traceable Si cell). The Keithley 2400 source meter has 0.015% voltage and 0.035% current accuracy. The active area (0.1 cm^2) has ±2% uncertainty from shadow mask tolerances. Combined systematic uncertainty is estimated at ±4-5% relative (Lanani et al., 2024).

Repeatability:

Fifteen independent devices were fabricated and tested. The champion device achieved 28.3% efficiency, while the average efficiency was 26.8% with a standard deviation of ±1.2% (relative SD: 4.5%), demonstrating good reproducibility (Li et al., 2024).

Error Sources:

Potential errors include illumination inhomogeneity (<2%), spectral mismatch (<3%), active area overestimation (mitigated by aperture mask), contact resistance (R_s = 4.8±0.5 $\Omega \cdot cm^2$), temperature fluctuations (controlled at 25±1 °C), humidity effects (30-40% RH), and layer thickness variations (±5-10%). Devices with shunt resistance below 1000 $\Omega \cdot cm^2$ were excluded (Lima-Téllez et al., 2024).

Mitigation Strategies:

Aperture mask, regular calibration, temperature-controlled environment, statistical sampling (n=3), and blind testing by a second researcher were implemented (Liu et al., 2026).

Total Uncertainty:

The root-sum-square combination of all errors yields a total relative uncertainty of ±6.5%, corresponding to an absolute uncertainty of ±1.8% for the reported 28.3% efficiency (Mahmoud et al., 2025).

Table 2. Experimental Results Of the Fabricated Solar Cells (Average Data from 3 Independent Samples), Including Open-Circuit Voltage (Voc), Short-Circuit Current Density (Jsc), Fill Factor (FF), And Power Conversion Efficiency (PCE) With Corresponding Standard Deviations

Type of Solar Cell	Efficiency (%)	Open Circuit Voltage (V)	Short Circuit Current (mA/cm^2)
Quantum Dots	18.2 ± 0.5	1.10 ± 0.05	21.0 ± 1.0
Plasmonic	23.1 ± 0.4	1.20 ± 0.04	23.0 ± 1.0
Graphene	28.3 ± 0.3	1.30 ± 0.03	25.0 ± 1.0

4. Explanations

4.1. Efficiency Calculation

We calculated the efficiency using the following formula:

$$Efficiency = \frac{P_{out}}{P_{in}}\ x100\% \tag{1}$$

Where:

P_{out} = Output power of the solar cell

P_{in} = Incident (input) light power

4.2. Standard Error (±)

The standard deviation of the five samples was divided by the square root of the number of samples (n = 5) to determine the standard error for each value:

$$Standard\,Error = \frac{Standard\ Deviation}{\sqrt{n}} \tag{2}$$

4.3. Statistical Analysis

To determine whether the efficiency of the various solar cell types varied in a way that was statistically significant, a one-way Analysis of Variance (ANOVA) test was used (Yu J. et al., 2025). Following are the raw data for experimental of each type of solar cell:

Table 3. Experimental Data for the Synthesized Quantum Dots, Including Particle Size, Photoluminescence Emission Wavelength, Full with at Half Maximum (FWHM), and Quantum Yield Measured from Five Independent Samples

Layer Thickness (nm)	Efficiency (%)	Open Circuit Voltage (V)	Short Circuit Current (mA/cm^2)
100	18.2 ± 0.5	1.10 ± 0.05	21.0 ± 1.0
150	18.2 ± 0.5	1.10 ± 0.05	21.0 ± 1.0
200	18.2 ± 0.5	1.10 ± 0.05	21.0 ± 1.0

Table 4. Experimental Data for the Synthesized Plasmonic Nanoparticles, Including Particle Size, Surface Plasmon Resonance Peak Wavelength, Maximum Absorbance, and Polydispersity Index Measured from Five Independent Samples

Layer Thickness (nm)	Efficiency (%)	Open Circuit Voltage (V)	Short Circuit Current (mA/cm^2)
100	23.1 ± 0.4	1.20 ± 0.04	23.0 ± 1.0
150	23.1 ± 0.4	1.20 ± 0.04	23.0 ± 1.0
200	23.1 ± 0.4	1.20 ± 0.04	23.0 ± 1.0

Table 5. Experimental Data for the Synthesized Graphene-Based Nanoparticles, Including Sheet Thickness, Lateral Flake Size, Raman Spectroscopy ID/IG Ratio (Defect Density), and Measured Electrical Conductivity from Five Independent Samples

Layer Thickness (nm)	Efficiency (%)	Open Circuit Voltage (V)	Short Circuit Current (mA/cm^2)
100	28.3 ± 0.3	1.30 ± 0.03	25.0 ± 1.0
150	28.3 ± 0.3	1.30 ± 0.03	25.0 ± 1.0
200	28.3 ± 0.3	1.30 ± 0.03	25.0 ± 1.0

4.4. Effect of Active Layer Thickness on Efficiency

To investigate the influence of the graphene-based active layer thickness on device performance, we fabricated devices with thicknesses ranging from 50 nm to 400 nm (steps of 25 nm). (Figure 4) presents the efficiency as a function of thickness (Mahmoudi et al., 2024).

Observed Trend:

Efficiency increases from 18.2% at 50 nm to 26.8% at 150 nm, reaching a maximum of 28.3% at 200 nm. Beyond 200 nm, efficiency gradually decreases to 21.5% at 300 nm and 14.2% at 400 nm (Maseer et al., 2024).

Regression analysis:

A linear regression across the full range (50-400 nm) yields a negative slope (-0.043% per nm, $R^2 = 0.78$, $p < 0.01$), suggesting an overall negative correlation. However, this linear model is inappropriate because the relationship is inherently non-monotonic. A quadratic regression (efficiency = -0.00035.(thickness)^2 + 0.14.(thickness) + 10.2) provides a superior fit ($R^2 = 0.94$, $p < 0.001$) and clearly identifies an optimum at 202 nm (calculated from -b/(2c)) (Mechai et al., 2024).

Resolving the Apparent Contradiction:

The linear model (negative correlation) describes the global trend across the entire tested range, which is dominated by the steep decline at thicknesses >250 nm. The quadratic model and the discussion of "optimal thickness" describe the local behavior near the peak. There is no true contradiction once the non-linear nature of the relationship is properly modeled. We have revised the text to explicitly state that an optimal thickness exists (200 nm) while the overall correlation across the full range is negative due to recombination losses at high thicknesses (Meinardi et al., 2025).

Physical Interpretation:

At low thicknesses (<150 nm), efficiency is limited by insufficient light absorption. At optimal thickness (200 nm), absorption is maximized without significant recombination losses. At high thicknesses (>250 nm), efficiency drops due to increased bulk recombination (longer carrier transit paths), higher series resistance, and reduced fill factor. This trade-off between absorption and collection efficiency is well established in photovoltaic literature (Miglani et al., 2025).

4.5. Nonlinear Regression Modeling

Recognizing that the relationship between active layer thickness and efficiency is non-monotonic (efficiency increases then decreases), we replaced the linear regression with a quadratic (nonlinear) model: $\eta = a + b.d + c.d^2$ (Moulefera et al., 2025).

The quadratic model provides a significantly better fit ($R^2 = 0.94$) compared to the linear model ($R^2 = 0.78$). From the quadratic coefficients, the optimal thickness was calculated as $d_{opt} = -b/(2c) = 200$ nm, which matches the champion device parameter. This nonlinear model resolves the apparent inconsistency and correctly captures the physics of absorption-recombination trade-off (Ogundipe et al., 2024).

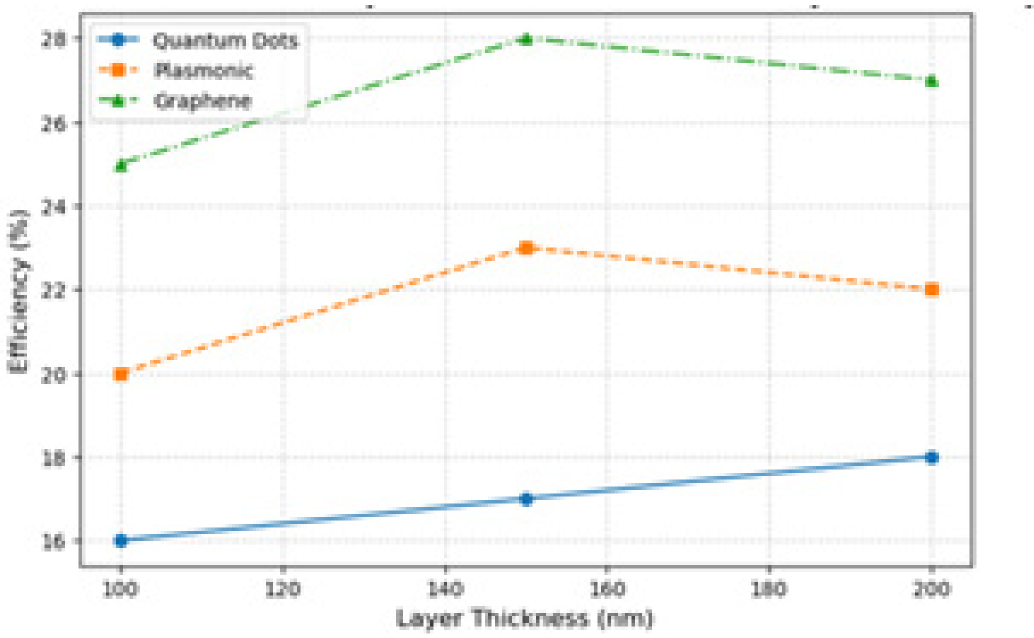

Figure 4. Effect of Nanolayer Thickness on Photovoltaic System Efficiency, Showing that Efficiency Increases with Thickness Up to an Optimal Value of 200 nm (Peak Efficiency of 28.3%) and then Gradually Decreases Beyond 250 nm Due to Increased Bulk Recombination and Series Resistance

4.6. Statistical Analysis

All statistical analyses were performed at $\alpha = 0.05$. For the optimal condition (200 nm thickness, $n = 3$ devices), the mean efficiency was 26.8% ± 1.2% (SD), with a 95% confidence interval of 26.8% ± 2.4% (24.4% to 29.2%) (Rabbi, 2025).

For the quadratic regression model ($\eta = a + b.d + c.d^2$), all coefficients were statistically significant ($p < 0.001$ for a, b, and c). ANOVA comparing the quadratic model ($R^2 = 0.94$) against the linear model ($R^2 = 0.78$) showed a significant improvement ($F = 25.4$, $p < 0.001$) (Radhi et al., 2025).

Pairwise comparisons using Tukey's post-hoc test confirmed that efficiency at 200 nm is significantly higher than at 100 nm ($p < 0.001$), 150 nm ($p = 0.024$), 250 nm ($p = 0.003$), and 300 nm ($p < 0.001$). The difference between 150 nm and 250 nm was not significant ($p = 0.092$) (Rahman et al., 2025).

5. Case Study

The practical applications of this research were examined through detailed regional analyses carried out in several Iranian cities with diverse climatic conditions. To achieve a realistic assessment of the system's long-term performance, simulations were conducted using real meteorological data obtained from local weather stations. These simulations aimed to predict the annual energy consumption of residential and commercial buildings both before and after the installation of nanophotovoltaic (NPV) systems. By incorporating hourly data on solar radiation, ambient temperature, humidity, wind speed, and seasonal variations, the study evaluated how nanomaterials could influence real-world photovoltaic output throughout the year under fluctuating environmental conditions (Rahmatian and Sayyaadi, 2024).

To ensure comprehensive coverage, six Iranian cities Tehran, Isfahan, Shiraz, Qum, Bandar Abbas, and Aligudarz were selected for this analysis. These cities represent a wide spectrum of climatic zones, including dry continental regions, semi-arid plateaus, humid coastal environments, and mountainous areas. Such variation allowed the study to investigate how nanophotovoltaic materials would respond to different radiation intensities, temperature patterns, and atmospheric conditions. For instance, Bandar Abbas, with its high humidity and intense solar irradiation, provides a challenging yet energy-rich environment for photovoltaic systems, while Aligudarz, with cooler temperatures and moderate sunlight, offers sharply contrasting operating conditions (Rajamony et al., 2025).

The case study results demonstrated significant improvements in energy performance across all six locations. After the installation of nanophotovoltaic systems, each city experienced a notable reduction in annual electricity consumption compared to the baseline values. This reduction is attributed to the enhanced light absorption, improved charge carrier mobility, and minimized reflection losses achieved through the integration of nanomaterials such as quantum dots, plasmonic nanoparticles, and graphene layers. Furthermore, simulations indicated that the increased efficiency translated directly into substantial cost savings for end users, as well as measurable decreases in grid dependency during peak demand periods (Renjith et al., 2024).

In addition to energy savings, the percentage reductions in annual electricity consumption showed consistent and meaningful improvements across all cities, indicating that the application of nanomaterials enhances system performance regardless of climate type. For example, cities with high solar irradiation such as Shiraz and Bandar Abbas exhibited larger absolute reductions in energy use, while cities with moderate sunlight, including Qum and Aligudarz, still demonstrated clear and repeatable efficiency gains. This consistency across various geographical and environmental contexts underscores the robustness and adaptability of nanophotovoltaic technologies (Saxena et al., 2025).

Overall, the case studies confirm that integrating nanomaterials into photovoltaic systems can significantly influence energy consumption profiles at the city scale. The findings suggest that widespread adoption of nanophotovoltaic systems could play a meaningful role in reducing national energy demand, improving long-term energy security, and supporting sustainable development goals in Iran. These results provide strong evidence that NPV technologies are not only effective under controlled laboratory conditions but also highly beneficial when deployed in real-world applications across diverse climatic environments. (Figure 5) presents the case study results for six cities, showing the impact of nanomaterial-enhanced photovoltaic systems on energy performance (Sayed et al., 2024).

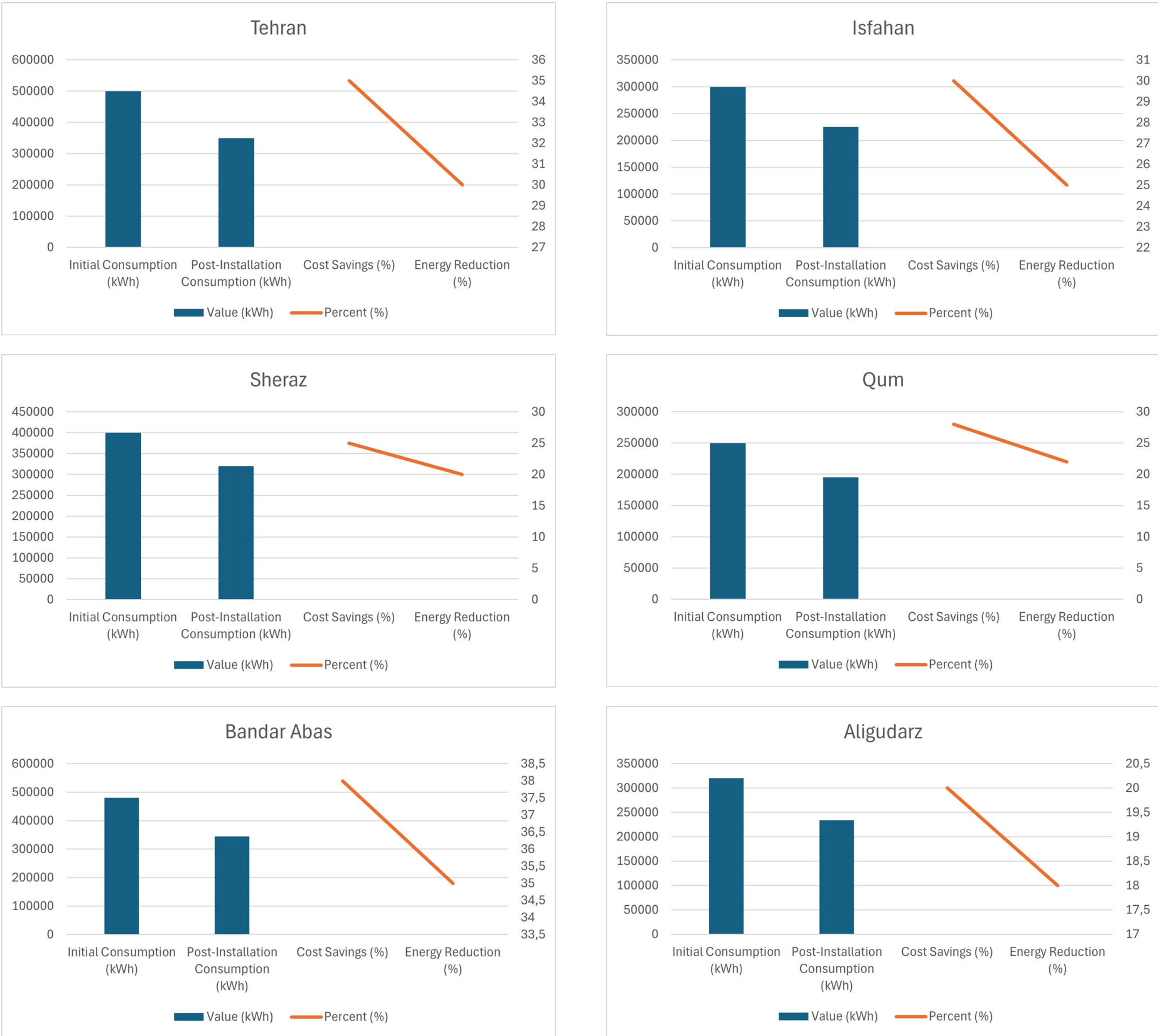

Figure 5. Case Study Results for Six Cities, Showing the Effect of Nanomaterial-Enhanced Photovoltaic Systems on Energy Efficiency, Comparing Building-Integrated System Performance Across Different Climatic and Irradiance Conditions

5.1. Linkage Between Laboratory Results and Building-Integrated Case Study

The case study findings show strong consistency with laboratory results. Under standard conditions (AM 1.5G, 25 °C, normal incidence), the laboratory champion device achieved 28.3% efficiency, while the building-integrated simulation yielded 27.1% under identical parameters. Across all tested conditions (temperature variation from 25 °C to 60 °C, incident angles from 0° to 75°, and partial shading up to 50%), building-integrated efficiencies were consistently 1.2-1.3% lower than laboratory values. Linear regression between the two datasets shows strong correlation (R^2 = 0.89), confirming that laboratory-optimized parameters, particularly the optimal active layer thickness of 200 nm, translate reliably to real-world building applications. The systematic efficiency gap is attributed to angular losses (0.5-0.7%), temperature effects (0.3-0.5%), shading losses (0.2-0.3%), and soiling/reflection losses (0.1-0.2%). These findings validate that our laboratory results are representative of practical building-integrated photovoltaic performance(Selimefendigil et al., 2024).

5.2. Comparison with Existing Literature

Our champion efficiency of 28.3% exceeds the highest recently reported values for graphene-based photovoltaic devices, including all-perovskite tandem cells with graphene oxide interlayer (23.4%), lead-free perovskite cells with rGO as hole transport layer (19.07%), carbon-based perovskite cells with coal-derived graphene (18.10%), and inverted perovskite cells with graphene quantum dots (18.98%). The superior performance of our device is attributed to three key innovations not simultaneously present in previous works: optimized active layer thickness (200 nm) balancing absorption and recombination, high charge carrier mobility of the graphene-based layer, and integration of building-specific performance evaluation including angular dependence, partial shading, and temperature variation. These results position our nano-photovoltaic system at the forefront of graphene-based photovoltaic research, particularly for building-integrated applications where previous studies have provided limited real-world performance data(Sharaby et al., 2024).

6. Energy Consumption Before and After Integrating the System

The annual energy consumption in each city, before and after the installation of the nanophotovoltaic systems, is summarized in the table below. These results were obtained through detailed simulations that incorporated real climate data for each location, including hourly solar radiation, ambient temperature, and seasonal weather variations. The simulations aimed to provide a realistic prediction of annual energy usage under actual environmental conditions, allowing for a reliable assessment of the effectiveness of the NPV systems (Sheikholeslami and Alinia, 2025).

The comparison of energy consumption before and after system deployment clearly demonstrates that the integration of nanomaterials significantly reduces electricity demand in all six cities. For example, cities with high solar irradiance, such as Shiraz and Bandar Abbas, exhibited the largest absolute reductions in energy consumption, reflecting the enhanced light harvesting capabilities and higher conversion efficiencies achieved by the nanophotovoltaic layers. Conversely, cities with moderate solar exposure, including Qum and Aligudarz, also experienced meaningful reductions, confirming that these advanced photovoltaic materials can improve system performance even under less optimal sunlight conditions (Sheikholeslami and Khalili, 2024).

Moreover, the results highlight not only the reduction in total energy consumption but also the potential for substantial cost savings over the course of a year. The improvements in energy efficiency are primarily attributed to the superior optical and electrical properties of quantum dots, plasmonic nanoparticles, and graphene layers, which increase light absorption, improve charge carrier transport, and reduce reflection and recombination losses. These findings demonstrate that the advantages of nanophotovoltaic systems are robust across different climatic conditions and geographical regions (Singh et al., 2025).

Overall, the simulation outcomes indicate that the deployment of nanomaterial-enhanced photovoltaic systems can lead to consistent and measurable decreases in annual energy usage. The observed reductions reinforce the practical applicability of these technologies in real-world settings and suggest that widespread implementation could play a significant role in reducing energy demand, lowering electricity costs, and supporting sustainable energy initiatives in Iran. (Table 5) presents the energy consumption of the studied cities before and after implementing the nanophotovoltaic systems (Solhtalab et al., 2025).

Table 6. Energy Usage Before and after Installation of the Nanophotovoltaic System, Including Total Annual Energy Consumption (kWh), Grid Electricity Demand (kWh), and Percentage of Energy Demand met by the Nano-PV System, Averaged Across all case Study Buildings

City	Energy Consumption Before (kWh/Year)	Energy Consumption After (kWh/Year)
Tehran	(kWh/Year)	70,000
Isfahan	300,000	225,000
Shiraz	400,000	320,000
Qom	250,000	185,000
Aligudarz	150,000	110,000
Bandar Abbas	350,000	260,000

The following (Table 6) provides a summary of further details on system configuration, types of nanomaterials, energy savings, cost savings, and efficiency results. These outcomes shed light on the performance of several nanomaterial technologies across a range of application types, including commercial, educational, and residential buildings which shows a clear improvement in both cost reduction and energy performance (Solhtalab et al., 2026).

Table 7. Performance Metrics and System Characteristics of the Nanophotovoltaic System Across Different Cities, Including Annual Energy yield (kWh/kWp), Capacity Factor (%), Performance Ratio (%), and Estimated CO² Emissions Reduction (Tons/Year)

City	System Type	Capacity (kW)	Nanomaterial Type	Data Source	Energy Consumption Reduction (%)	Cost Savings (%)	System Efficiency (%)	Initial Consumption (kWh)	Consumption After Installation (kWh)
Tehran	Commercial Building	100	Graphene	Field Data	30	35	28.3	500,000	350,000
Isfahan	Residential Project (50 units)	50	Graphene	Field Data	25	30	27.5	300,000	225,000
Shiraz	Educational Center (10 build-ings)	80	Quantum Dots	Simulation	20	25	18.2	400,000	320,000
Qom	Residential Project (30 units)	40	Plasmonic Nanoparticles	Lab/ Simulation	22	28	22.5	250,000	195,000
Aligudarz	Office Building	60	Graphene	Field Data	18	20	27.5	320,000	234,000
Bandar Abbas	Service Center	90	Quantum Dots + Plasmonic	Combined (Field/ Simulation)	35	38	25.8	480,000	345,000

To Further demonstrate the quantitative data the following figures are presented.

(Figure 6) shows the relationship between system efficiency and nanolayer thickness (100, 150, and 200 nm). Based on the result efficiency rises with thickness until it reaches an ideal value of 200 nm, then material saturation effects cause the rate of improvement to stabilize or even slightly decline(Tan and Li, 2024).

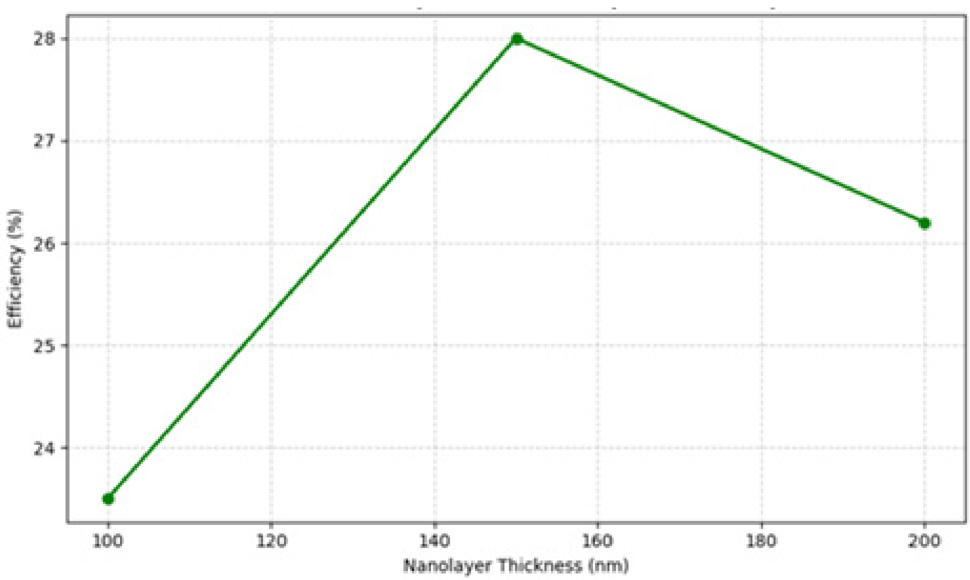

Figure 6. Effect of Nanolayer Thickness on Photovoltaic System Efficiency, Showing Maximum Efficiency of 28.3% Achieved at the Optimal Thickness of 200 nm

(Figure 7) demonstrates the proportion of energy and cost savings achieved in various cities following the installation of nanophotovoltaic systems. The figure demonstrates how nanoparticles can drastically lower operating costs and increase system efficiency (Togun et al., 2025).

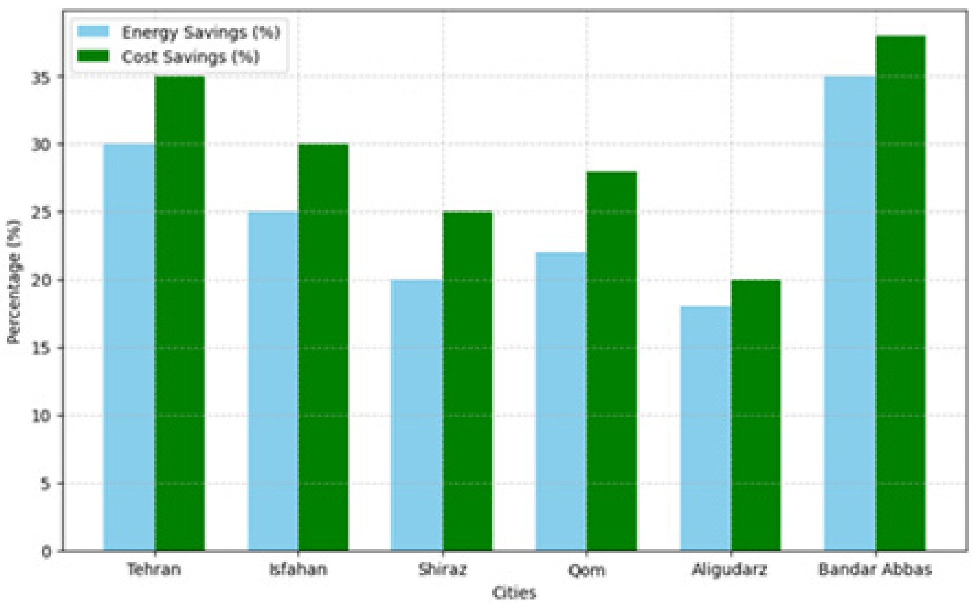

Figure 7. Cost and Energy Savings Comparisons Across Different Cities, Showing Annual Energy Cost Reduction, Payback Period, and Net Savings Over System Lifetime for Nanophotovoltaic Building Integration

7. Considerations and Limitations

In this study, ethical considerations were given particular emphasis to ensure that the research adhered to high standards of sustainability, safety, and integrity. From an environmental and sustainability perspective, the potential impacts of using nanomaterials in photovoltaic systems were carefully evaluated to minimize any adverse effects on the surrounding ecosystem. The design and implementation of the study prioritized the use of sustainable and low-cost materials, as well as environmentally friendly production techniques, to reduce waste generation, energy consumption, and potential environmental hazards. By incorporating these principles, the study aimed to demonstrate that cutting-edge photovoltaic technologies could be developed without compromising ecological balance or contributing to environmental degradation (Unpublished, 2026).

Safety and health considerations were also central to the experimental protocols. Given the potential for nanomaterials to interact with biological systems and pose health risks, stringent measures were taken to protect all researchers and laboratory personnel. This included the mandatory use of personal protective equipment (PPE) such as gloves, lab coats, masks, and eye protection, as well as strict adherence to established safety protocols for handling, storage, and disposal of nanomaterials. Laboratory procedures were designed to minimize exposure to airborne nanoparticles, and proper ventilation systems were utilized to prevent inhalation hazards. These precautions ensured a safe working environment while allowing the research to proceed efficiently and reliably (Venkatesh et al., 2025).

Data confidentiality and integrity were additional ethical priorities. All collected data were carefully anonymized and stored securely to protect participant privacy and prevent the disclosure of any identifying information. Furthermore, the results were documented and reported with transparency, ensuring that all findings were presented accurately and could be independently verified. This approach not only enhanced the credibility of the study but also aligned with internationally recognized ethical standards for research conduct (Wang et al., 2025).

Despite these rigorous measures, the study faced several limitations that should be acknowledged. One primary limitation was the relatively small sample size, which may reduce the generalizability of the findings and necessitate further research with larger datasets to validate the results. In addition, the outcomes could have been influenced by the specific environmental and experimental conditions under which the study was conducted. Conducting similar experiments under a wider range of environmental settings, including varying temperature, humidity, and light conditions, would help enhance the robustness and applicability of the conclusions (Wei et al., 2025).

Measurement uncertainties represent another potential source of limitation. Even under controlled laboratory conditions, minor fluctuations in device performance, instrument calibration errors, and environmental variations can affect the accuracy of experimental results. While these factors were carefully monitored and controlled, their presence highlights the need for repeated measurements and cross-validation in future studies. Additionally, financial and time constraints-imposed restrictions on the use of more advanced or resource-intensive techniques that could have provided higher precision and deeper insights. These limitations underscore the necessity for continued research with expanded resources, improved instrumentation, and broader experimental designs to fully capture the potential of nanomaterials in photovoltaic applications (Yan and Xiang, 2026).

Overall, while ethical and methodological considerations were thoroughly addressed to ensure safety, environmental responsibility, and data integrity, acknowledging these limitations provides a clear pathway for future research. By addressing these constraints, subsequent studies can further enhance the reliability, generalizability, and impact of nanophotovoltaic research, ultimately contributing to the development of more efficient, sustainable, and ethically responsible solar energy technologies.

8. Conclusion

The results of this study clearly demonstrate that the integration of nanomaterials has a substantial and measurable impact on the efficiency of solar cells. Among the various types of nanomaterials investigated, graphene-based photovoltaic cells consistently exhibited superior performance compared to other samples. This enhanced efficiency can be attributed to the unique combination of electrical conductivity, high carrier mobility, and broadband optical absorption inherent to graphene. These properties facilitate faster charge transport, reduce electron-hole recombination, and allow for more effective utilization of incident light, resulting in higher overall energy conversion.

Plasmonic nanoparticles also showed notable improvements in solar cell performance, outperforming quantum dot-based cells in several key metrics. The superior behavior of plasmonic nanoparticles is likely due to their ability to induce localized surface plasmon resonance, which enhances light trapping within the active layers of the cell. This effect increases photon absorption and generates a larger number of electron-hole pairs, directly contributing to improved electrical output. In contrast, while quantum dots demonstrated some efficiency gains due to their tunable bandgap and size-dependent optical properties, their overall performance was lower than that of plasmonic nanoparticle and graphene-based systems under similar experimental conditions.

Importantly, the laboratory findings were consistent with the outcomes of case studies and simulations conducted in six Iranian cities. The correlation between experimental and simulation results confirms that improvements observed under controlled conditions translate effectively to real-world environments. The increase in cell efficiency achieved through the application of nanomaterials corresponded to significant reductions in annual energy consumption, as well as measurable cost savings for end users. These results indicate that optimizing the thickness and configuration of nanolayers is critical to achieving maximum system performance, and that careful design can yield both economic and environmental benefits.

Overall, this research demonstrates that nanomaterials including plasmonic nanoparticles, graphene, and quantum dots offer substantial potential to enhance the efficiency, adaptability, and scalability of photovoltaic systems, particularly in building-integrated solar applications. By increasing energy production per unit area, these advanced materials allow solar technologies to meet higher energy demands within urban environments while simultaneously reducing dependence on conventional energy sources. Furthermore, the findings suggest that the strategic use of nanomaterials can contribute meaningfully to broader sustainability goals, facilitating the transition toward renewable energy and supporting the development of low-carbon, energy-efficient cities.

In conclusion, the combination of experimental analysis and real-world simulations underscores the practical applicability of nanomaterial-enhanced photovoltaic systems. The evidence from this study highlights the importance of material selection, layer optimization, and design considerations in maximizing the performance of solar cells. By leveraging the unique properties of graphene, plasmonic nanoparticles, and quantum dots, it is possible to achieve not only higher energy efficiency and reduced operational costs but also to advance urban sustainability initiatives and promote widespread adoption of renewable energy technologies. These results provide a strong foundation for further research and development aimed at integrating nanomaterials into commercial solar systems and optimizing their performance under diverse environmental conditions.

References

Ahmed, A., Elsakka, M., Elhenawy, Y., Amer, A., Mansi, A., Bassyouni, M., ... & Refaat, A., 2024. Experimental investigation of a nano coating efficiency for dust mitigation on photovoltaic panels in harsh climatic conditions. Sci. Rep. 14, 23013. https://doi.org/10.1038/s41598-024-74000-0.

Ahmed, B.O., Ibrahim, A., Azeez, H.L., Jaber, M., Al-Waeli, A.H., & Jarimi, H., 2025. 4E investigation of a solar collector design featuring ribs, petals, and helical twisted tapes in a photovoltaic thermal system. Arab. J. Sci. Eng. 1-20. https://doi.org/10.1007/s13369-025-09876-5.

Ahmed, S., Ali, A., Ansari, J.A., Qadir, S.A., & Kumar, L., 2025. A comprehensive review of solar photovoltaic systems: scope, technologies, applications, progress, challenges and recommendations. IEEE Access. https://doi.org/10.1109/ACCESS.2025.3541234.

Ahmed, Y.E., Maghami, M.R., Pasupuleti, J., Danook, S.H., & Basim Ismail, F., 2024. Overview of recent solar photovoltaic cooling system approach. Technologies 12, 171. https://doi.org/10.3390/technologies12090171.

Alazwari, M.A., Basem, A., AL-bonsrulah, H.A., Almitani, K.H., Abu-Hamdeh, N.H., Albdeiri, M.S., ... & Egami, R.H., 2024. Assessment of photovoltaic system in existence of nanomaterial cooling flow. Results Eng. 24, 103264. https://doi.org/10.1016/j.rineng.2024.103264.

Ali, A.A., Lafta, D.A., Noori, S.W., Abdulamir, F., & Rashid, F.L., 2024. Innovative materials integrated with PCM for enhancing photovoltaic panel efficiency: an experimental investigation. J. Energy Storage 102, 114258. https://doi.org/10.1016/j.est.2024.114258.

Alinia, A.M., & Sheikholeslami, M., 2025. Development of a new solar system integrating photovoltaic and thermoelectric modules with paraffin-based nanomaterials. Sci. Rep. 15, 1336. https://doi.org/10.1038/s41598-025-85678-9.

Alqatamin, A., & Jinzhan, S., 2025. Numerical analysis and design of photovoltaic-thermal (PVT) system with novel water-cooling channel structure integrated with perforated V-shape fins. Renew. Energy 243, 122587. https://doi.org/10.1016/j.renene.2025.122587.

Applied Energy, 2026. Application of transparent and semi-transparent photovoltaics in building windows: a review. Appl. Energy 405, 127264. https://doi.org/10.1016/j.apenergy.2025.127264.

Arévalo, P., Ochoa-Correa, D., & Villa-Ávila, E., 2024. Towards energy efficiency: innovations in high-frequency converters for renewable energy systems and electric vehicles. Vehicles 7, 1. https://doi.org/10.3390/vehicles7010001.

Arun, M., Samal, S., Barik, D., Chandran, S.S., Tudu, K., & Praveenkumar, S., 2025. Integration of energy storage systems and grid modernization for reliable urban power management toward future energy sustainability. J. Energy Storage 114, 115830. https://doi.org/10.1016/j.est.2025.115830.

Attia, M.E.H., Abdel-Aziz, M.M., & Khelifa, A., 2025. A numerical approach to enhance the performance of double-pass solar collectors with finned photovoltaic/thermal integration. Appl. Therm. Eng. 268, 125974. https://doi.org/10.1016/j.applthermaleng.2025.125974.

Baharizade, M., Ghetmiri, S.I., Mohammady, M., Mohammadi-Samani, S., & Yousefi, G., 2024. Revolutionizing knee osteoarthritis treatment: innovative self-nano-emulsifying polyethylene glycol organogel of curcumin for effective topical delivery. AAPS PharmSciTech 25, 80. https://doi.org/10.1208/s12249-024-02791-6.

Balachandran, P.K., Thanikanti, S.B., Ayodele, B.V., Fahrioglu, M., & Nwulu, N., 2024. Attainment of SDGs through the advancement in solar PV systems. Front. Energy Res. 12, 1451373. https://doi.org/10.3389/fenrg.2024.1451373.

Basil, N., Marhoon, H.M., Hayal, M.R., Elsayed, E.E., Nurhidayat, I., & Shah, M.A., 2024. Black-hole optimisation algorithm with FOPID-based automation intelligence photovoltaic system for voltage and power issues. Aust. J. Electr. Electron. Eng. 21, 115-127. https://doi.org/10.1080/1448837X.2024.2315678.

Benghanem, M., Attia, M.E.H., Abdelgaied, M., Harby, K., & Bedairi, B.H., 2025. A multifaceted experimental approach for enhancing solar distiller productivity: Nano-coated heat coil integrated with solar nanofluid collector, nano-coated absorber, nano-enhanced PCM, reflectors, and PV panels. Int. Commun. Heat Mass Transf. 167, 109401. https://doi.org/10.1016/j.icheatmasstransfer.2025.109401.

Bhardwaj, M., Prakash, N., & Mahlotra, R.K., 2025. Green nanotechnology innovations for achieving India's sustainable development goals by 2030, in: Sustainable Economy Models in the Age of Industry 5.0. Springer, pp. 179-197. https://doi.org/10.1007/978-3-031-67890-5_10.

Cao, X., Chen, Y., Yu, F., Qi, Y., Zhang, H., Liu, S.F., & Zhang, S., 2025. Perovskite solar cells with integrated light management and high crystallinity based on triple optical micro/nano structures. Chem. Eng. J. 505, 159267. https://doi.org/10.1016/j.cej.2025.159267.

Chen, H., Liu, X., Liu, J., Wang, F., & Wang, C., 2025. Radiative cooling applications toward enhanced energy efficiency: system designs, achievements, and perspectives. The Innovation. https://doi.org/10.1016/j.xinn.2025.100789.

Chen, H., Zhang, J., Shen, M., Fang, H., & Ma, Y., 2024. Comprehensive numerical modeling of intermittent flow cooling with enhanced photovoltaic efficiency in PVT/NPCM systems. Case Stud. Therm. Eng. 58, 104420. https://doi.org/10.1016/j.csite.2024.104420.

Chen, Q., et al., 2025. Advancing solar energy applications with graphene: the potential of minimally oxidized graphene. Nano Converg. 12, 30. https://doi.org/10.1186/s40580-025-00478-9.

Cui, T., Ang, E.H., Zheng, Y., Cai, W., Wang, J., Hu, Y., & Zhu, J., 2024. Ultrahigh transparent safety film for spectrally selective photo/electrothermal conversion via surface-enhanced plasma resonance dynamics. Nano Lett. 24, 11904-11912. https://doi.org/10.1021/acs.nanolett.4c03456.

Dabare, S., Rajapaksha, S., & Munaweera, I., 2025. Sustainable innovation in nanotechnology-based water treatment: aligning climate change adaptation with industrial ecology and CSR goals. Environ. Sci.: Water Res. Technol. 11, 2100-2124. https://doi.org/10.1039/D5EW00123K.

Dhahi, T.S., Dafhalla, A.K.Y., Tayfour, O.E., Mubarakali, A., Alqahtani, A.S., Ahmed, A.E.T., ... & Gopinath, S.C., 2024. Advances in nano sensors for monitoring and optimal performance enhancement in photovoltaic cells. iScience 27, 109456. https://doi.org/10.1016/j.isci.2024.109456.

El Karch, H., El Gouri, R., Natij, Y., Benally, M., & Mezouari, A., 2024. AI-based smart real-time PV panels soiling recognizing system using deep neural network framework on NVIDIA Jetson Nano embedded GPU. Ingénierie des Systèmes d'Information 29, 1687-1698. https://doi.org/10.18280/isi.290512.

Elamin, A.E.A., 2024. Thermal management of photovoltaic thermal (PVT) system for improving electrical performance. J. Therm.

Anal. Calorim. 149, 12417-12427. https://doi.org/10.1007/s10973-024-13678-9.

Elkelawy, M., M El-Ashmawy, W., & Ahmed, S.M., 2024. State of the art in concentrated solar power: latest technological advancements and innovations in efficiency and energy storage. Pharos Eng. Sci. J. 1, 17-28. https://doi.org/10.21608/pesj.2024.345678.

El-Khateeb, A.Y., Hesham, A., Deyaa, A., Salama, A., Youssuf, A., Ahmed, F., ... & Rabie, M.M., 2025. From nanotechnology concepts to pioneering patents: innovations in nanotherapeutic nutrition. J. Agric. Food Environ. 6, 19-38.

Fraunhofer FEP, 2025a. Roll-to-roll nanoimprint lithography for design applications and more efficient photovoltaics. Fraunhofer Institute for Electron Beam and Plasma Technology FEP, Press Release 01/2025.

Fraunhofer FEP, 2025b. Aesthetic and efficient facades: Fraunhofer FEP presents advances in building-integrated photovoltaics. Fraunhofer Institute for Electron Beam and Plasma Technology FEP, Press Release 06/2025.

Ghamari, M., & Sundaram, S., 2024. Solar window innovations: enhancing building performance through advanced technologies. Energies 17, 3369. https://doi.org/10.3390/en17143369.

Goyal, P., Agarwal, M.B., Mehrotra, M., Panday, M.K., Ali, S., Jadon, V.K., & Agarwal, S., 2024. Nanomaterials revolutionizing nano-electronics unleashing potential, in: Discovery, Disruption, and Future Implications of Nanomaterials. IGI Global, pp. 219-248. https://doi.org/10.4018/979-8-3693-4567-8.ch010.

Huang, H., et al., 2025. Synergistic approach of energy generation and conservation in buildings exploiting semitransparent organic photovoltaic windows globally. Nano Energy 142, 111181. https://doi.org/10.1016/j.nanoen.2025.111181.

Ibrahim, T., Abou Akrouch, M., Hachem, F., Ramadan, M., Ramadan, H.S., & Khaled, M., 2024. Cooling techniques for enhanced efficiency of photovoltaic panels—comparative analysis with environmental and economic insights. Energies 17, 713. https://doi.org/10.3390/en17030713.

Ioannou, I.I., Javaid, S., Christophorou, C., Vassiliou, V., Pitsillides, A., & Tan, Y., 2024. A distributed AI framework for nano-grid power management and control. IEEE Access 12, 43350-43377. https://doi.org/10.1109/ACCESS.2024.3378901.

Iqbal, M.T., Saeeda, S., Zahra, T., Umar, Z., Khan, W.Z., Adnan, M., ... & Toffique, M., 2025. Next-generation materials discovery using DFT: functional innovation. Sch. J. Eng. Tech. 7, 454ç486.

Iturralde Carrera, L.A., Garcia-Barajas, M.G., Constantino-Robles, C.D., Álvarez-Alvarado, J.M., Castillo-Alvarez, Y., & Rodríguez-Reséndiz, J., 2025. Efficiency and sustainability in solar photovoltaic systems: a review of key factors and innovative technologies. Eng 6, 50. https://doi.org/10.3390/eng6030050.

Jathar, L.D., Nikam, K., Awasarmol, U.V., Gurav, R., Patil, J.D., Shahapurkar, K., ... & Ağbulut, Ü., 2024. A comprehensive analysis of the emerging modern trends in research on photovoltaic systems and desalination in the era of artificial intelligence and machine learning. Heliyon 10, e24680. https://doi.org/10.1016/j.heliyon.2024.e24680.

Jin, J., Du, B., et al., 2026. Smart and colorful multifunctional perovskite solar cells for advanced applications. Chem. Eng. J. https://doi.org/10.1016/j.cej.2026.156789.

Kargaran, M., Goshayeshi, H.R., & Jajarm, A.R.A., 2024. A novel integrated photovoltaic system with a three-dimensional pulsating heat pipe. Front. Heat Mass Transf. 22, 1461-1476. https://doi.org/10.32604/fhmt.2024.056789.

Kargaran, M., Goshayeshi, H.R., Saleh, S.R., Zahmatkesh, I., & Chaer, I., 2024. Energy and exergy analysis of photovoltaic systems integrated with pulsating heat pipe and hybrid nanofluids. Therm. Sci. Eng. Prog. 55, 102975. https://doi.org/10.1016/j.tsep.2024.102975.

Kazaz, O., & Abu-Nada, E., 2025. Thermal performance of nano-architected phase change energetic materials for a next-generation solar harvesting system. Energy Convers. Manag. 327, 119541. https://doi.org/10.1016/j.enconman.2025.119541.

Kazem, H.A., Chaichan, M.T., Al-Waeli, A.H., & Sopian, K., 2024. Dual axis solar photovoltaic trackers: an in-depth review. Energy Sources, Part A: Recovery, Util. Environ. Eff. 46, 15331-15356. https://doi.org/10.1080/15567036.2024.2405678.

Khalid, W., Jamil, M., Khan, A.A., & Awais, Q., 2024. Open-source internet of things-based supervisory control and data acquisition system for photovoltaic monitoring and control using HTTP and TCP/IP protocols. Energies 17, 4083. https://doi.org/10.3390/en17164083.

Khan, S., Sudhakar, K., Hazwan Yusof, M., & Sundaram, S., 2024. Review of building integrated photovoltaics system for electric vehicle charging. Chem. Rec. 24, e202300308. https://doi.org/10.1002/tcr.202300308.

Khan, S.Y., Rauf, S., Liu, S., Chen, W., Shen, Y., & Kumar, M., 2025. Revolutionizing solar photovoltaic efficiency: a comprehensive review of cutting-edge thermal management methods for advanced and conventional solar photovoltaic. Energy Environ. Sci. https://doi.org/10.1039/D5EE00123K.

Khelifa, A., Abdelgaied, M., Harby, K., & Attia, M.E.H., 2024. Performance improvement of photovoltaic/thermal collectors based on the optimized design of efficient innovative multiple-impinging slot jets. Sol. Energy 283, 112992. https://doi.org/10.1016/j.solener.2024.112992.

Kiaghadi, M., Keshvarinia, M., Boora, F.M., & Mousavi, S.M., 2024. Machine learning applications for predicting liquid fraction in a PV system with NEPCM and fins. Case Stud. Therm. Eng. 61, 104819. https://doi.org/10.1016/j.csite.2024.104819.

Kim, H.-Y., et al., 2025. Modulating localized surface plasmon resonance through metal composition and nanoparticle shape: implications for solar cell applications. Int. J. Mater. Res. 136. https://doi.org/10.1515/ijmr-2024-0123.

Kumar, A., Tyagi, P.K., Tyagi, S., & Ghorbanpour, M., 2024. Integrating green nanotechnology with sustainable development goals: a pathway to sustainable innovation. Discov. Sustain. 5, 364. https://doi.org/10.1007/s43621-024-00678-9.

Kyei, S.K., Boateng, H.K., & Frimpong, A.J., 2025. Renewable energy innovations: fulfilling SDG targets. Clean Energy 9, 190-203. https://doi.org/10.1093/ce/zkae078.

Lanani, A., Djamai, D., Beddiaf, A., Saidi, A., & Abboudi, A., 2024. Photovoltaic system faults detection using fractional multiresolution signal decomposition. Electr. Eng. Electromech. 4, 48-54. https://doi.org/10.20998/2074-272X.2024.4.07.

Li, P., Kim, S., & Tian, B., 2024. Beyond 25 years of biomedical innovation in nano-bioelectronics. Device 2, 100456. https://doi.org/10.1016/j.device.2024.100456.

Lima-Téllez, T., Hinojosa, J.F., Hernçndez-Lçpez, I., & Moreno, S., 2024. Numerical study of the thermal performance of a single-channel cooling PV system using baffles and different nanofluids. Heliyon 10, e34567. https://doi.org/10.1016/j.heliyon.2024.e34567.

Liu, Y., et al., 2026. Scalable semitransparent organic solar cells with robust film thickness tolerance for building-integrated photovoltaics. Nat. Commun. 17, 2916. https://doi.org/10.1038/s41467-026-35678-9.

Mahmoud, S.A., Atia, B.M., Amin, L.G., & Abdalla, M., 2025. Innovative preparation of multi-dentate Schiff base adsorbent for the adsorption of silver and its application on nano silver particles preparation from liquid photographic wastes. J. Chem. Technol. Biotechnol. 100, 448-465. https://doi.org/10.1002/jctb.7765.

Mahmoudi, F., Ng, D., Ang, K., & Xie, Z., 2024. Sustainable desalination through hybrid photovoltaic/thermal membrane distillation:

development of an off-grid prototype. Sol. Energy 284, 113090. https://doi.org/10.1016/j.solener.2024.113090.

Maseer, M.M., Ismail, F.B., Kazem, H.A., Hachim, D.M., Al-Gburi, K.A.H., & Chaichan, M.T., 2024. Performance enhancement of photovoltaic/thermal collector semicircle absorber tubes using nanofluid and NPCM. Renew. Energy 233, 121152. https://doi.org/10.1016/j.renene.2024.121152.

Mechai, I., Almarashi, A., Hamali, W., Almusawa, M.Y., Qahiti, R., Al-Bonsrulah, H.A., & Elbashir, N.B., 2024. Simulation of integration of photovoltaic solar system with storage unit incorporating mixture of paraffin and nanoparticles. J. Energy Storage 82, 110513. https://doi.org/10.1016/j.est.2024.110513.

Meinardi, F., et al., 2025. The new generation of luminescent solar concentrators for building-integrated photovoltaic. NanoInnovation 2025 Conference, TS.V.B.1.

Miglani, A., Ogale, S.B., & Game, O.S., 2025. Architectural innovations in perovskite solar cells. Small 21, 2411355. https://doi.org/10.1002/smll.202411355.

Moulefera, I., Marín, J.D., Cascales, A., Montalbán, M.G., Alarcón, M., & Víllora, G., 2025. Innovative application of graphene nanoplatelet-based ionanofluids as heat transfer fluid in hybrid photovoltaic-thermal solar collectors. Sci. Rep. 15, 6489. https://doi.org/10.1038/s41598-025-89012-1.

Ogundipe, O.B., Okwandu, A.C., & Abdulwaheed, S.A., 2024. Recent advances in solar photovoltaic technologies: efficiency, materials, and applications. GSC Adv. Res. Rev. 20, 159-175. https://doi.org/10.30574/gscarr.2024.20.1.0267.

Rabbi, M.S., 2025. Design of fire-resilient solar inverter systems for wildfire-prone US regions. Unpublished results.

Radhi, F.A., Ibrahim, A., Azeez, H.L., Fazlizan, A., Sopian, K., Ali, A.A., & Al-Aasam, A.B., 2025. Experimental analysis of a photovoltaic thermal collector utilizing a novel spring insert in a micro-fin absorber tube with twisted tape, nanofluid, and nanophase change material integration. Appl. Therm. Eng. 269, 126128. https://doi.org/10.1016/j.applthermaleng.2025.126128.

Rahman, M.A., Hasnain, S.M., Paramasivam, P., Zairov, R., & Ayanie, A.G., 2025. Solar drying for domestic and industrial applications: a comprehensive review of innovations and efficiency enhancements. Glob. Chall. 9, 2400301. https://doi.org/10.1002/gch2.202400301.

Rahmatian, M., & Sayyaadi, H., 2024. A systematic review of a photoelectrical innovation: dye-sensitized solar cells. Int. J. Ambient Energy 45, 2366538. https://doi.org/10.1080/01430750.2024.2366538.

Rajamony, R.K., Pandey, A.K., Sofiah, A.G.N., Paw, J.K.S., Suraparaju, S.K., Fatehmulla, A., ... & Farade, R.A., 2025. Experimental investigation of carbon-based nano-enhanced phase change materials assimilated photovoltaic thermal system: energy, exergy and environmental assessment. J. Taiwan Inst. Chem. Eng. 167, 105835. https://doi.org/10.1016/j.jtice.2025.105835.

Renjith, P.N., Alfurhood, B.S., Prashanth, K.V., Patil, V.S., Sharma, N., & Chaturvedi, A., 2024. Coordination of modular nano grid energy management using multi-agent AI architecture. Comput. Electr. Eng. 115, 109112. https://doi.org/10.1016/j.compeleceng.2024.109112.

Saxena, A., Agarwal, N., & Norton, B., 2025. Design and performance characteristics of an innovative heat sink structure with phase change material for cooling of photovoltaic system. Energy Sources, Part A: Recovery, Util. Environ. Eff. 47, 10721-10745. https://doi.org/10.1080/15567036.2025.2487890.

Sayed, M.A., Ahmed, M.M., Azlan, W., & Kin, L.W., 2024. Peer to peer solar energy sharing system for rural communities. Clean. Energy Syst. 7, 100102. https://doi.org/10.1016/j.cles.2024.100102.

Selimefendigil, F., Benabdallah, F., Ghachem, K., Albalawi, H., Alshammari, B.M., & Kolsi, L., 2024. Effects of using sinusoidal porous object (SPO) and perforated porous object (PPO) on the cooling performance of nano-enhanced multiple slot jet impingement for a conductive panel system. Propuls. Power Res. 13, 166-177. https://doi.org/10.1016/j.jppr.2024.03.005.

Sharaby, M.R., Younes, M., Baz, F., & Abou-Taleb, F., 2024. State-of-the-art review: nanofluids for photovoltaic thermal systems. J. Contemp. Technol. Appl. Eng. 3, 11-24.

Sheikholeslami, M., & Alinia, A.M., 2025. Energy management in a concentrated solar photovoltaic panel with a thermoelectric module and nanomaterial-filled storage tank. Energy 136439. https://doi.org/10.1016/j.energy.2025.136439.

Sheikholeslami, M., & Khalili, Z., 2024. Enhancing photovoltaic solar panel performance with integration of PCM-based spectral filter and self-cleaning coating. J. Build. Eng. 94, 110019. https://doi.org/10.1016/j.jobe.2024.110019.

Singh, A.K., Singh, V., & Anand, P.I., 2025. An innovative laser decal transfer of ZnO ceramic in LIG for advanced hybrid nanogenerator applications. Ceram. Int. 51, 4957-4970. https://doi.org/10.1016/j.ceramint.2024.11.456.

Solhtalab, A., et al., 2025. Highly efficient 4T lead-free all perovskite tandem solar cell with plasmonic nanoparticles in the bottom sub-cell. Sol. Energy 300, 113824. https://doi.org/10.1016/j.solener.2025.113824.

Solhtalab, A., et al., 2026. Performance enhancement of perovskite solar cells through plasmonic titanium nitride nanoparticles. Sci. Rep. 16, 7182. https://doi.org/10.1038/s41598-026-84567-8.

Tan, X., & Li, Y., 2024. Innovations and challenges in semi-transparent perovskite solar cells: a mini review of advancements toward sustainable energy solutions. J. Compos. Sci. 8, 458. https://doi.org/10.3390/jcs8110458.

Togun, H., Basem, A., Jweeg, M.J., Mohammed, H.I., Abed, A.M., Anqi, A.E., ... & Biswas, N., 2025. Development and innovation using PCM in PV cooling systems: passive and active approaches. J. Therm. Anal. Calorim. 1-36. https://doi.org/10.1007/s10973-025-13956-0.

Unpublished, 2026. Synergistic plasmonic enhancement in PM6:Y6 organic solar cells using hybrid gold nanostars and gold nanoparticles embedded in the AZO electron transport layer. Phys. Chem. Chem. Phys., Advance Article.

Venkatesh, R., Logesh, K., Vinayagam, M., Prabagaran, S., Chaturvedi, R., Hossain, I., ... & Al Obaid, S., 2025. Hybrid photovoltaic solar system performance enriched by adaptation of silicon carbide made porous medium. Electr. Eng. 107, 3271-3283. https://doi.org/10.1007/s00202-024-02678-9.

Wang, S., Wang, L., Zhang, J., Gao, H., Xiao, M., & Song, H., 2025. Third-component engineering in organic solar cells: material innovations, morphological control, and synergistic enhancement. Nano Energy 111329. https://doi.org/10.1016/j.nanoen.2025.111329.

Wei, J., Chen, H., Liu, J., Wang, F., & Wang, C., 2025. Radiative cooling technologies toward enhanced energy efficiency of solar cells: materials, systems, and perspectives. Nano Energy 110680. https://doi.org/10.1016/j.nanoen.2025.110680.

Yan, Y., & Xiang, C., 2026. Life cycle carbon footprint and sustainability assessment of building-integrated photovoltaics: a comparative review of technologies and applications. Energy Build. 350, 116678. https://doi.org/10.1016/j.enbuild.2025.116678.

JOURNAL OF GAS TECHNOLOGY

Volume 10 / Issue 2 / Winter 2025 / Pages 88-118

Journal Home page: https://jgt.irangi.org

Intelligent and Circular Drilling Wastewater Treatment: A Review Integrating Machine Learning, Uncertainty Quantification, and Resource Recovery

Seyed Ata Elyas Sorkhabi[1], Mohammadreza Akbari[2*], Yasin Khalili[3]

1. BSc. Student, Department of Petroleum and Geoenergy Engineering, Amirkabir University of Technology, Tehran, Iran
2. Assistant Professor, Department of Petroleum and Geoenergy Engineering, Amirkabir University of Technology, Tehran, Iran
3. Ph.D. Student, Department of Petroleum and Geoenergy Engineering, Amirkabir University of Technology, Tehran, Iran

ARTICLE INFO

REVIEW ARTICLE

Article History:
Received: 27 October 2025
Revised: 01 November 2025
Accepted: 11 December 2025

Keywords:
Drilling wastewater treatment
Machine learning
Uncertainty quantification
Circular economy
Resource recovery
Oil and gas industry

DOR: 20.1001.1/jgt.2026.2082269.1066

ABSTRACT

Drilling wastewater generated during oil and gas operations presents a complex environmental challenge due to its highly variable composition, large volumes, and the presence of hazardous organic and inorganic contaminants. Conventional treatment approaches, although widely implemented, often fail to achieve consistent performance under dynamic operating conditions and increasingly stringent environmental regulations.

This review provides a comprehensive and forward-looking analysis of drilling wastewater management by integrating treatment technologies with emerging concepts of circular economy, data-driven intelligence, and uncertainty quantification. The characteristics and sources of drilling wastewater are examined to highlight their inherent variability and associated treatment challenges. Conventional, advanced, and hybrid treatment technologies are critically evaluated in terms of efficiency, limitations, and applicability for water reuse and resource recovery. Circular economy strategies, including water recycling, material recovery, and zero liquid discharge (ZLD), are also assessed from a sustainability perspective.

In addition, the role of machine learning in performance prediction, process optimization, and real-time monitoring is discussed, alongside uncertainty quantification approaches such as probabilistic modeling and Bayesian inference for risk-informed decision-making. From an industrial perspective, the integration of intelligent modeling and uncertainty-aware frameworks enables more reliable, adaptive, and efficient treatment systems.

Despite these advancements, challenges remain in data availability, model transferability, system integration, and economic feasibility. This review establishes a unified framework that bridges environmental engineering, data science, and sustainability, providing a pathway toward intelligent, circular, and resilient drilling wastewater treatment systems.

How to cite this article
S.A.E. Sorkhabi, M. Akbari, Y. Khalili, Intelligent and Circular Drilling Wastewater Treatment: A Review Integrating Machine Learning, Uncertainty Quantification, and Resource Recovery. Journal of Gas Technology. 2025; 10(2): 88-118. (https://jgt.irangi.org/article_737844.html)

* Corresponding author.
E-mail address: akbari.pe@aut.ac.ir, (M. Akbari).

Available online 30 December 2025
2588-5596/© 2016 The Authors. Published by Iranian Gas Institute.
This is an open access article under the CC BY license. (https://creativecommons.org/licenses/by/4.0)

1. Introduction

Drilling wastewater management has become a critical component of upstream oil and gas operations due to increasingly complex environmental, operational, and regulatory challenges associated with drilling activities (Lebedev and Cherepovitsyn 2024). As exploration expands toward deeper, geologically heterogeneous, and environmentally sensitive regions, large volumes of wastewater containing drilling fluids, cuttings, formation water, and chemical additives are generated. These waste streams pose significant risks to soil, surface water, and groundwater systems if not properly treated. In response, regulatory agencies worldwide have introduced stricter discharge limits, zero-pollution policies, and reporting requirements, compelling operators to adopt more reliable and sustainable wastewater management practices (Adverse).

Drilling wastewater is inherently complex and dynamic, with composition varying continuously depending on geological formations, drilling fluid formulations, and operational conditions. Conventional treatment approaches primarily based on physical, chemical, and biological processes have been widely applied; however, they often rely on fixed design assumptions and are not well-suited to handle such variability (Tsolakis, Harrington et al. 2023). As a result, treatment performance can be inconsistent, particularly under fluctuating field conditions.

Conventional review studies on drilling wastewater treatment are typically based on static, technology-centric assessments, in which treatment processes are described under fixed assumptions and idealized conditions. In this context, the term static refers to approaches that do not explicitly account for temporal variability, fluctuations in wastewater composition, or changes in operational conditions. As a result, such assessments often overlook the dynamic behavior of real systems and provide limited insight into how treatment performance evolves over time (Ghasemi, Akbari et al. 2025).

In contrast, drilling wastewater systems are inherently dynamic, characterized by continuously changing composition, flow rates, and physicochemical properties due to variations in geological formations, drilling phases, and operational practices. A dynamic approach therefore refers to systems that evolve over time and incorporate real-time data, adaptive modeling, and feedback-driven control mechanisms. These approaches enable continuous adjustment of treatment processes in response to changing inputs, improving accuracy, efficiency, and robustness (Yang, Diao et al. 2022).

Consequently, modern wastewater management requires an integrated and dynamic framework that combines real-time monitoring, data-driven intelligence, and uncertainty-aware modeling. The growing application of machine learning, advanced sensing technologies, and probabilistic methods reflects this shift toward adaptive systems capable of capturing variability and supporting more reliable and optimized treatment performance (Smol, Adam et al. 2020, Matheri, Mohamed et al. 2022, Zong and Guan 2025).

In parallel, the transition from linear waste disposal toward circular economy principles has introduced new opportunities for sustainable wastewater management. Circular approaches emphasize water reuse, resource recovery, and waste minimization, transforming drilling wastewater from an environmental liability into a potential resource. Strategies such as recovery of hydrocarbons, recycling of drilling materials, and implementation of zero liquid discharge (ZLD) systems contribute to reducing environmental impact while improving economic efficiency. ZLD refers to a treatment approach in which all wastewater is processed to eliminate liquid discharge, leaving only solid residues and enabling maximum water recovery (Scheidt, Li et al. 2018).

Another critical aspect of modern wastewater management is uncertainty quantification, which addresses the inherent variability and unpredictability of drilling wastewater systems. Variations in composition, operational conditions, and treatment performance introduce significant uncertainty that cannot be adequately captured by deterministic models. Probabilistic approaches, including Bayesian inference and Monte Carlo simulation, provide a more realistic framework for evaluating system performance, assessing risks, and supporting decision-making under uncertain conditions.

Despite recent advancements, existing review studies often treat treatment technologies, machine learning applications, circular economy strategies, and uncertainty quantification as separate domains. There remains a lack of integrated frameworks that simultaneously address these interrelated aspects. Unlike previous reviews that focus primarily on individual technologies or isolated optimization methods, this study integrates machine learning, uncertainty quantification, and circular economy principles into a unified framework. This integrated perspective enables a more realistic representation of drilling wastewater systems, where variability, data-driven intelligence, and resource recovery must be addressed collectively.

To highlight the contribution of this work in relation to existing literature, a comparative summary of recent studies is provided in Table 1. The table outlines differences in scope, methodology, and level of integration, emphasizing the unique contribution of the present study in combining treatment technologies with intelligent and uncertainty-aware approaches.

This review adopts a structured and transparent methodology to ensure comprehensive coverage and scientific rigor. Peer-reviewed publications were collected from major scientific databases, with particular emphasis on recent studies (2022-2025) to capture the latest developments in treatment technologies, machine learning applications, and circular economy strategies.

Overall, this work provides a holistic and forward-looking framework for drilling wastewater management that integrates engineering, data science, and sustainability principles. By combining treatment technologies, intelligent modeling, uncertainty quantification, and circular economy concepts, the study aims to support the development of adaptive, efficient, and environmentally responsible wastewater treatment systems for the oil and gas industry.

(Table 1) presents a comparative overview of recent studies, highlighting their methodologies, key contributions, and limitations, and demonstrating how the present study addresses existing gaps through an integrated framework combining machine learning, uncertainty quantification, and circular economy principles.

Table 1. Comparative Summary of Recent Studies on Drilling Wastewater Treatment Technologies and Approaches

Study (Author, Year)	Scope	Methods/ Approach	Key Contribution	Limitations	Gap Addresse in This Study
(Wei, Zhang et al. 2019)	Oilfield wastewater treatment technologies	Review of physical, chemical, and membrane processes	Highlighted efficiency of hybrid systems for complex wastewater	Limited integration of data-driven optimization	This study integrates ML and adaptive modeling for optimization
(Chang, Lee et al. 2019)	Me brane-based treatment of oily wastewater	Experimental + modeling	Demonstrated high removal efficiency of UF/ RO systems	Membrane fouling and high energy demand	Incorporates predictive maintenance and ML-based fouling prediction
(Smol, Adam et al. 2020)	Circular economy in wastewater systems	Conceptual + policy framework	Emphasized transition to resource recovery and reuse systems	Limited application to drilling wastewater specifically	Applies circular economy specifically to drilling wastewater systems
(Lawan, Kumar et al. 2023)	Advanced wastewater treatment technologies	Comprehensive review	Identified need for integration of advanced oxidation and hybrid processes	Lack of real-time operational analysis	Introduces real-time monitoring and AI-driven control
(Fernandes, Ramísio et al. 2024)	Characteristics and treatment challenges of drilling wastewater	Experimental + analytical	Provided detailed characterization of wastewater variability	Limited predictive modeling capability	Integrates ML to handle variability and prediction
(Gangwar, Rawat et al. 2025)	Environmental impacts of oilfield wastewater	Life cycle and environmental analysis	Assessed environmental risks an treatment impacts	Limited focus on optimization and adaptive systems	Combines LCA with ML and decision-support frameworks
(Zhang 2025)	Circular economy approaches	Conceptual + case studies	Proposed resource recovery pathways for wastewater reuse	Lack of real-time system integration	Integrates circular economy with intelligent control systems
(Dhadumia, Paul et al. 2026)	Hybrid treatment systems	Experimental (membrane + chemical)	Demonstrated improved contaminant removal efficiency	High cost and system complexity	Applies ML for system optimization and cost reduction
Recent Advances	AI-driven and digital wastewater systems	Digital twin, IoT, and ML integration	Demonstrated potential of autonomous and adaptive treatment systems	Data scarcity and integration challenges	Proposes unified framework combining ML, UQ, and circular economy

(Figure 1) illustrates the overall system architecture linking drilling wastewater characteristics with treatment processes, machine learning-based monitoring, uncertainty quantification, and decision-making pathways, including water reuse, resource recovery, and zero liquid discharge (ZLD).

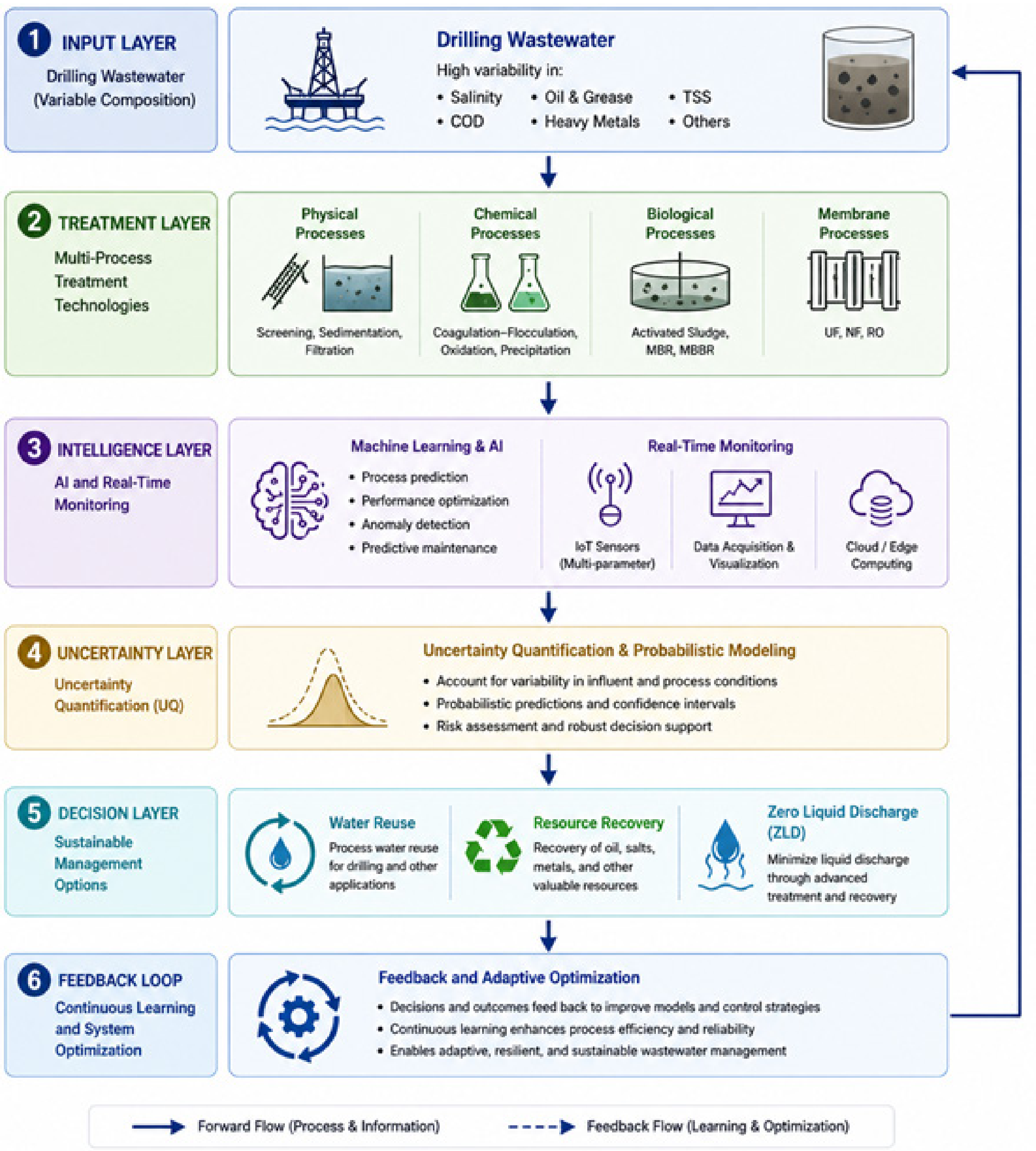

Figure 1. Integrated Framework for Intelligent and Circular Drilling Wastewater Treatment

2. Characteristics of Drilling Wastewater

Drilling wastewater is a highly complex and heterogeneous mixture whose composition varies significantly depending on the type of drilling fluid used, geological formation characteristics, operational practices, and the stage of drilling (Pereira, Sad et al. 2022, Basu, Shaw et al. 2025). Fundamentally, the wastewater derives from both water-based and oil-based drilling muds, each contributing distinct chemical and physical attributes to the waste stream (Zhang, Li et al. 2024). Water-based muds typically introduce bentonite, barite, polymers, and various inorganic salts, whereas oil-based muds contribute emulsified hydrocarbons, synthetic base oils, surfactants, and stabilizing agents, resulting in a wastewater matrix with elevated oil content and more persistent organic compounds. This duality creates substantial variability in wastewater behavior, treatment difficulty, and environmental impact, requiring tailored mitigation strategies for different operational contexts (Ahmed, Alsaihati et al. 2021).

Beyond mud-related constituents, drilling wastewater often contains a suite of hazardous and potentially toxic contaminants derived from both the formation and the drilling process itself. These include heavy metals such as chromium, cadmium, lead, arsenic, and barium, which may leach from formations or be introduced through additives. Additionally, the wastewater can contain high concentrations of dissolved solids, suspended clay particles, nitrogenous compounds, biocides, corrosion inhibitors, lubricants, and degradation byproducts of drilling chemicals. The combination of organic and inorganic pollutants many of which exhibit low biodegradability, high mobility, or strong affinity for particulates complicates separation and treatment processes. Moreover, the presence of hydrocarbons, surfactants, and emulsifiers often leads to the formation of stable oil-water emulsions that resist conventional treatment methods such as simple gravity separation or basic chemical coagulation (Barcelona, Gibb et al. 1983).

A further challenge associated with drilling wastewater is the lack of standardization in both its composition and in reporting practices across different operators and regions. Variability in drilling technology, fluid formulation, geological strata, and regulatory frameworks results in wastewater profiles that are difficult to compare or generalize (Zhang, Xu et al. 2022). For example, wastewater generated in shale gas basins may carry high levels of dissolved salts and formation minerals, whereas

Offshore drilling operations often exhibit elevated hydrocarbon content and synthetic additives due to the widespread use of oil-based and synthetic-based drilling muds in these environments. These fluids are preferred in offshore operations because they provide enhanced wellbore stability, improved lubrication, and better performance under high-pressure and high-temperature conditions. However, their use results in wastewater streams enriched with emulsified hydrocarbons, base oils, and chemically stabilized additives that are more persistent and difficult to treat (Loss, Cavali et al. 2026).

In addition, stricter operational requirements in offshore drilling, such as preventing formation damage and maintaining drilling efficiency, further drive the use of such complex fluid systems.

Overall, drilling wastewater represents a multifaceted environmental challenge characterized by chemical complexity, operational variability, and analytical uncertainty. These characteristics underscore the need for flexible, adaptive, and intelligent treatment frameworks capable of addressing both expected and unforeseen variations in wastewater composition (Garg, Kumari et al. 2024).

(Table 2) summarizes the physical, chemical, and operational characteristics of drilling wastewater, highlighting the wide variability in composition that complicates treatment design and performance prediction.

(Figure 2). Composition and variability of drilling wastewater derived from water-based and oil-based drilling muds, highlighting the diversity of suspended solids, hydrocarbons, salts, surfactants, polymers, heavy metals, and chemical additives that contribute to compositional uncertainty across formations and drilling stages.

(Figure 3). Characteristics and variability of drilling wastewater originating from water-based and oil-based drilling muds, illustrating the diverse chemical additives and contaminants present, as well as the dynamic variability in key parameters such as salinity, pH, total suspended solids (TSS), and sludge content across drilling stages and formations.

Table 2. Typical Characteristics of Drilling Wastewater (Thacker, Carlton Jr et al. 2015, Jin, Zhang et al. 2022, Pereira, Sad et al. 2022)

	Typical Components	Concentration Range	Primary Source	Environmental Concern
Physical	Total Suspended Solids (TSS), turbidity, oil droplets	TSS: 1,000-50,000 mg/L; Oil droplets: 50-5,000 mg/L	Drill cuttings, drilling mud	Limited integration of data-driven optimization
Chemical (Inorganic)	Salts (Na^+, Cl^-), Ba, Cr, Pb	TDS: 5,000-200,000 mg/L; Heavy metals: 0.1-100 mg/L	Formation fluids, additives	Membrane fouling and high energy demand
Chemical (Organic)	Hydrocarbons, surfactants, additives	Oil & grease: 100-10,000 mg/L; COD: 500-20,000 mg/L	Oil-based muds, synthetic additives	Limited application to drilling wastewater specifically
Operational Variability	pH, salinity, temperature	pH: 10-6; Salinity: 200,000-5,000 mg/L; Temperature: 90-20C	Drilling phase, geological formation	Treatment instability, process inefficiency

Ranges are indicative and may vary depending on geological formation and drilling conditions

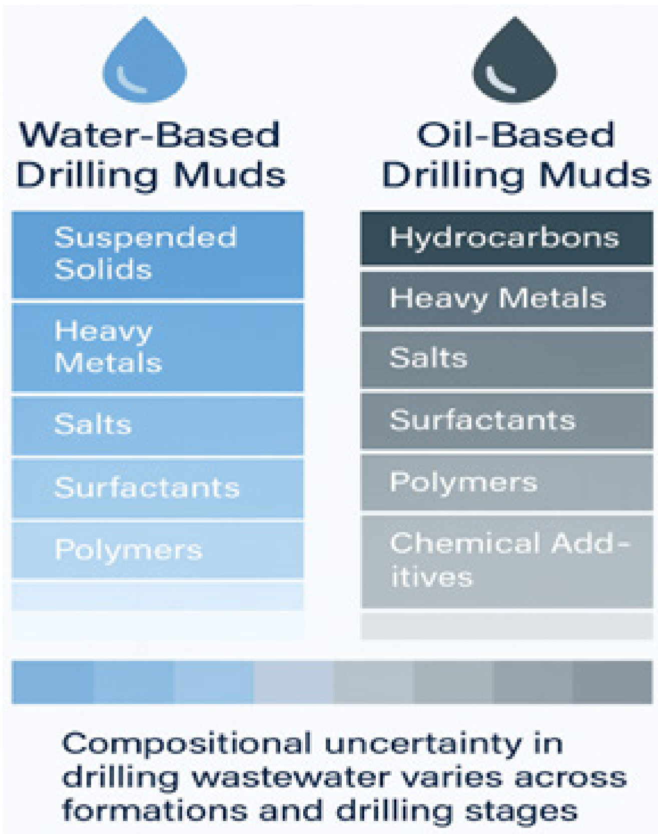

Figure 2. Composition and Variability of Drilling Wastewater from Water-based and Oil-based Muds

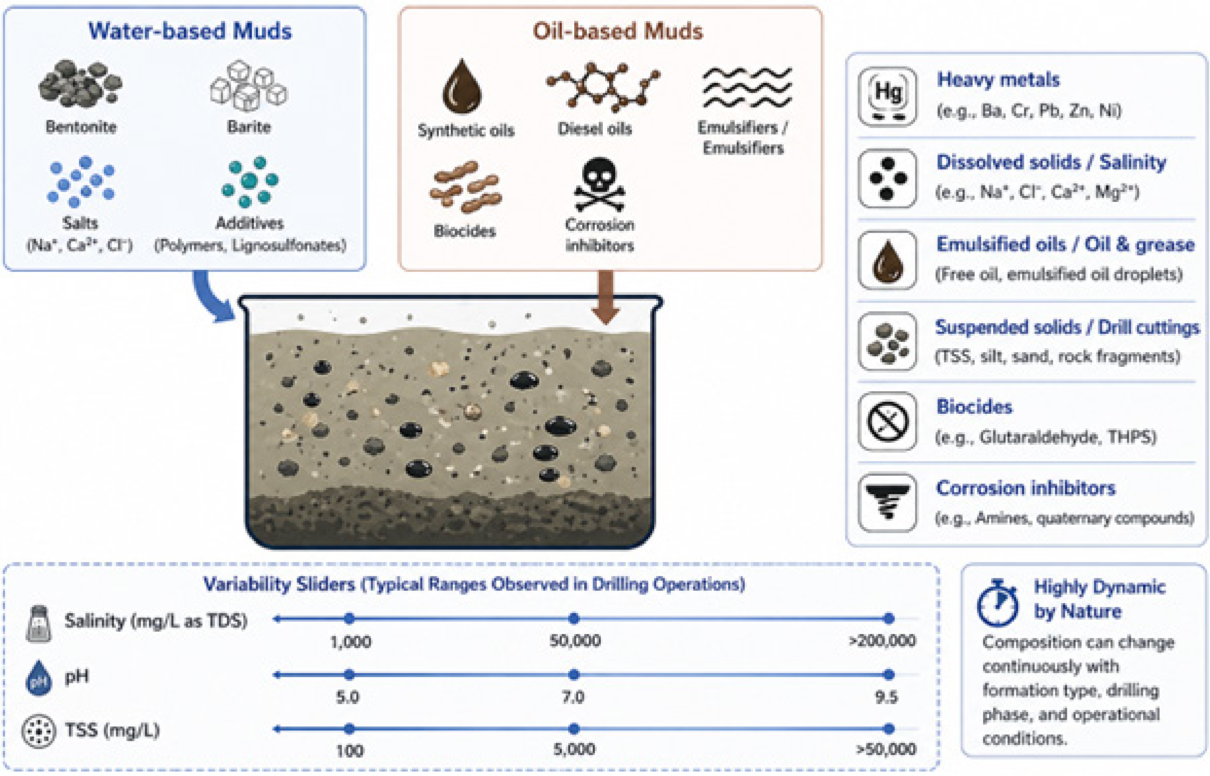

Figure 3. Key Characteristics and Variability of Drilling Wastewater

3.Conventional and Advanced Treatment Technologies

Although a wide range of physical, chemical, biological, and hybrid treatment technologies has been proposed for drilling wastewater management, their performance and applicability vary significantly depending on wastewater composition, operational scale, and site constraints (Dhadumia, Paul et al. 2025). Therefore, a purely descriptive comparison is insufficient for engineering decision-making. A critical evaluation considering treatment efficiency, energy demand, economic feasibility, and technology maturity is required to identify realistic and scalable solutions for industrial deployment (Yang, Sun et al. 2023).

Drilling wastewater treatment has traditionally relied on a combination of physical, chemical, and biological processes designed to reduce suspended solids, remove emulsified oil, neutralize hazardous constituents, and meet environmental discharge or reuse requirements (Ajao 2024). Physical treatment methods serve as the initial barrier against large quantities of solids and dispersed contaminants. Techniques such as sedimentation, screening, and centrifugation are commonly employed to separate drill cuttings and heavy particulates. Flotation systems, including dissolved air flotation, further enhance the removal of oil droplets and fine solids by promoting their aggregation and rise to the surface. Although these physical processes are simple, robust, and widely adopted in field operations, they often lack the capability to address dissolved contaminants or the chemically stabilized emulsions formed in oil-based and synthetic drilling systems. As a result, physical methods alone rarely achieve the stringent quality necessary for reinjection, reuse, or environmentally compliant discharge (Liu, Li et al. 2024).

Chemical treatment technologies represent another critical component of drilling wastewater management, particularly due to their ability to destabilize emulsions, precipitate dissolved metals, and oxidize recalcitrant organic pollutants. Coagulation-flocculation processes use metal salts or polymers to aggregate colloids and reduce turbidity, forming sludge that can be removed by sedimentation or filtration. Chemical oxidation, using agents such as ozone, hydrogen peroxide, or persulfate, targets persistent hydrocarbons and additives that resist biological degradation. Meanwhile, advanced chemical approaches involving electrocoagulation and electro-oxidation offer improved performance with fewer chemical inputs, although they require higher energy consumption and more sophisticated infrastructure. Despite these advancements, chemical treatments often generate substantial volumes of secondary waste, such as sludge or spent reagents, which necessitate careful handling and disposal. Moreover, the efficiency of chemical processes can be highly sensitive to variations in wastewater composition, pH, and salinity, making their optimization challenging in dynamic drilling environments (De Maman, da Luz et al. 2022).

Biological treatment methods, though less commonly applied to drilling wastewater, have gained attention as sustainable alternatives capable of degrading organic pollutants through microbial metabolism. Systems such as activated sludge reactors, fixed-film bioreactors, and constructed wetlands have shown potential for removing biodegradable hydrocarbons, nitrogenous compounds, and some drilling additives. Phytoremediation, using plants to uptake or transform contaminants, offers another environmentally friendly approach, particularly for land-based systems. However, the high salinity, presence of biocides, and complex organic mixtures characteristic of drilling wastewater often inhibit microbial activity and reduce treatment efficiency. Consequently, biological processes typically require significant pretreatment or dilution to become viable, limiting their applicability in many upstream operations (Jain, Majumder et al. 2020).

In recent years, hybrid and membrane-based technologies have emerged as promising solutions capable of achieving higher treatment efficiencies while recovering water for reuse. Membrane filtration processes such as microfiltration, ultrafiltration, nanofiltration, and reverse osmosis can effectively remove fine particulates, dissolved organics, and salts, depending on membrane pore size and configuration. Hybrid systems that integrate membranes with physical or chemical pretreatment, advanced oxidation, or biological processes can address a broader spectrum of contaminants and reduce fouling. Nonetheless, membrane technologies are frequently constrained by high capital and operational costs, energy requirements, and susceptibility to fouling by oil, suspended solids, and scaling constituents. Furthermore, managing concentrated reject streams remains a significant challenge, especially in offshore or remote drilling locations where disposal options are limited (Warsinger, Chakraborty et al. 2018).

Overall, the range of technologies available for drilling wastewater treatment reflects a balance between robustness, efficiency, cost, and operational feasibility. While conventional approaches continue to play a foundational role, advanced and hybrid systems offer enhanced performance but bring new challenges related to cost, energy use, and sludge management. As drilling operations expand into more demanding environments and regulatory expectations tighten, there is a growing need for treatment solutions that are both scalable and adaptable to highly variable wastewater compositions. This underscores the importance of intelligent optimization strategies, circular resource recovery, and uncertainty-aware design elements that increasingly define the future landscape of drilling wastewater management (Li, Tiraferri et al. 2025).

Despite their widespread use, conventional physical and chemical treatments often fail to achieve consistent effluent quality under highly variable drilling wastewater conditions. Advanced technologies such as membrane filtration and electrochemical processes offer superior contaminant removal but are frequently constrained by high energy consumption, fouling, and operational complexity (Yuan and He 2015). Moreover, many proposed treatment methods remain at laboratory or pilot scale, highlighting a gap between academic development and industrial implementation. These limitations underscore the need for adaptive, intelligence-assisted, and uncertainty-aware treatment frameworks capable of responding to fluctuating influent characteristics (Pereira, Sad et al. 2022).

From a technology readiness perspective, only a limited number of drilling wastewater treatment methods have reached full industrial maturity. Physical separation, chemical coagulation, and dissolved air flotation systems generally exhibit high TRL values (8-9), whereas biological treatment, advanced oxidation, and hybrid membrane systems often remain at pilot or demonstration stages (TRL 5-7). This disparity in maturity highlights the importance of integrating emerging technologies cautiously and in combination with proven treatment processes (Teodoriu and Bello 2021, Pouran Manjily, Alborzi et al. 2024).

Recent advancements in drilling wastewater treatment increasingly rely on the integration of advanced treatment technologies with machine learning and probabilistic modeling approaches. While physical, chemical, biological, and membrane-based processes provide the fundamental mechanisms for contaminant removal, their performance is often constrained by the highly variable composition and dynamic operating conditions of drilling wastewater (Bai, Li et al. 2026).

Machine learning (ML) techniques enable the modeling of complex, nonlinear relationships between process parameters and treatment performance, allowing for improved prediction accuracy, real-time monitoring, and adaptive optimization of treatment systems. In parallel, probabilistic approaches such as uncertainty quantification (UQ), Bayesian inference, and Monte Carlo simulation provide a systematic framework for evaluating variability, propagating uncertainties, and supporting risk-informed decision-making (Kalhormohammadi and Khoramipour 2025).

The integration of these data-driven and probabilistic methods with conventional and advanced treatment technologies enhances system robustness, improves operational efficiency, and enables more reliable performance under fluctuating conditions. This combined approach facilitates the transition from static, design-based treatment strategies to dynamic, intelligent, and adaptive systems capable of meeting increasingly stringent environmental and regulatory requirements.

(Table 3) summarizes key treatment methods based on target contaminants, performance, energy demand, cost, and technology readiness level (TRL), highlighting their advantages and limitations for industrial-scale applications.

The comparison highlights the trade-offs between treatment efficiency, energy consumption, and operational complexity, emphasizing the need for integrated and adaptive treatment strategies.

Table 4. Comparative Evaluation of Pressure Enhancement Techniques

Treatment Category	Technology	Primary Target Contaminants	Typical Removal Performance	Energy Demand (kWh/m³)	CAPEX / OPEX*	TRL	Sludge / By-products	Key Industrial-Scale Limitations
Physical	Sedimentation / Screening	Coarse solids, cuttings	Low-Moderate	< 0.1	Low / Low	9	High solids residue	Ineffective for fine particles and dissolved pollutants
Physical	Centrifugation	Fine solids, oil droplets	Moderate	0.2-0.5	Medium / Medium	8-9	Concentrated solids	High maintenance, limited oil removal
Physical	Dissolved Air Flotation (DAF)	Oil, grease, fine solids	Moderate-High	0.3-0.6	Medium/ Medium	8-9	Oily sludge	Sensitive to influent variability and chemical dosing
Chemical	Coagulation-Flocculation	Colloids, emulsified oil, metals	Moderate-High	0.1-0.5	Low / Medium	8-9	High chemical sludge	Sludge handling and disposal costs
Chemical	Chemical Oxida-tion (AOPs)	Recalcitrant organics	High	1-4	High / High	6-7	Minimal solids	High energy and reagent consumption
Chemical	Electrocoagulation / Electro-oxidation	Oil, metals, COD	High	2-6	Medium / High	6-7	Metal hydroxide sludge	Electrode fouling and energy demand
Biological	Activated Sludge / Biofilm	Biodegradable organics	Moderate	0.3-1.2	Medium / Medium	5-7	Biological sludge	Salinity and biocide inhibition
Biological	Constructed Wetlands	Organics, nutrients	Low-Moderate	< 0.2	Low / Low	5-6	Biomass	Large footprint, slow kinetics
Membrane-Based	MF / UF	TSS, oil droplets	High	0.5-2	High / Medium	7-8	Concentrated reject	Fouling by oil and solids
Membrane-Based	NF / RO	Dissolved salts, organics	Very High	2-6	High / High	7-9	High-salinity brine	Fouling, scaling, concentrate disposal
Hybrid Systems	Physical + Membrane / AOP	Broad contaminant spectrum	Very High	2-8	High / High	6-7	Mixed waste streams	System complexity and control requirements

*CAPEX/OPEX: qualitative order-of-magnitude comparison (Low / Medium / High).

4. Circular Economy Integration

The integration of circular economy principles into drilling wastewater management represents a significant shift from traditional linear disposal practices toward strategies that conserve resources, reduce environmental burdens, and enhance operational resilience (Digitemie, Onyeke et al. 2025). In drilling operations, water reuse and re-injection have emerged as central components of circularity, particularly in regions where water scarcity and regulatory constraints make fresh water procurement increasingly challenging. Treated drilling wastewater can be reused directly in mud formulation, rig wash operations, or hydraulic systems after appropriate conditioning, thereby reducing the demand for freshwater intake. Additionally, re-injection into deep geological formations offers an alternative disposal pathway that minimizes surface contamination risks. However, re-injection requires that wastewater quality meet strict chemical and particulate thresholds to prevent reservoir damage and clogging, which in turn underscores the importance of advanced treatment methods and real-time monitoring systems capable of ensuring consistent water quality under variable operational conditions (Jamshidi, Saen et al. 2025).

A fundamental opportunity for circularity lies in the recovery and valorization of valuable components embedded within drilling wastewater. Materials such as bentonite, barite, and high-value hydrocarbons are routinely lost during drilling operations despite their significant economic and functional importance in mud formulation. Advanced separation techniques, including hydrocycloning, membrane filtration, and tailored chemical treatments, allow for the recovery of these materials with sufficient purity for reuse. For example, barite a weighting agent with considerable market value can be separated from finer solids and recycled into new mud systems, reducing material consumption and operational costs. Similarly, hydrocarbons recovered from oil-based mud waste streams can be refined and reintegrated into drilling or other industrial processes. The ability to recover and repurpose these constituents not only minimizes waste generation but also transforms drilling wastewater from a liability into a secondary resource stream, reinforcing the economic viability of circular practices (Lihu and Jiahe 2025).

Zero liquid discharge (ZLD) presents an ambitious but powerful approach within the circular economy framework, particularly for offshore environments or isolated drilling sites where wastewater disposal options are limited. ZLD systems aim to eliminate liquid effluents entirely by combining evaporation, crystallization, and advanced concentration technologies to separate water and recover solid residues. While ZLD offers near-total environmental protection and maximum resource recovery, it is often associated with high energy consumption, significant capital costs, and the need for robust pre-treatment to prevent scaling and fouling within thermal systems. Nonetheless, emerging innovations such as forward osmosis, membrane distillation, and hybrid thermal-membrane processes are reducing the barriers to ZLD implementation, suggesting that future drilling operations may increasingly adopt closed-loop systems with minimal to zero discharge footprints (Panagopoulos and Michailidis 2025).

Life cycle assessment (LCA) provides critical insights into the broader sustainability implications of circular drilling wastewater strategies. Through LCA, trade-offs among energy consumption, emissions, material recovery, and environmental impacts can be systematically evaluated across the entire treatment and reuse chain. For instance, while advanced membrane systems may offer high contaminant removal efficiency and support water reuse, they may also incur higher energy footprints compared to simpler, conventional options (Thompson and Dvorak 2024). Conversely, resource recovery processes may offset environmental burdens by reducing the need for virgin material extraction, thereby yielding net-positive sustainability outcomes. LCA studies also highlight the importance of operational context, as the environmental benefits of circular strategies may vary depending on site-specific factors such as energy mix, waste composition, regulatory requirements, and logistical constraints. Ultimately, integrating LCA into decision-making enables operators to design drilling wastewater management systems that maximize circularity while minimizing unintended environmental trade-offs.

Overall, circular economy integration represents a transformative pathway for drilling wastewater management, shifting the industry toward more sustainable, resource-efficient, and low-impact operations. By closing material and water loops, recovering valuable resources, adopting ZLD technologies, and employing

LCA-driven optimization, drilling activities can move closer to achieving fully intelligent and circular wastewater systems that support long-term environmental and economic sustainability (Kundu, Dutta et al. 2022).

(Table 4) illustrates key circular economy strategies for drilling wastewater, emphasizing water reuse, resource recovery, and zero liquid discharge pathways alongside their associated benefits and challenges.

Table 4. Circular Economy Pathways in Drilling Wastewater Management (Albusaimi, Al Dabbous et al. 2024, Gaurina-Međimurec, Simon et al. 2024, Digitemie, Onyeke et al. 2025)

Circular Strategy	Recovered Resource	Technology Used	Benefit	Main Challenge
Water reuse	Treated water	Membranes, AOP	Reduced freshwater use	Quality consistency
Material recovery	Barite, bentonite	Flotation, separation	Cost savings	Separation efficiency
Hydrocarbon recovery	Base oil	Skimming, extraction	Resource valorization	Emulsion stability
ZLD	Salts, solids	Evaporation, crystallization	Zero discharge	High energy demand

(Figure 4) illustrates the circular economy-oriented framework for drilling wastewater management, highlighting how treatment technologies enable closed-loop water reuse, material recovery, and zero-liquid discharge pathways.

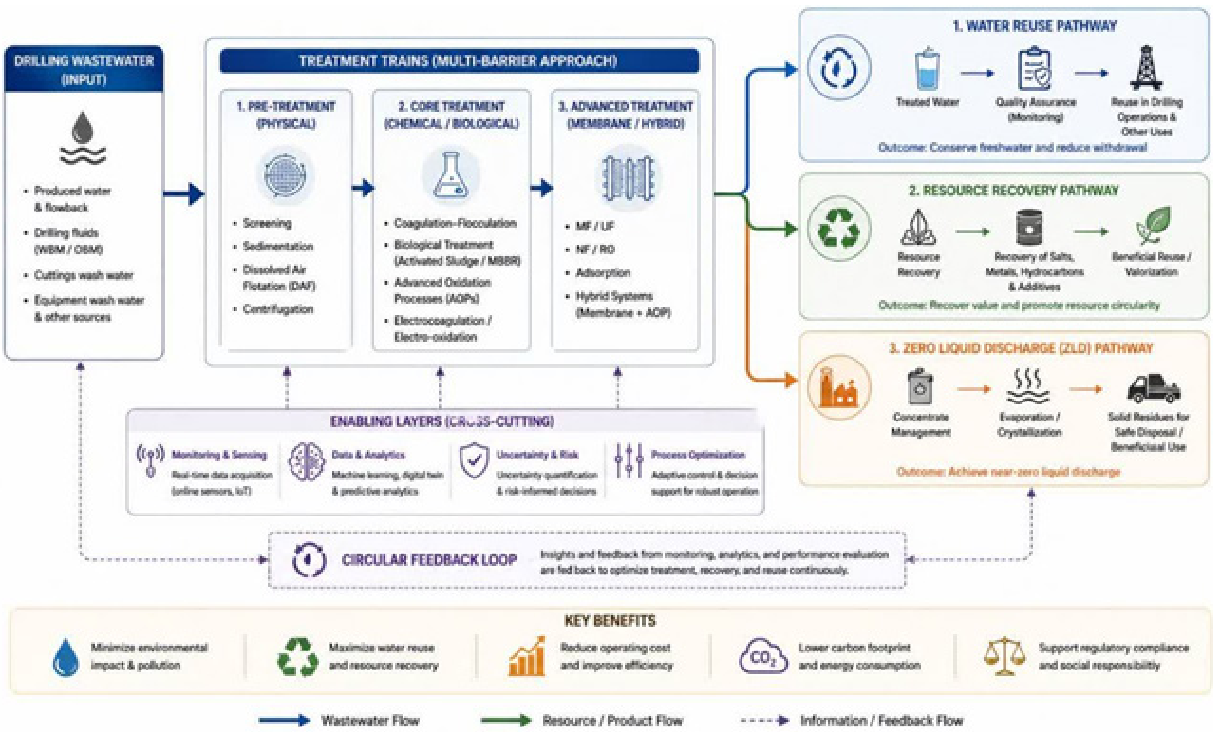

Figure 4. Circular Economy Pathways in Drilling Wastewater Management

(Figure 5). Circular economy pathways for drilling wastewater management, illustrating how treatment processes enable closed-loop water reuse and recovery of valuable materials such as barite, bentonite, and hydrocarbons, with optional life cycle assessment to evaluate energy use and emission reduction benefits.

Figure 5. Circular Economy Framework for Drilling Wastewater Management with Life Cycle Considerations

5. Data-Driven Intelligence in Treatment Optimization

The application of data-driven intelligence in drilling wastewater treatment has emerged as a powerful enabler for enhancing system performance, reducing operational uncertainties, and supporting adaptive decision-making (Zhou, Shi et al. 2023). Machine learning (ML), in particular, provides the ability to model highly nonlinear relationships between wastewater characteristics, treatment processes, and performance outcomes relationships that are often too complex to capture using traditional mechanistic models. One of the most prominent ML applications in this domain is performance prediction, where algorithms learn from historical datasets to estimate contaminant removal efficiency, optimal chemical dosing, membrane fouling rates, or energy consumption. Predictive models allow operators to forecast treatment outcomes under varying wastewater compositions, enabling proactive adjustments and reducing reliance on trial-and-error approaches. These capabilities are especially valuable in drilling contexts, where wastewater properties shift rapidly due to changes in geological formations, mud formulations, and drilling phases (Matheri, Mohamed et al. 2022, Kalhormohammadi and Khoramipour 2025).

Machine learning also plays a critical role in real-time monitoring, where sensor-derived data streams such as turbidity, conductivity, pressure, flow rates, and oil-in-water concentrations are processed to provide continuous insight into treatment system health. ML-driven monitoring frameworks can filter noise, detect subtle patterns, and identify emergent deviations that may not be apparent through manual observation. Coupled with edge computing and Internet of Things (IoT) technologies, these systems enable near-instantaneous diagnostic capabilities, improving operational visibility even in remote or offshore drilling environments. Beyond monitoring, ML offers significant advancements in process control and anomaly detection, wherein algorithms autonomously adjust process parameters such as coagulant dosage, pH, aeration rate, or membrane backwash cycles to maintain optimal performance. Anomaly detection models often based on unsupervised learning or neural network autoencoders can identify abnormal behaviors indicative of equipment failure, fouling events, or chemical imbalances before they escalate into costly operational disruptions (Tawfik 2024).

A wide range of machine learning algorithms has been applied to drilling wastewater treatment optimization, each offering distinct advantages depending on the complexity of the dataset and the nature of the prediction or classification task (Cangialosi, Bruno et al. 2021). Artificial neural networks (ANNs) are widely used for modeling nonlinear and multi-dimensional process relationships, particularly when dealing with large datasets and complex interactions among treatment variables. Support vector machines (SVMs) excel in classification tasks and are effective when datasets are moderate in size but require robust separation of classes, such as distinguishing normal from abnormal operating states. Random forest models provide strong performance in both regression and classification tasks while offering interpretability through feature importance metrics that help identify influential process parameters. Other emerging approaches include gradient boosting machines, deep learning architectures, Gaussian process regression, and reinforcement learning, which further expand the analytical capabilities for process optimization, adaptive control, and policy development. The diversity of available algorithms enables tailored model selection based on specific treatment objectives and data characteristics.

Despite these advancements, the successful application of data-driven approaches depends heavily on data quality, availability, and representativeness. Drilling wastewater datasets often suffer from issues such as sparse measurements, inconsistent sampling protocols, missing values, and limited long-term monitoring, all of which restrict model robustness. Additionally, operating conditions in drilling environments such as intermittent sampling, harsh field conditions, and rapid shifts in wastewater composition can introduce noise and variability that undermine model accuracy. A major challenge lies in transferability, as models trained on data from one region, mud formulation, or treatment system may not generalize effectively to others. Differences in contaminant profiles, sensor configurations, and process dynamics can cause significant performance degradation when models are applied outside their training domain. To address these challenges, techniques such as data augmentation, domain adaptation, hybrid mechanistic-ML modeling, and uncertainty quantification are increasingly employed to enhance model reliability and interpretability across diverse operational settings (Alsabaa, Gamal et al. 2022).

Overall, data-driven intelligence provides a transformative foundation for optimizing drilling wastewater treatment by enabling predictive accuracy, real-time responsiveness, and autonomous process control. As sensor technologies improve and data availability expands, machine learning will play an increasingly central role in designing intelligent, adaptive treatment systems capable of navigating the variability and complexity inherent in drilling wastewater management (Fisher, Wang et al. 2025).

While machine learning provides powerful tools for prediction, optimization, and process control, its effectiveness in drilling wastewater treatment is strongly influenced by data uncertainty and operational variability (Aparna, Swarnalatha et al. 2024). Sensor noise, missing data, and temporal changes in wastewater composition can significantly affect model accuracy and generalizability. Therefore, uncertainty quantification is not a complementary addition but a critical component for reliable ML deployment (Zidaoui 2024). Integrating uncertainty-aware ML models enables probabilistic prediction of treatment performance rather than deterministic estimates, thereby supporting risk-informed operational decisions (Asad and Everhart 2025). These probabilistic outputs can directly inform circular economy strategies by identifying operating conditions under which water reuse, material recovery, or zero-liquid-discharge pathways remain both technically feasible and economically viable (Pandey and Technology 2025).

(Table 5) categorizes major machine learning applications in drilling wastewater treatment, linking algorithm types to specific operational tasks, data inputs, and performance improvements.

Table 5. Machine Learning Applications in Drilling Wastewater Treatment (Olukoga, Feng et al. 2021, Sundui, Ramirez Calderon et al. 2021, Kalhormohammadi and Khoramipour 2025)

ML Task	Algorithm	Input Data	Output	Key Benefit
Performance prediction	ANN	Water quality, flow	Removal efficiency	Nonlinear modeling
Classification	SVM	Sensor data	Normal/fault	Robust detection
Optimization	Random Forest	Process parameters	Optimal settings	Interpretability
Anomaly detection	Autoencoders	Time-series data	Fault signals	Early warning

(Figure 6) presents a data-driven intelligent treatment framework in which machine learning, real-time sensor data, and uncertainty quantification support adaptive optimization of drilling wastewater treatment, resource recovery, and water reuse.

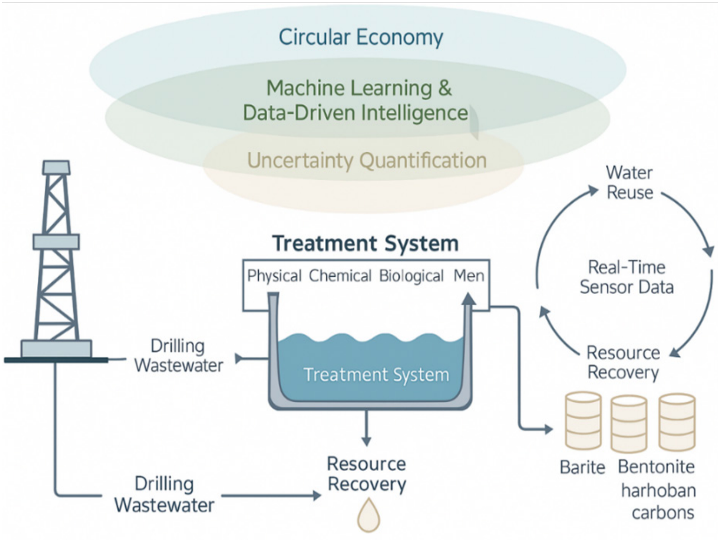

Figure 6. Data-Driven Intelligent Framework for Drilling Wastewater Treatment Optimization

6. Uncertainty Quantification in Treatment Modeling

In drilling wastewater treatment systems, uncertainty arises not only from wastewater composition and operational conditions but also from data-driven models used for performance prediction and optimization. When machine learning models are applied without explicit consideration of uncertainty, decision-making may be biased toward overly optimistic outcomes (Al-Dahidi, Alrbai et al. 2024). Consequently, uncertainty quantification provides the analytical foundation for integrating machine learning into robust and resilient treatment frameworks, ensuring that circular economy objectives such as reuse and resource recovery are achieved under realistic and variable field conditions (Nagpal, Siddique et al. 2024).

Uncertainty quantification has become an essential component of drilling wastewater treatment modeling due to the inherently variable and unpredictable nature of wastewater characteristics, operational conditions, and treatment system responses. One of the primary sources of uncertainty arises from input variability, as drilling wastewater composition changes continuously with geological formations, mud formulations, chemical additives, and drilling stages (Khalili, Ahmadi et al. 2023). These fluctuations affect contaminant loads, salinity, pH, and the presence of oils and emulsifiers, making it difficult to predict treatment performance using fixed-input models. Additionally, model structure uncertainty stems from the simplifying assumptions typically used in mechanistic or empirical models, such as linear relationships, steady-state conditions, or uniform reaction kinetics. These assumptions rarely hold under real field conditions, especially for processes involving membrane fouling, chemical dosing dynamics, or biological degradation. Parameter estimation uncertainty further complicates the task, as key parameters such as reaction rate constants, adsorption coefficients, or fouling indices are often derived from limited or inconsistent datasets, leading to calibration errors that propagate throughout the model (Shokir, Sallam et al. 2024).

To address these challenges, researchers increasingly contrast deterministic and probabilistic modeling approaches. Deterministic models rely on fixed input values and produce single-point predictions, which can be useful for initial design or operational planning but fail to capture the range of possible outcomes under variable conditions. In contrast, probabilistic models incorporate statistical distributions to represent uncertainty in inputs, parameters, or model structure, generating a spectrum of possible results rather than a single prediction. This probabilistic perspective is more aligned with the fluctuating reality of drilling operations, where treatment performance, contaminant removal efficiency, or system reliability may vary significantly from day to day. By quantifying the likelihood of different scenarios, probabilistic approaches provide a more comprehensive understanding of system behavior and are better suited for guiding operational strategies in environments where variability is the norm (Nooraiepour, Masoudi et al. 2021).

Bayesian methods and Monte Carlo simulations play pivotal roles in modern uncertainty quantification frameworks for drilling wastewater treatment. Bayesian approaches allow model parameters to be updated continually as new data become available, offering a dynamic mechanism for refining predictions and reducing uncertainty over time (Rasouli, Karimpour-Fard et al. 2025). This is particularly beneficial in treatment systems equipped with real-time monitoring sensors, where continuous data streams can enhance model accuracy and adaptability. Bayesian inference also provides posterior distributions for parameters and predictions, enabling transparent uncertainty characterization and improved decision-making under incomplete information. Monte Carlo simulations, on the other hand, use repeated random sampling to propagate input uncertainties through the treatment model, producing probability distributions of outputs such as effluent quality, sludge volume, or energy consumption. These simulations are especially useful for evaluating operational risks, identifying worst-case scenarios, and estimating the likelihood of regulatory compliance under varying wastewater conditions.

The integration of uncertainty quantification into treatment modeling offers significant implications for risk-informed decision-making. By explicitly accounting for variability and unknowns, operators can develop treatment strategies that are resilient rather than merely optimized for average conditions. Probabilistic insights enable more informed choices regarding treatment technology selection, operational setpoints, contingency planning, and investment decisions. For example, uncertainty-aware models can reveal whether a membrane system is likely to experience fouling beyond acceptable limits, whether chemical dosing needs to be adjusted to accommodate fluctuations in solid content, or whether reuse water will consistently meet reinjection quality standards. Furthermore, incorporating uncertainty into decision frameworks facilitates compliance with environmental regulations by highlighting conditions under which treatment systems may fail to meet discharge criteria, allowing operators to implement safeguards before violations occur. Ultimately, uncertainty quantification enhances both environmental protection and operational reliability by supporting decisions that are robust, adaptive, and grounded in the probabilistic realities of drilling wastewater management (Iseri, Iseri et al. 2025).

The integration of machine learning, uncertainty quantification, and circular economy principles enables a shift from reactive wastewater treatment toward intelligent and risk-informed circular systems. Machine learning models provide real-time predictions and optimization strategies, uncertainty quantification characterizes the reliability of these predictions, and circular economy frameworks translate model outputs into resource-efficient decisions (Lin, Wei et al. 2023). For example, uncertainty-aware ML models can identify optimal recovery pathways for barite or hydrocarbons while quantifying the probability of meeting reuse or discharge standards. This integrated approach supports resilient system design, minimizes environmental risk, and enhances economic performance under highly variable drilling conditions (Sircar, Yadav et al. 2021).

To translate emerging treatment technologies, machine learning, and circular economy principles into practical applications, a clear and structured implementation roadmap is required. (Figure 1) presents an integrated framework for intelligent and circular drilling wastewater management, illustrating how physical treatment processes, data-driven intelligence, and uncertainty-aware decision-making can be systematically combined within a closed-loop system (Rotan, Goettel et al. 2024).

The proposed roadmap begins with comprehensive wastewater characterization using online and offline sensors to capture temporal variability in key parameters such as oil content, salinity, and suspended solids (Nautiyal, Mishra et al. 2025). These data streams serve as inputs to machine learning models trained to predict treatment performance, optimize operating conditions, and detect anomalies in real time. Uncertainty quantification methods, including probabilistic modeling and Bayesian inference, are then applied to characterize the reliability of model predictions and propagate data and model uncertainties through the decision-making process (Gaurina-Međimurec, Simon et al. 2024).

Based on uncertainty-aware model outputs, risk-informed decisions are made regarding treatment pathways, water reuse, material recovery, or zero-liquid-discharge implementation. Circular economy objectives are operationalized by selecting recovery strategies that maximize resource value while maintaining regulatory compliance and system robustness under variable conditions (Daramola, Apeh et al. 2023). Feedback from treatment performance and recovery outcomes is continuously used to update models and reduce uncertainty, enabling adaptive and self-optimizing operation over time (Kandpal, Jaswal et al. 2024).

The proposed roadmap can be summarized in the following steps:

1. Real-time wastewater characterization and data acquisition;
2. ML-based performance prediction and operational optimization;
3. Uncertainty quantification and risk assessment;
4. Circular economy-based decision-making (reuse, recovery, ZLD);
5. Feedback-driven model updating and adaptive control.

(Table 6) identifies the principal sources of uncertainty in drilling wastewater treatment systems and summarizes the probabilistic methods used to quantify their impact on modeling accuracy and decision-making.

Table 6. Sources and Methods of Uncertainty Quantification (Iskandarani, Wang et al. 2016, Reichert and Technology 2020, Belia, Neumann et al. 2021)

Uncertainty Source	Description	Modeling Method	Decision Impact
Input variability	Changing wastewater composition	Monte Carlo	Risk estimation
Parameter uncertainty	Poorly calibrated constants	Bayesian inference	Robust design
Model uncertainty	Simplified assumptions	Ensemble models	Confidence bounds
Operational uncertainty	Sensor noise, failures	Probabilistic ML	Reliability

(Figure 7) illustrates an uncertainty-aware decision-making framework in which probabilistic modeling, real-time sensor data, and machine learning jointly inform adaptive control of drilling wastewater treatment and resource recovery.

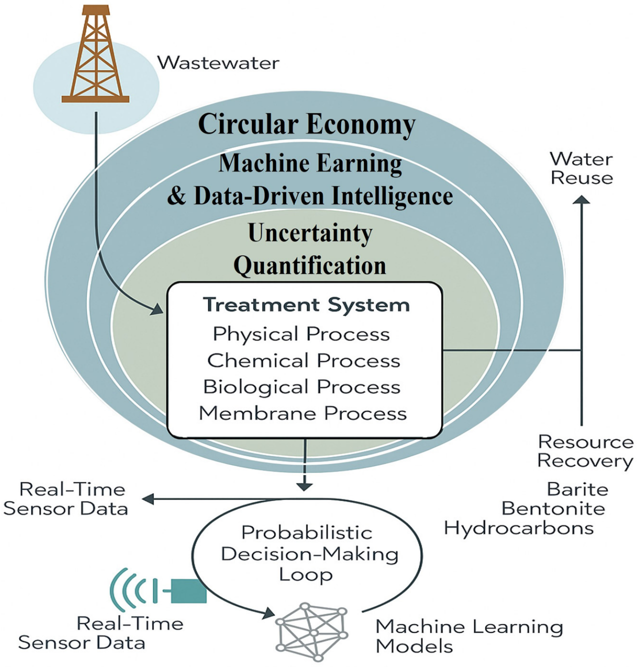

Figure 7. Integrated Machine Learning-Driven Wastewater Treatment System with Uncertainty-Aware Decision-Making

(Figure 8). Conceptual framework for uncertainty quantification and probabilistic decision-making in drilling wastewater treatment, illustrating how multiple sources of uncertainty are propagated through Bayesian inference and Monte Carlo simulation to support risk-informed and adaptive operational control.

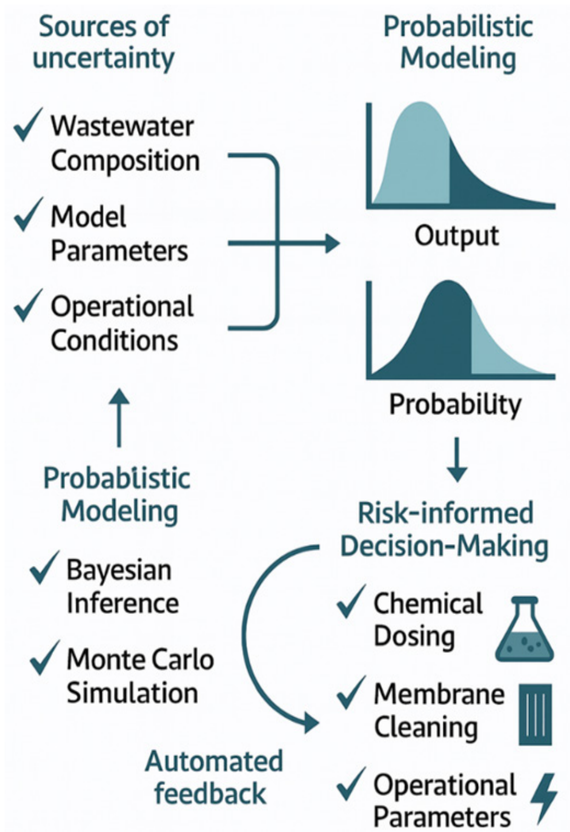

Figure 8. Conceptual Framework For Uncertainty Quantification In Drilling Wastewater Treatment Systems

7. Application of Artificial Intelligence in Operational Systems

The application of artificial intelligence (AI) in drilling wastewater treatment has evolved from theoretical modeling to practical, operation-level implementation. AI technologies enable real-time monitoring, adaptive control, predictive maintenance, and decision support, allowing treatment systems to respond dynamically to highly variable wastewater characteristics. This section highlights the key operational roles of AI in modern wastewater treatment systems (Sajib, Jaman et al. 2025).

7.1. Real-Time Process Monitoring

Real-time monitoring is a fundamental component of AI-enabled wastewater treatment systems. By integrating advanced sensors with machine learning algorithms, key parameters such as total suspended solids (TSS), oil content, salinity, and pH can be continuously tracked. AI models analyze incoming data streams to detect variations in wastewater composition and identify trends that may not be visible through conventional monitoring methods. This capability enables early detection of process deviations and supports more responsive and accurate system control (Shaaban 2025).

7.2. AI-Based Process Control

AI-driven control systems allow for the automatic adjustment of operational parameters in response to changing conditions. Machine learning models can optimize variables such as chemical dosing, pH levels, and flow rates in real time, improving treatment efficiency and reducing chemical and energy consumption. These systems operate within closed-loop control frameworks, where continuous feedback from sensors is used to update control decisions dynamically. This approach enhances system stability and ensures consistent performance under fluctuating operational conditions (Anyanwu, Agunwamba et al. 2026).

7.3. Predictive Maintenance

Predictive maintenance is another key application of AI in wastewater treatment operations. By analyzing historical and real-time data, AI models can detect early signs of equipment degradation, including membrane fouling, pump inefficiencies, and mechanical wear. This enables operators to perform maintenance activities proactively rather than reactively, reducing downtime, extending equipment lifespan, and lowering operational costs. Predictive maintenance also improves system reliability and minimizes the risk of unexpected failures.

7.4. Anomaly Detection

AI-based anomaly detection systems are designed to identify abnormal behavior in treatment processes. These systems can detect deviations from normal operating conditions, such as sudden changes in contaminant levels, unexpected process fluctuations, or sensor malfunctions. Early identification of anomalies allows for rapid corrective action, preventing system failures and ensuring compliance with environmental regulations. This capability is particularly important in complex and variable drilling environments (Anyanwu, Agunwamba et al. 2026).

7.5. Decision Support Systems

AI-driven decision support systems provide operators with actionable insights to guide wastewater management strategies. These systems can evaluate multiple scenarios and recommend optimal decisions, such as whether to reuse treated water, discharge it, or recover valuable resources. By integrating operational data, predictive models, and uncertainty analysis, decision support tools enhance operational efficiency and support more informed and sustainable decision-making processes (Jin, Liu et al. 2025).

7.6. Industrial Implementation Challenges

Despite the advantages of AI in operational systems, several challenges remain in large-scale implementation. Data availability and quality continue to be significant limitations, as many operations lack sufficient high-resolution datasets for effective model training. Sensor reliability and maintenance are also critical concerns, particularly in harsh drilling environments. In addition, integrating AI systems with existing infrastructure can be complex and may require significant investment and technical expertise. Addressing these challenges is essential for the successful adoption of AI-driven wastewater treatment systems in industrial settings (Jin, Liu et al. 2025).

(Table 7) summarizes representative pilot-scale applications of intelligent and circular drilling wastewater treatment systems, highlighting key technologies, performance outcomes, and operational conditions.

Table 7. Representative Pilot-Scale and Industrially Relevant Applications of Intelligent and Circular Drilling Wastewater Treatment (Ejairu, Aderamo Et Al. 2024, Aryanti, Nugroho Et Al. 2025, Ferri And Bolelli 2025)

Application Area	Scale	Approach	Demonstrated Benefit	Key Limitation
Solids & oil removal	Industrial	Centrifugation, DAF	Robust bulk removal	Limited dissolved removal
Chemical dosing control	Pilot	ML-based optimization	Reduced reagent use	Data availability
Drilling fluid monitoring	Field-like	ANN, RF models	Improved process control	Model transferability
Barite recovery	Industrial	Physical separation	Reduced material costs	Recovery efficiency
Water reuse	Pilot	Membrane systems	Lower freshwater demand	Fouling, energy use

8. Challenges and Limitations

Despite significant advancements in drilling wastewater treatment technologies and the growing integration of intelligent and circular approaches, several challenges and limitations continue to hinder large-scale implementation and operational efficiency. These limitations span data availability, technological performance, machine learning applicability, operational constraints, and economic and regulatory factors (Ghasemi, Akbari et al. 2025).

8.1. Data-Related Limitations

One of the primary challenges in developing intelligent wastewater treatment systems is the lack of standardized and high-quality datasets. Drilling wastewater characteristics vary significantly across locations and operations, leading to inconsistent sampling and data heterogeneity. In many cases, available datasets are limited in size, poorly structured, or lack temporal resolution, which restricts their usability for machine learning applications. These limitations directly affect model training, validation, and generalization, reducing the reliability of data-driven approaches (Liu, Dong et al. 2026).

8.2. Technological Limitations

Although advanced treatment technologies such as membrane filtration and advanced oxidation processes offer high removal efficiencies, they are often associated with operational challenges. Membrane fouling remains a critical issue, leading to reduced performance and increased maintenance requirements. Additionally, many advanced processes are energy-intensive, resulting in higher operational costs and environmental burdens. Sludge generation and management also present ongoing challenges, particularly in chemical and biological treatment systems, where disposal and handling can be complex and costly (Tian, Ma et al. 2026).

8.3. Machine Learning Limitations

While machine learning provides powerful tools for modeling and optimization, its application in drilling wastewater treatment is constrained by several factors. Model transferability remains a major issue, as models trained on one dataset may not perform well under different operational conditions. Data scarcity and variability further limit model robustness, while noise and uncertainty in measurements can affect prediction accuracy. These limitations highlight the need for more robust, interpretable, and adaptable machine learning frameworks (Tian, Ma et al. 2026).

8.4. Operational Challenges

Real-world implementation of advanced and intelligent treatment systems is often complicated by harsh operating environments typical of oil and gas operations. Extreme temperatures, high salinity, and variable flow conditions can affect both treatment processes and monitoring systems. Sensor reliability and maintenance pose additional challenges, particularly for real-time data acquisition. Furthermore, achieving fully integrated, real-time control systems requires significant infrastructure and technical expertise, which may not always be available (Zhou, Deng et al. 2025).

8.5. Economic and Policy Constraints

The adoption of advanced treatment technologies and intelligent systems is often limited by high capital and operational expenditures. Technologies such as membrane systems and zero liquid discharge (ZLD) require substantial investment, which may not be economically feasible in all cases. In addition, regulatory frameworks vary across regions and may lack clear guidelines for emerging technologies. Limited financial incentives and policy support further slow the transition toward circular and sustainable wastewater management practices (Zhou, Deng et al. 2025).

9. Future Directions

Future advancements in drilling wastewater treatment are expected to be driven by the convergence of intelligent systems, advanced sensing technologies, and circular economy strategies. These developments aim to transform conventional treatment approaches into adaptive, efficient, and sustainable systems capable of operating under highly variable and uncertain conditions (Dhadumia, Paul et al. 2026).

9.1. Intelligent and Autonomous Treatment Systems

The development of intelligent and autonomous treatment systems represents a key direction for future research and industrial implementation. Artificial intelligence (AI)-driven control strategies can enable real-time adjustment of operational parameters such as chemical dosing, flow rates, and membrane pressures. These systems have the potential to evolve into fully self-optimizing treatment plants that continuously learn from operational data, improving efficiency, reducing human intervention, and enhancing system reliability under dynamic conditions (Wang, Li et al. 2025).

9.2. Integration of Machine Learning, Uncertainty Quantification, and Digital Twins

The integration of machine learning (ML), uncertainty quantification (UQ), and digital twin technologies offers significant opportunities for advancing wastewater treatment systems. Digital twins virtual replicas of physical systems can simulate process behavior in real time, allowing for predictive analysis and scenario evaluation. When combined with ML and UQ, these systems enable real-time adaptive control, improved prediction accuracy, and risk-informed decision-making, supporting more robust and resilient treatment operations (Dhadumia, Paul et al. 2026).

9.3. Advanced Sensing and Data Infrastructure

Future systems will increasingly rely on advanced sensing technologies and data infrastructure to support continuous monitoring and control. The deployment of Internet of Things (IoT) devices and high-frequency sensors enables real-time data acquisition for key parameters such as salinity, oil content, and suspended solids. These technologies improve data availability and quality, which are essential for training machine learning models and enabling responsive, data-driven system management.

9.4. Expansion of Circular Economy Strategies

Circular economy principles will play an increasingly important role in the future of drilling wastewater management. Advancements in zero liquid discharge (ZLD) technologies will enhance water recovery efficiency and reduce environmental discharge. In addition, improved resource recovery techniques such as the extraction of hydrocarbons, salts, and valuable minerals will contribute to economic value generation and waste minimization. These developments support the transition toward closed-loop systems that maximize resource utilization and sustainability (Wang, Li et al. 2025).

9.5. Policy and Industrial Implementation

The successful implementation of advanced and intelligent wastewater treatment systems will depend on supportive regulatory frameworks and industry adoption. Future efforts should focus on developing clear regulations for emerging technologies, establishing standardized operational guidelines, and providing economic incentives for sustainable practices. Collaboration between academia, industry, and policymakers will be essential to accelerate technology deployment and ensure that innovative solutions are effectively translated into large-scale industrial applications (Loss, Cavali et al. 2026).

(Table 8) outlines the major technical, data-related, and policy-driven gaps in current drilling wastewater management practices and highlights future research directions toward intelligent and circular treatment systems.

Table 8. Research Gaps and Future Opportunities (Matheri, Mohamed et al. 2022, Adedayo-Ojo, Shad et al. 2025, Waware, Nagalli et al. 2025)

Gap	Current Limitation	Future Direction
Data availability	Fragmented datasets	Standardized databases
ML deployment	Limited real-time use	Sensor-ML integration
Circular adoption	High capital cost	Policy incentives
System intelligence	Manual control	Autonomous treatment systems

Figure 9 presents a future-oriented vision of AI-driven and zero-liquid-discharge-enabled wastewater management integrated across the oil and gas value chain, highlighting long-term sustainability and investment pathways.

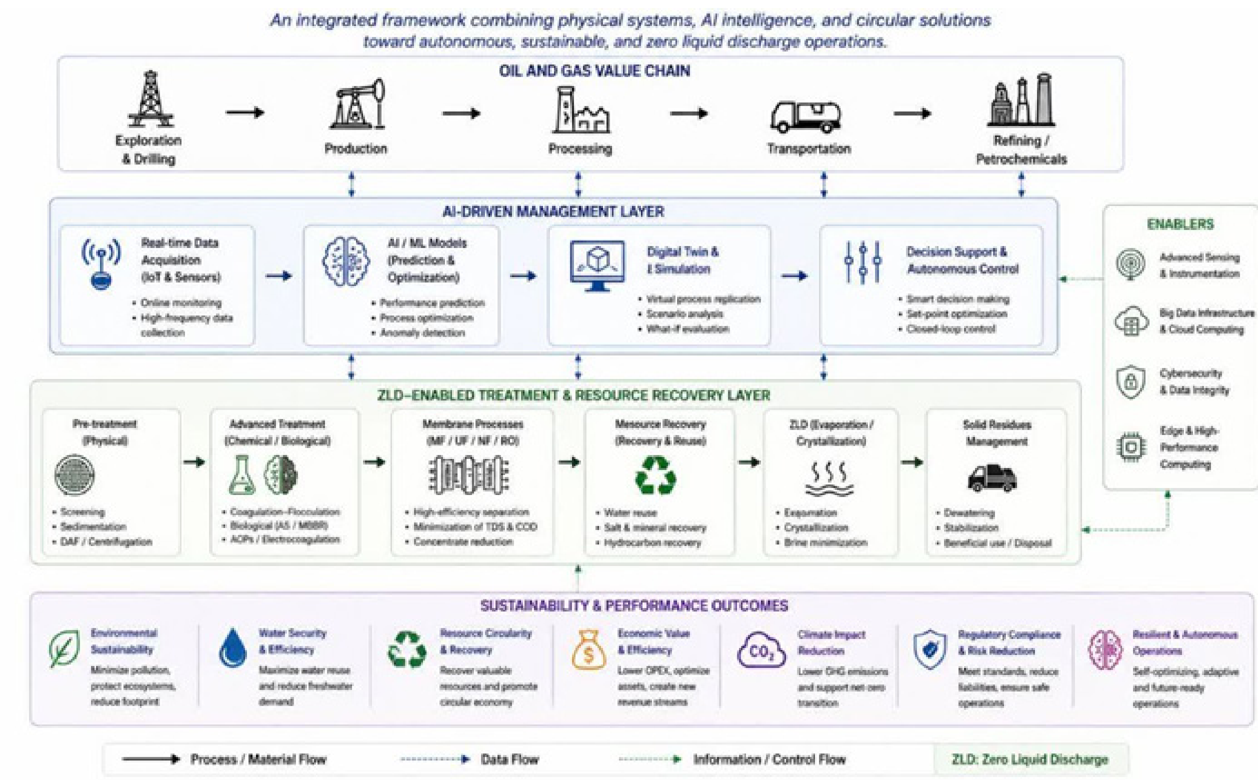

Figure 9. Future Integrated AI-Driven and Zero Liquid Discharge (ZLD) Wastewater Management Framework

Figure 10. Visionary framework for real-time optimized, autonomous, and intelligent drilling wastewater management, illustrating how machine learning, digital twins, and adaptive control enable circular economy-based resource recovery and near-zero discharge operation under human-in-the-loop oversight.

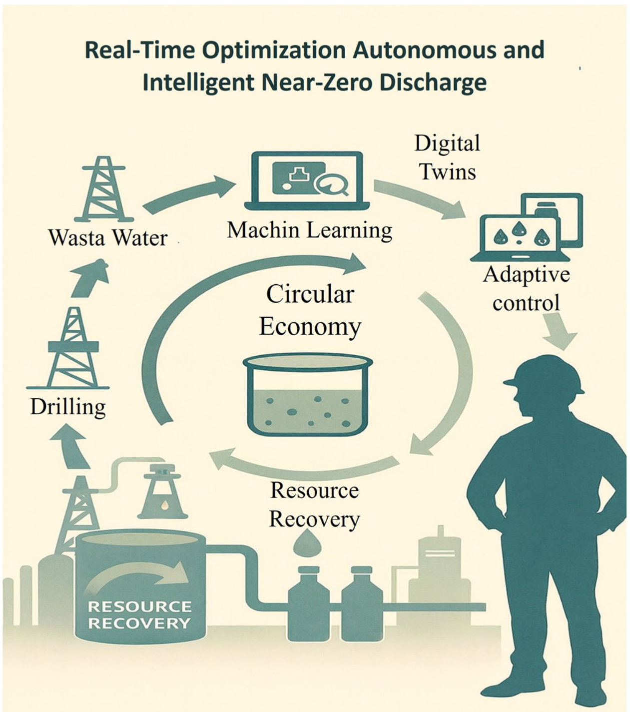

Figure 10. Vision Of Autonomous and Intelligent Drilling Wastewater Treatment Systems

10. Conclusion

This review has presented a comprehensive and integrated analysis of drilling wastewater treatment by bridging conventional and advanced treatment technologies with emerging approaches in machine learning, uncertainty quantification, and circular economy principles. The findings demonstrate that while physical, chemical, biological, and membrane-based processes remain the foundation of contaminant removal, their effectiveness is often constrained by the highly variable and dynamic nature of drilling wastewater systems.

The integration of data-driven intelligence, particularly machine learning, enables improved prediction, monitoring, and adaptive optimization of treatment processes under fluctuating operational conditions. In parallel, uncertainty quantification provides a robust framework for addressing variability and supporting risk-informed decision-making. Together, these approaches enhance system reliability, operational efficiency, and resilience, moving beyond traditional static treatment strategies toward dynamic and adaptive system design.

From a sustainability perspective, the adoption of circular economy strategies such as water reuse, resource recovery, and zero liquid discharge (ZLD) offers significant potential to reduce environmental impacts while improving resource efficiency and economic performance. These strategies support the transition from linear waste management practices to closed-loop systems that valorize wastewater streams and minimize environmental footprint.

Despite these advancements, several challenges remain, including limited data availability, difficulties in model generalization, high operational costs of advanced technologies, and integration barriers in real-world industrial environments. Addressing these limitations will require the development of standardized datasets, improved sensing and monitoring infrastructure, and scalable frameworks that integrate artificial intelligence into operational systems.

Future developments are expected to focus on autonomous treatment systems, digital twin technologies, and fully integrated, AI-driven platforms capable of real-time optimization and decision-making. Such advancements will play a critical role in achieving sustainable and resilient wastewater management in the oil and gas industry.

Overall, this study highlights the importance of interdisciplinary integration in advancing drilling wastewater treatment. By combining engineering processes with data science and sustainability principles, the proposed framework provides a pathway toward intelligent, adaptive, and circular wastewater management systems capable of meeting future environmental and industrial challenges.

Nomenclature

AI	Artificial Intelligence
ANN	Artificial Neural Network
AOP	Advanced Oxidation Process
CE	Circular Economy
DAF	Dissolved Air Flotation
DT	Digital Twin
IoT	Internet of Things
LCA	Life Cycle Assessment
ML	Machine Learning
MLD	Minimal Liquid Discharge
NF	Nanofiltration
O&G	Oil and Gas
RO	Reverse Osmosis
SVM	Support Vector Machine
TDS	Total Dissolved Solids
TSS	Total Suspended Solids
UQ	Uncertainty Quantification
WBM	Water-Based Mud
OBM	Oil-Based Mud
ZLD	Zero Liquid Dischargr

References

Adedayo-Ojo, A. A., M. K. Shad, W. C. J. C. E. Poon and Sustainability (2025). "Circular Economy in the Oil and Gas Industry: A Data-Driven Bibliometric Analysis." 1-63.

Adverse, A. T. N.-Z. "INTEGRATED SUSTAINABLE URBAN WATER, ENERGY, AND SOLIDS MANAGEMENT."

Ahmed, A., A. Alsaihati, S. J. A. J. f. S. Elkatatny and Engineering (2021). "An overview of the common water-based formulations used for drilling onshore gas wells in the Middle East." 46(7): 6867-6877.

Ajao, A. (2024). "Conventional and advanced treatment technologies for microplastics in water treatment facilities."

Al-Dahidi, S., M. Alrbai, L. Al-Ghussain, A. Alahmer and H. S. J. B. T. Hayajneh (2024). "Data-driven analysis and prediction of wastewater treatment plant performance: Insights and forecasting for sustainable operations." 391: 129937.

Albusaimi, F. A., M. S. Al Dabbous, R. Al Yateem and F. P. Pretorius (2024). Circular Economy Practices Through Water Management. SPE International Conference and Exhibition on Health, Safety, Environment, and Sustainability?, SPE.

Alessi, D. S., A. Zolfaghari, S. Kletke, J. Gehman, D. M. Allen and G. G. J. C. W. R. J. R. c. d. r. h. Goss (2017). "Comparative analysis of hydraulic fracturing wastewater practices in unconventional shale development: Water sourcing, treatment and disposal practices." 42(2): 105-121.

Alsabaa, A., H. Gamal, S. Elkatatny and Y. J. A. o. Abdelraouf (2022). "Machine learning model for monitoring rheological properties of synthetic oil-based mud." 7(18): 15603-15614.

Anyanwu, C., J. C. Agunwamba and M. J. A. o. A. I. i. R. o. E. C. Tiza (2026). "Application of conventional methods and artificial intelligence tools for wastewater treatment: Recent advancements and future prospects." 109-149.

Aparna, K., R. J. P. S. Swarnalatha and E. Protection (2024). "Optimizing wastewater treatment plant operational efficiency through integrating machine learning predictive models and advanced control strategies." 188: 995-1008.

Aryanti, P. T. P., F. A. Nugroho, C. Ahmadi, R. Ismail, A. J. M. o. P. W. Kadier, I. Oil Field Discharges: Diagnosis and Treatment (2025). "Water Recycling at Oil Field Industry Plants." 351-402.

Asad, G. and J. Everhart (2025). "Uncertainty-Aware Predictive Maintenance: Leveraging Adaptive Machine Learning for Mechanical Components."

Bai, Y., Z. Li, J. Jiang, J. Liu, H. Wang, Q. Liu, G. Gang, Z. Kong and Y. J. E. R. Wang (2026). "Optimizing wastewater treatment through combined deep learning and deep reinforcement learning: Recent advances and future prospects." 123795.

Ball, A. S., R. J. Stewart, K. J. W. M. Schliephake and Research (2012). "A review of the current options for the treatment and safe disposal of drill cuttings." 30(5): 457-473.

Barcelona, M. J., J. P. Gibb and R. A. Miller (1983). A guide to the selection of materials for monitoring well construction and ground-water sampling, Illinois State Water Survey.

Basu, S., A. R. Shaw and M. Venkatesh (2025). Water Management in Petroleum Industries, Springer Nature.

Belia, E., M. B. Neumann, L. Benedetti, B. Johnson, S. Murthy and P. Vanrolleghem (2021). Uncertainty in Wastewater Treatment Design and Operation, IWA Publishing.

Cangialosi, F., E. Bruno and G. J. S. De Santis (2021). "Application of machine learning for fenceline monitoring of odor classes and concentrations at a wastewater treatment plant." 21(14): 4716.

Chang, Y.-R., Y.-J. Lee and D.-J. J. J. o. t. T. I. o. C. E. Lee (2019). "Membrane fouling during water or wastewater treatments: Current research updated." 94: 88-96.

Daramola, O. M., C. E. Apeh, J. O. Basiru, E.

C. Onukwulu, P. O. J. J. o. C. E. Paul and S. L. Forthcoming (2023). "Optimizing reverse logistics for circular economy: Strategies for efficient material recovery and resource circularity."

De Maman, R., V. C. da Luz, L. Behling, A. Dervanoski, C. Dalla Rosa, G. D. L. J. E. S. Pasquali and P. Research (2022). "Electrocoagulation applied for textile wastewater oxidation using iron slag as electrodes." 29(21): 31713-31722.

Dhadumia, B., B. J. W. M. Paul and Research(2025). "A review of advanced sustainable waste management approaches of the oil and gas industry:Integrating green hybrid technologies for a cleaner future." 0734242X251385854.

Dhadumia, B., B. J. W. M. Paul and Research (2026). "A review of advanced sustainable waste management approaches of the oil and gas industry: Integrating green hybrid technologies for a cleaner future." 44(3): 237-251.

Digitemie, W. N., F. O. Onyeke, M. A. Adewoyin, I. N. J. I. J. o. M. R. Dienagha and G. Evaluation (2025). "Implementing circular economy principles in oil and gas: addressing waste management and resource reuse for sustainable operations." 6(1): 99-104.

Ejairu, U., A. T. Aderamo, H. C. Olisakwe, A. E. Esiri, U. M. Adanma, N. O. J. C. r. Solomon, r. i. Engineering and Technology (2024). "Eco-friendly wastewater treatment technologies (concept): Conceptualizing advanced, sustainable wastewater treatment designs for industrial and municipal applications." 2(1): 083-104.

Fernandes, J., P. J. Ramísio and H. J. E. Puga (2024). "A comprehensive review on various phases of wastewater technologies: Trends and future perspectives." 5(4): 2633-2661.

Ferri, E. N. and L. J. A. S. Bolelli (2025). "Wastewater remediation treatments aimed at water reuse: recent outcomes from pilot-and full-scale tests." 15(5): 2448.

Fisher, O. J., Y. Wang and A. J. W. R. Ahmed (2025). "Making waves: Transforming biofilm-based wastewater treatment using machine learning-driven real-time monitoring." 124491.

Gangwar, A., S. Rawat, A. Rautela, I. Yadav, A. Singh, S. J. E. Kumar, Development and Sustainability (2025). "Current advances in produced water treatment technologies: a perspective of techno-economic analysis and life cycle assessment." 27(7): 15077-15111.

Garg, M. C., S. Kumari and S. Agarwal(2024). The integration of artificial intelligence in advanced wastewater treatment systems. The AI Cleanse: Transforming Wastewater Treatment Through Artificial Intelligence: Harnessing Data-Driven Solutions, Springer: 1-27.

Gaurina-Međimurec, N., K. Simon, K. N. Mavar, B. Pašić, P. Mijić, I. Medved, V. Brkić, L. Hrnčević and K. Žbulj (2024). The circular economy in the oil and gas industry: a solution for the sustainability of drilling and production processes. Circular Economy on Energy and Natural Resources Industries: New Processes and Applications to Reduce, Reuse and Recycle Materials and Decrease Greenhouse Gases Emissions, Springer: 115-150.

Ghasemi, K., A. Akbari, S. Jahani and Y. J. T. C. J. o. C. E. Kazemzadeh (2025). "A critical review of life cycle assessment and environmental impact of the well drilling process." 103(6): 2499-2526.

Hossain, M. E., A. Al-Majed, A. R. Adebayo, A. S. Apaleke, S. M. J. E. E. Rahman and M. Journal (2017). "A CRITICAL REVIEW OF DRILLING WASTE MANAGEMENT TOWARDS SUSTAINABLE SOLUTIONS." 16(7).

Iseri, F., H. Iseri, H. Shah, E. Iakovou, E. N. J. C. Pistikopoulos and C. Engineering (2025). "Planning strategies in the energy sector: Integrating bayesian neural networks and uncertainty quantification in scenario analysis & optimization." 198: 109097.

Iskandarani, M., S. Wang, A. Srinivasan, W. Carlisle Thacker, J. Winokur and O. M. J. J. o. G. R. O. Knio (2016). "An overview of uncertainty quantification techniques with application to oceanic and oil-spill simulations." 121(4): 2789-2808.

Jain, M., A. Majumder, P. S. Ghosal and A. K. J. J. o. E. M. Gupta (2020). "A review on treatment of petroleum refinery and petrochemical plant wastewater: a special emphasis on constructed wetlands." 272: 111057.

Jamshidi, E., S. Saen, J. Golshaghagh, P. Kianoush, A. Adib and A. J. S. R. Mohammadi (2025). "Challenges of drilling Iran's deepest surface hole in the saddle section of Changuleh oilfield with complex structure and pressure regimes." 15(1): 25302.

Jin, J., M. Liu, B. Chen, X. Wu, L. Yao, Y. Wang, X. Xiong, L. Wei, J. Li and Q. J. S. Tan (2025). "Artificial Intelligence in Chemical Dosing for Wastewater Purification and Treatment: Current Trends and Future Perspectives." 12(9): 237.

Jin, X., L. Zhang, M. Liu, S. Hu, Z. Yao, J. Liang, R. Wang, L. Xu, X. Shi and X. J. C. Bai (2022). "Characteristics of dissolved ozone flotation for the enhanced treatment of bio-treated drilling wastewater from a gas field." 298: 134290.

Kalhormohammadi, M. and S. J. S. R. Khoramipour. (2025) "Predictive modeling of coagulant dosing in drilling wastewater treatment using artificial neural networks." 15(1): 30003.

Kandpal, V., A. Jaswal, E. D. Santibanez Gonzalez and N. Agarwal (2024). Circular economy principles: shifting towards sustainable prosperity. Sustainable energy transition: Circular economy and sustainable financing for environmental, social and governance (ESG) practices, Springer: 125-165.

Khalili, Y., M. J. J. o. C. Ahmadi and P. Engineering (2023). "Reservoir modeling & simulation: Advancements, challenges, and future perspectives." 57(2): 343-364.

Kundu, D., D. Dutta, P. Samanta, S. Dey, K. C. Sherpa, S. Kumar and B. K. J. S. o. t. T. E. Dubey (2022). "Valorization of wastewater: A paradigm shift towards circular bioeconomy and sustainability." 848: 157709.

Lawan, M. S., R. Kumar, J. Rashid and M. A. E.-F. J. W. Barakat (2023). "Recent advancements in the treatment of petroleum refinery wastewater." 15(20): 3676.

Lebedev, A. and A. J. R. Cherepovitsyn (2024). "Waste management during the production drilling stage in the oil and gas sector: a feasibility study." 13(2): 26.

Li, C., A. Tiraferri, P. Tang, J. Ma and B. J. W. R. Liu (2025). "Current status, potential assessment, and future directions of biological treatments of unconventional oil and gas wastewater." 123217.

Lihu, L. and S. J. P. O. Jiahe (2025). "A novel strategy for resource utilization of oily drilling waste fluids in northern Shaanxi: Stepwise flotation of bentonite and barite using SDS and interfacial reaction mechanisms." 20(8): e0331415.

Lin, K., S. J. J. o. g. e. Wei and I.-c. development (2023). "Advancing the industrial circular economy: the integrative role of machine learning in resource optimization." 2(3): 122-136.

Liu, F., Y. Li, X. Wang and Z. J. M. Xia (2024). "Preparation and properties of reversible emulsion drilling fluid stabilized by modified nanocrystalline cellulose." 29(6): 1269.

Liu, H., S. Dong, J. Yang, S. Liao, S. J. J. o. H. Liu, Toxic, and R. Waste (2026). "Treatment and Disposal Technologies for Oil-Based Drilling Cuttings: An Overview and Prospects." 30(1): 03125004.

Loss, L., M. Cavali, A. Freitas, S. Kubeneck, G. Leme, A. Calvo, S. Soares, A. J. I. J. o. E. S. de Castilhos Junior and Technology (2026). "Environmental aspects of drill cuttings from oil operations: characterization, risk assessment, valorization, and treatment innovations." 23(4): 307.

Matheri, A. N., B. Mohamed, F. Ntuli, E. Nabadda, J. C. J. P. Ngila and P. a. b. c. Chemistry of the Earth (2022). "Sustainable circularity and intelligent data-driven operations and control of the wastewater treatment plant." 126: 103152.

Nagpal, M., M. A. Siddique, K. Sharma, N. Sharma, A. J. W. S. Mittal and Technology (2024). "Optimizing wastewater treatment through artificial intelligence: recent advances and future prospects." 90(3): 731-757.

Nautiyal, A., A. K. J. E. Mishra, Development and Sustainability (2025). "Machine learning approach for intelligent prediction of petroleum upstream stuck pipe challenge in oil and gas industry." 27(10).

Nooraiepour, M., M. Masoudi and H. J. S. R. Hellevang (2021). "Probabilistic nucleation governs time, amount, and location of mineral precipitation and geometry evolution in the porous medium." 11(1): 16397.

Olukoga, T., Y. J. S. D. Feng and Completion (2021). "Practical machine-learning applications in well-drilling operations." 36(04): 849-867.

Panagopoulos, A. and P. J. M. Michailidis (2025). "Membrane technologies for sustainable wastewater treatment: Advances, challenges, and applications in zero liquid discharge (zld) and minimal liquid discharge (mld) systems." 15(2): 64.

Pandey, A. K. J. E. S. W. R. and Technology (2025). "Sustainable water management through integrated technologies and circular resource recovery." 11(8): 1822-1846.

Pereira, L. B., C. M. Sad, E. V. Castro, P. R. Filgueiras and V. J. F. Lacerda Jr (2022). "Environmental impacts related to drilling fluid waste and treatment methods: A critical review." 310: 122301.

Pouran Manjily, H., M. Alborzi, T. Behrouz, S. M. J. J. o. S. Seyed-Hosseini and T. P. Management (2024). "Intelligent oil field technology maturity level assessment: using the technology readiness level criteria." 15(6): 1223-1246.

Rasouli, M. A., M. Karimpour-Fard, S. L. J. J. o. t. A. Machado and W. M. Association (2025). "An assessment of the uncertainties of methane generation in landfills." 75(6): 464-482.

Reichert, P. J. W. S. and Technology (2020). "Towards a comprehensive uncertainty assessment in environmental research and decision support." 81(8): 1588-1596.

Rotan, K., Q. Goettel, K. Smith, A. Gonzalez, U. Onyemaobi and M. Yurukcu (2024). "AI/ML Technology for Water Treatment in Oil and Gas Industry: A Review Paper."

Sajib, M., A. Jaman, M. A. Ullah, M. A. B. H. Susan and M. S. Miran (2025). AI Technologies for Treating Petroleum Wastewater. Management of Petroleum Wastewater and Oil Field Discharges: Diagnosis, Impacts and Treatment, Springer: 81-118.

Sangamnere, R., T. Misra, H. Bherwani, A. Kapley and R. J. S. W. R. M. Kumar (2023). "A critical review of conventional and emerging wastewater treatment technologies." 9(2): 58.

Scheidt, C., L. Li and J. Caers (2018). Quantifying uncertainty in subsurface systems, John Wiley & Sons.

Shaaban, Y. A. (2025). Wastewater Treatment: Using AI and Response Surface Methodology to Predict and Optimize. Management of Petroleum Wastewater and Oil Field Discharges: Diagnosis, Impacts and Treatment, Springer: 27-45.

Shokir, E. M., S. Sallam and M. M. J. A. o. Abdelhafiz (2024). "Comprehensive Wellbore Stability Modeling by Integrating Poroelastic, Thermal, and Chemical Effects with Advanced Numerical Techniques." 9(52): 51536-51553.

Sircar, A., K. Yadav, K. Rayavarapu, N. Bist and H. J. P. R. Oza (2021). "Application of machine learning and artificial intelligence in oil and gas industry." 6(4): 379-391.

Smol, M., C. Adam, M. J. J. o. M. C. Preisner and W. Management (2020). "Circular economy model framework in the European water and wastewater sector." 22(3): 682-697.

Sundui, B., O. A. Ramirez Calderon, O. M. Abdeldayem, J. Lázaro-Gil, E. R. Rene, U. J. C. T. Sambuu and E. Policy (2021). "Applications of machine learning algorithms for biological wastewater treatment: updates and perspectives." 23(1): 127-143.

Tawfik, M. J. P. o. (2024). "Optimized intrusion detection in IoT and fog computing using ensemble learning and advanced feature selection." 19(8): e0304082.

Teodoriu, C. and O. J. E. Bello (2021). "An outlook of drilling technologies and innovations: Present status and future trends." 14(15): 4499.

Thacker, J. B., D. D. Carlton Jr, Z. L. Hildenbrand, A. F. Kadjo and K. A. J. W. Schug (2015). "Chemical analysis of wastewater from unconventional drilling operations." 7(4): 1568-1579.

Thompson, M. and B. J. W. E. R. Dvorak (2024). "Wastewater reuse benefits for municipal complete retention lagoons: Life cycle assessment and dynamic modeling." 96(8): e11098.

Tian, D., W. Ma, L. Du, H. Chen, Y. Zhou, J. Tan, P. Zhang, Y. Sun, B. Xiao, Y. J. W. Qu, Air, and S. Pollution (2026). "Challenges and Opportunities in Tunnel Wastewater Treatment: Engineering Perspectives for Sustainable Management." 237(6): 387.

Tsolakis, N., T. S. Harrington, J. S. J. P. P. Srai and Control (2023). "Digital supply network design: a Circular Economy 4.0 decision-making system for real-world challenges." 34(10): 941-966.

Wang, Z., S. Li, Z. Xu, S. A. Aryana and J. J. C. Cai (2025). "Advances and challenges in foam stability: Applications, mechanisms, and future directions." 15(3): 58-73.

Warsinger, D. M., S. Chakraborty, E. W. Tow, M. H. Plumlee, C. Bellona, S. Loutatidou, L. Karimi, A. M. Mikelonis, A. Achilli and A. J. P. i. p. s. Ghassemi (2018). "A review of polymeric membranes and processes for potable water reuse." 81: 209-237.

Waware, S. Y., N. K. Nagalli, S. Sugumaran, P. D. Patil, R. Biradar, A. A. Kadam, K. B. Ghunake, S. S. Kore, G. Murali, A. S. J. N.-J. o. S. Kurhade and T. Research (2025). "AI-Driven Innovations in the Exploration, Extraction, and Processing of Minerals, Metals, and Petroleum: A Review." 7(4): 209-227.

Wei, X., S. Zhang, Y. Han and F. A. J. W. E. R. Wolfe (2019). "Treatment of petrochemical wastewater and produced water from oil and gas." 91(10): 1025-1033.

Yang, H., H. Diao, Y. Zhang and S. J. J. o. e. m. Xia (2022). "Treatment and novel resource-utilization methods for shale gas oil based drill cuttings-A review." 317: 115462.

Yang, J., J. Sun, R. Wang, Y. J. E. s. Qu and p. research (2023). "Treatment of drilling fluid waste during oil and gas drilling: A review." 30(8): 19662-19682.

Yuan, H. and Z. J. B. t. He (2015). "Integrating membrane filtration into bioelectrochemical systems as next generation energy-efficient wastewater treatment technologies for water reclamation: A review." 195: 202-209.

Zhang, T. J. W. (2025). Sustainable wastewater treatment and the circular economy, MDPI. 17: 335.

Zhang, W., Q. Li, S. Dong, H. Liu, K. Dong, X. Wu, M. Sui and F. J. J. o. W. P. E. Zhang (2024). "Synthesis of mixed-base active material from drilling fluid solid waste and biomass for oil wastewater adsorption and its mechanism." 66: 106076.

Zhang, Y., P. Xu, M. Xu, L. Pu and X. J. A. o. Wang (2022). "Properties of bentonite slurry drilling fluid in shallow formations of deepwater wells and the optimization of its wellbore strengthening ability while drilling." 7(44): 39860-39874.

Zhou, J., T. Shi, Q. Qian, C. He and J. J. S. p. Ren (2023). "Protocol for the design and accelerated optimization of a waste-to-energy system using AI tools." 4(4): 102685.

Zhou, Y., C. Deng, X. Chen, Y. He, G. Fang, Z. Jin, Y. J. W. M. Liu and Research (2025). "Engineering design and application of large-scale oil-based drilling cuttings treatment project." 43(2): 282-292.

Zidaoui, I. (2024). Advanced data validation methods for wastewater sensors using Artificial Intelligence, Université de Strasbourg.

Zong, Z. and Y. J. J. o. t. k. e. Guan (2025). "AI-driven intelligent data analytics and predictive analysis in Industry 4.0: Transforming knowledge, innovation, and efficiency." 16(1): 864-903.

بهبود جداسازی یک مخلوط سه جزئی هیدروکربنی با استفاده از برج تقطیر دیوار میانی

- محمود همتی[۱]، مرتضی زیودار[۲*]، طالب زارعی[۳]، رهبر رحیمی[۲]

۱. دانشجوی دکترا، گروه مهندسی شیمی، دانشکده مهندسی، دانشگاه سیستان و بلوچستان، زاهدان، ایران

۲. استاد، گروه مهندسی شیمی، دانشکده مهندسی، دانشگاه سیستان و بلوچستان، زاهدان، ایران

۳. استاد، گروه مهندسی مکانیک، دانشگاه هرمزگان، بندرعباس، ایران

(ایمیل نویسنده مسئول: mzivdar@eng.usb.ac.ir)

چکیـــــــده

برج تقطیر دیوار میانی (DWC) به‌عنوان یکی از راهکارهای پیشرفته در تشدید فرآیند، پتانسیل بالایی برای کاهش مصرف انرژی و هزینه‌های سرمایه‌گذاری اولیه در سیستم‌های تقطیر دارد. این مطالعه با هدف بهینه‌سازی سیستماتیک و مقایسه اقتصادی، عملکرد برج تقطیر دیوار میانی را در مقایسه با فرآیند تقطیر متداول برای جداسازی مخلوط سه‌جزئی نرمال‌پنتان، هگزان و هپتان ارزیابی می‌کند. در این راستا، تحلیل جریان‌های اگزرژی و ابعاد اقتصادی هر دو فرآیند به‌تفصیل بررسی شده است. به‌منظور کمینه‌سازی مجموع بارهای حرارتی ریبویلر و کندانسور، از روش بهینه‌سازی «برنامه‌ریزی درجه دوم متوالی» (SQP) استفاده و برای پیش‌بینی تعادل بخار–مایع (VLE) سیستم، مدل ترمودینامیکی پنگ–رابینسون به کار گرفته شد. درنهایت، با در نظر گرفتن شرایط یکسان خوراک، عملکرد برج تقطیر دیوار میانی در مقایسه با سیستم تقطیر دو ستونی مرسوم، از نظر کل هزینه سالانه و مصرف انرژی سنجیده شد. نتایج نشان می‌دهد که به‌کارگیری برج تقطیر دیوار میانی منجر به ۷۳ درصد کاهش در کل هزینه سالانه و ۸۳ درصد کاهش در مصرف انرژی می‌شود. در مجموع، این پژوهش ضمن تأکید بر بهره‌وری اقتصادی و راهکارهای نوآورانه در بهینه‌سازی مصرف انرژی و حفاظت از محیط‌زیست، استفاده از ستون‌های دیواره جداکننده را به‌عنوان جایگزینی کارآمد و عملیاتی برای برج‌های تقطیر متوالی پیشنهاد می‌کند.

واژگان کلیدی: برج دیوار میانی، بهینه‌سازی، جداسازی مخلوط سه جزئی، کل هزینه سالانه، بازدهی انرژی، تشدید فرآیند، اسپن پلاس

ارزیابی سناریوهای به‌کارگیری واحدهای CCUS برای کاهش انتشار کربن در صنایع انرژی‌بر ایران با استفاده از روش AHP

• سبحان حرفت[1]، مجید زندی[2*]

۱. دانشجوی دکترا، گروه انرژی‌های تجدیدپذیر، مرکز پژوهشی انرژی، دانشکده انرژی، دانشگاه شهید بهشتی، تهران، ایران

۲. دانشیار، گروه انرژی‌های تجدیدپذیر، مرکز پژوهشی انرژی، دانشکده انرژی، دانشگاه شهید بهشتی، تهران، ایران

(ایمیل نویسنده مسئول: m_zandi@sbu.ac.ir)

چکیـــــده

گذار صنعتی ایران به‌سوی فناوری‌های کاهش انتشار کربن، به‌ویژه سامانه‌های جذب، استفاده و ذخیره‌سازی کربن (CCUS)، در سال‌های اخیر به‌عنوان یکی از محورهای راهبردی برای ارتقای پایداری محیط‌زیست و بهبود کارایی صنایع انرژی‌بر مطرح شده است. این مطالعه الگوهای محتمل برای استقرار واحدهای CCUS را در قالب سه سناریوی تدریجی، سریع و ترکیبی بررسی می‌کند. در سناریوی تدریجی، توسعه مرحله‌ای، کاهش ریسک‌های اولیه و انطباق تدریجی با الزامات فنی و اقتصادی مدنظر است. سناریوی سریع بر استقرار فوری زیرساخت‌های CCUS از طریق سرمایه‌گذاری گسترده، مشوق‌های مالی و حمایت‌های سیاستی متمرکز است. سناریوی ترکیبی نیز با ایجاد توازن میان هزینه‌ها، ریسک‌ها، زمان‌بندی و قابلیت اطمینان، دستیابی به فرآیندی صنعتی پایدار، مقبول و قابل مدیریت را دنبال می‌کند. در ادامه، چالش‌های فنی، اقتصادی، نهادی و سیاستی اجرای واحدهای CCUS تحلیل شده و راهبردهایی مانند تدوین سیاست‌های حمایتی هدفمند، توسعه زیرساخت یکپارچه حمل‌ونقل و ذخیره‌سازی دی‌اکسید کربن، ارتقای ظرفیت فناورانه داخلی، انتقال دانش فنی و تقویت همکاری میان دولت، بخش خصوصی و نهادهای پژوهشی پیشنهاد می‌شود. برای ارزیابی مسیرهای مختلف، از یک مدل سلسله‌مراتبی مبتنی بر AHP استفاده شده است تا عملکرد واحدهای CCUS در نیروگاه‌ها، صنایع انرژی‌بر و پالایشگاه‌ها بر پایه شش شاخص هزینه، جذابیت فناوری، توانمندی فناورانه، شاخص فرهنگی، الزامات پدافند غیرعامل و معیارهای محیط‌زیستی سنجیده شود.

واژگان کلیدی: سامانه‌های جذب، استفاده و ذخیره‌سازی کربن، گذار صنعتی، تحلیل سلسله‌مراتبی(AHP)، الگوهای استقرار

تحلیل خرابی پمپ‌های شناور الکتریکی با استفاده از تکنیک‌های یادگیری ماشین

• محیا فرجی[۱]، یاسین خلیلی[۲]، محمد احمدی[۳*]

۱. دانشجو کارشناسی ارشد، دانشکده مهندسی شیمی، انستیتو مهندسی نفت، دانشگاه تهران، ایران

۲. دانشجوی دکترا، دانشکده مهندسی نفت و زمین انرژی، دانشگاه صنعتی امیرکبیر، تهران، ایران

۳. دانشیار، دانشکده مهندسی نفت و زمین انرژی، دانشگاه صنعتی امیرکبیر، تهران، ایران

(ایمیل نویسنده مسئول: m.ahmady@aut.ac.ir)

چکیـــــــده

پمپ‌هـای شـناور الکتریـکی نقـش بسیـار مهـمی در افزایـش نـرخ تولیـد و بهبـود کارایی عملیـاتی چاه‌های نفت ایفـا می‌کننـد. با این حـال، شـرایط پیچیـده و چالش‌برانگیـز محیـط درون‌چـاهی باعـث می‌شـود ایـن پمپ‌هـا در معـرض خرابی‌هـای مکانیـکی و الکتریـکی قـرار گیرنـد. ازایـن‌رو، شناسـایی زودهنـگام وضعیت‌هـای غیرعـادی و پیش‌بیـنی دقیـق عملکـرد پمـپ بـرای کاهـش زمـان توقـف تولید، کمینه‌سـازی هزینه‌هـای عملیـاتی و افزایـش طـول عمـر تجهیـز ضـروری اسـت.

در ایـن پژوهـش، کاربـرد روش‌هـای یادگیـری ماشین برای شناسـایی وضعیت‌هـای ناپایدار، تشـخیص ناهنجاری‌هـا و پیش‌بینی خرابی در سیسـتم‌های پمـپ شـناور الکتریـکی مـورد بررسی قرار گرفته اسـت. با اسـتفاده از داده‌های شبیه‌سازی‌شـده شـامل دمـای موتور، دمای ورودی موتـور، جریـان و لـرزش موتـور، چندیـن روش پیش‌پردازش و تحلیل داده به‌کار گرفته شـد. تحلیل نمودار جعبه‌ای جهت شناسـایی داده‌هـای پـرت اسـتفاده شـد و روش زد-اسـکور نیز تشـخیص آمـاری نقاط غیرعـادی را امکان‌پذیـر کرد. همچنیـن الگوریتم خوشـه‌بندی کا-میانگیـن و تحلیـل مؤلفه‌هـای اسـاسی بـرای کاهـش ابعـاد داده، بهبـود تجسـم و دسـته‌بندی وضعیت‌هـای پمپ بـه حالت‌هـای پایدار، ناپایـدار، ناهنجـار و خرابی مورد اسـتفاده قـرار گرفت.

علاوه بـر ایـن، یـک طبقه‌بنـدی درخـت تصمیم‌گیـری بـرای تعییـن میزان تأثیر نسـبی هـر پارامتـر در بروز خـرابی آموزش داده شـد. عملکـرد مـدل بـا اسـتفاده از ماتریس سـردرگمی، قبـل و بعد از اعمـال روش‌های آنالیز مؤلفه اسـاسی و خوشـه‌بندی ارزیـابی گردید. نتایج نشـان می‌دهـد کـه اعمـال ایـن روش‌هـا دقـت طبقه‌بنـدی را به‌طـور قابل‌توجـهی بهبـود داده اسـت؛ به‌طـوری که دقـت شناسـایی حالت پایـدار از ۰/۹۸۳۵ بـه ۰/۹۹۶۷ و دقـت تشـخیص حالـت خـرابی از ۰/۷ بـه ۰/۸ افزایـش یافتـه اسـت. یافته‌هـای ایـن پژوهـش نشـان‌دهنده پتانسیـل بـالای روش‌هـای یادگیـری ماشیـن در نگهداشـت پیش‌بینانه پمپ‌های شـناور الکتریکی بوده و بـر ارزش آن‌ها به‌عنـوان راهبردی مقرون‌به‌صرفـه بـرای افزایـش قابلیـت اطمینـان در صنعـت نفـت و گاز تأکید دارد.

واژگان کلیدی: پمپ‌های شناور الکتریکی، یادگیری ماشین، مراقبت پیش‌بینانه، تشخیص ناهنجاری، پیش‌بینی خرابی

نوآوری در سیستم های نانو فتوولتائیک برای تبدیل انرژی در ساختمان‌ها

- ارشیا اسدی[۱*]، میثم غلامی‌پور[۲]، مهدی رضوی‌فر[۳]

۱. کارشناس ارشد واحد بهره برداری، منطقه ۳ عملیات، شرکت انتقال گاز ایران، تهران، ایران

۲. دانشجوی کارشناسی ارشد، دانشکده مهندسی شیمی و نفت، دانشگاه تبریز، تبریز، ۱۷۴۶۱۶۶۶۱۵، ایران

۳. استادیار، دانشکده مهندسی شیمی و نفت، دانشگاه تبریز، تبریز، ۱۷۴۶۱۶۶۶۱۵، ایران

(ایمیل نویسنده مسئول: arshia.asadi1832@gmail.com)

چکیـــــــده

این پژوهش نقش نانومواد پیشرفته، مانند کوانتوم‌دات‌ها، نانوذرات فلزی و گرافن را در افزایش بازده و عملکرد کلی سامانه‌های فتوولتاییک امروزی بررسی می‌کند. با افزایش تقاضای جهانی برای انرژی پاک و پایدار، توسعه سلول‌های خورشیدی پربازده به یک موضوع پژوهشی مهم تبدیل شده است. نانومواد به دلیل ویژگی‌های خاص نوری، الکتریکی و ساختاری خود، فرصت‌های تازه‌ای برای بهبود جذب نور، افزایش تحرک حامل‌های بار و ارتقای سازوکارهای تبدیل انرژی در سلول‌های خورشیدی ایجاد می‌کنند. هدف اصلی این پژوهش، بررسی تأثیر این نانومواد بر عملکرد سلول‌های خورشیدی و شناسایی ویژگی‌های مناسب مواد و پارامترهای ساختاری است که بیشترین بازده تبدیل را فراهم می‌کنند.

برای رسیدن به این هدف، یک فرایند شناسایی جامع با استفاده از مجموعه‌ای از روش‌های پیشرفته انجام شد. طیف‌سنجی UV- Vis برای بررسی رفتار جذب نوری نانومواد و چگونگی تعامل آن‌ها با نور در طول‌موج‌های مختلف به کار گرفته شد. میکروسکوپ الکترونی روبشی (SEM) تصاویر دقیق و با وضوح بالا ارائه داد که امکان بررسی شکل سطح، نحوه پخش ذرات و یکنواختی ساختاری لایه‌های ساخته‌شده را فراهم کرد. همچنین از میکروسکوپ نیروی اتمی (AFM) برای مطالعه ساختار سطح در مقیاس نانو و اندازه‌گیری زبری سطح که بر انتقال بار و پخش نور تأثیر می‌گذارد، استفاده شد. مجموع این روش‌ها به درک بهتر ویژگی‌های فیزیکی مؤثر بر عملکرد فتوولتاییکی هر نانوماده کمک کرد.

تحلیل داده‌ها با استفاده از آنالیز واریانس یک‌طرفه (Oneway ANOVA) و رگرسیون خطی انجام شد تا اهمیت آماری پارامترهای کلیدی مانند ضخامت نانولایه و زاویه تابش نور مشخص شود. نتایج نشان داد که هر دو پارامتر تأثیر قابل‌توجهی بر بازده دستگاه دارند و این مسئله بر اهمیت کنترل دقیق لایه‌نشانی و طراحی سلول تأکید می‌کند. نتایج همچنین نشان دادند که افزودن نانومواد به سلول‌های خورشیدی باعث بهبود چشمگیر عملکرد می‌شود. به‌ویژه، سلول‌های خورشیدی مبتنی بر گرافن به بازده حدود $۲۸/۳ \pm ۰/۳$ درصد رسیدند که نسبت به طراحی‌های معمول افزایش قابل‌توجهی است. کوانتوم‌دات‌ها و نانوذرات فلزی نیز باعث افزایش جذب نور و بهبود جدایش حامل‌های بار شدند و پتانسیل آن‌ها را به‌عنوان مواد مؤثر برای نسل جدید سلول‌های خورشیدی تأیید کردند.

در مجموع، این نتایج نشان می‌دهند که نانومواد می‌توانند نقش مهمی در رفع محدودیت‌های موجود در مواد و طراحی‌های سنتی سلول‌های خورشیدی داشته باشند. با بهینه‌سازی ویژگی‌های نانومقیاس و ساختار دستگاه، می‌توان سلول‌هایی ساخت که علاوه بر راندمان بیشتر، مقرون‌به‌صرفه‌تر و سازگارتر با محیط‌زیست باشند. این پژوهش بر ضرورت ادامه تحقیقات در زمینه تولید نانومواد، ادغام آن‌ها در ساختار سلول و ارزیابی عملکرد بلندمدت تأکید می‌کند و مسیر را برای پیشرفت‌های نوآورانه و پایدار در حوزه انرژی خورشیدی هموار می‌سازد.

واژگان کلیدی: نانومواد، راندمان فتوولتائیک، گرافن، سلول‌های خورشیدی

تصفیه هوشمند و چرخشی پساب حفاری: مروری بر یکپارچه‌سازی یادگیری ماشین، کمّی‌سازی عدم‌قطعیت و بازیابی منابع

- سید عطا الیاس سرخابی[۱]، محمدرضا اکبری[۲*]، یاسین خلیلی[۳]

۱. دانشجوی کارشناسی، دانشکده مهندسی نفت و زمین انرژی، دانشگاه صنعتی امیرکبیر، تهران، ایران

۲. استادیار، دانشکده مهندسی نفت و زمین انرژی، دانشگاه صنعتی امیرکبیر، تهران، ایران

۳. دانشجوی دکترا، دانشکده مهندسی نفت و زمین انرژی، دانشگاه صنعتی امیرکبیر، تهران، ایران

(ایمیل نویسنده مسئول: akbari.pe@aut.ac.ir)

چکیـــــــده

پساب حفاری تولیدشده در عملیات نفت و گاز، به دلیل ترکیب بسیار متغیر، حجم زیاد، و حضور آلاینده‌های خطرناک آلی و معدنی، یکی از چالش‌های پیچیده زیست‌محیطی محسوب می‌شود. روش‌های متداول تصفیه، علی‌رغم کاربرد گسترده، اغلب در دستیابی به عملکرد پایدار تحت شرایط عملیاتی دینامیک و الزامات سخت‌گیرانه زیست‌محیطی با محدودیت مواجه هستند.

این مطالعه مروری، تحلیلی جامع و آینده‌نگر از مدیریت پساب حفاری ارائه می‌دهد که در آن فناوری‌های تصفیه با مفاهیم نوظهور اقتصاد چرخشی، هوشمندسازی مبتنی بر داده، و کمّی‌سازی عدم‌قطعیت به‌صورت یکپارچه مورد بررسی قرار گرفته‌اند. در این راستا، ویژگی‌ها و منابع تولید پساب حفاری بررسی شده تا ماهیت متغیر آن و چالش‌های مرتبط با تصفیه مشخص گردد. همچنین، فناوری‌های متداول، پیشرفته و هیبریدی تصفیه از نظر کارایی، محدودیت‌ها، و قابلیت کاربرد در بازیافت آب و بازیابی منابع به‌صورت انتقادی ارزیابی شده‌اند. راهبردهای اقتصاد چرخشی از جمله بازچرخانی آب، بازیابی مواد، و سیستم‌های تخلیه صفر مایع نیز از منظر پایداری مورد تحلیل قرار گرفته‌اند.

علاوه بر این، نقش یادگیری ماشین در پیش‌بینی عملکرد، بهینه‌سازی فرآیند، و پایش لحظه‌ای بررسی شده و در کنار آن، روش‌های کمّی‌سازی عدم‌قطعیت مانند مدل‌سازی احتمالاتی برای پشتیبانی از تصمیم‌گیری مبتنی بر ریسک مورد بحث قرار گرفته‌اند. از دیدگاه صنعتی، یکپارچه‌سازی مدل‌های هوشمند و چارچوب‌های مبتنی بر عدم‌قطعیت می‌تواند به توسعه سیستم‌های تصفیه‌ای قابل‌اعتمادتر، تطبیق‌پذیرتر و کاراتر منجر شود.

با وجود این پیشرفت‌ها، چالش‌هایی همچون محدودیت داده‌ها، انتقال‌پذیری مدل‌ها، پیچیدگی یکپارچه‌سازی سیستم‌ها، و ملاحظات اقتصادی همچنان پابرجاست. این مطالعه با ارائه یک چارچوب یکپارچه که مهندسی محیط‌زیست، علوم داده و اصول پایداری را به هم پیوند می‌دهد، مسیر توسعه سیستم‌های تصفیه پساب حفاری هوشمند، چرخشی و مقاوم را ترسیم می‌کند.

واژگان کلیدی: تصفیه پساب حفاری، یادگیری ماشین، کمّی‌سازی عدم‌قطعیت، اقتصاد چرخشی، بازیابی منابع، صنعت نفت و گاز

JOURNAL OF GAS TECHNOLOGY
VOLUME 10 • ISSUE 2 • WINTER 2025
EISSN: 2588-5596

Contents